AD_____

Award Number: W81XWH-06-1-0116

TITLE: Role of Caveolin-1 in Prostate Cancer Angiogenesis

PRINCIPAL INVESTIGATOR: Timothy C. Thompson, Ph.D.

CONTRACTING ORGANIZATION: The University of Texas
M. D. Anderson Cancer Center
Houston, TX 77030

REPORT DATE: December 2008

TYPE OF REPORT: Annual

PREPARED FOR: U.S. Army Medical Research and Materiel Command
Fort Detrick, Maryland 21702-5012

REPORT DOCUMENTATION PAGE

Form Approved
OMB No. 0704-0188

1. REPORT DATE	2. REPORT TYPE	3. DATES COVERED
1 Dec 2008	Annual	15 Nov 2007 – 14 Nov 2008

4. TITLE AND SUBTITLE

Role of Caveolin-1 in Prostate Cancer Angiogenesis

5a. CONTRACT NUMBER

5b. GRANT NUMBER
W81XWH-06-1-0116

5c. PROGRAM ELEMENT NUMBER

6. AUTHOR(S)

Timothy C. Thompson, Ph.D.

E-Mail: timthomp@mdanderson.org

5d. PROJECT NUMBER

5e. TASK NUMBER

5f. WORK UNIT NUMBER

7. PERFORMING ORGANIZATION NAME(S) AND ADDRESS(ES)

The University of Texas
M. D. Anderson Cancer Center
Houston, TX 77030

8. PERFORMING ORGANIZATION REPORT NUMBER

9. SPONSORING / MONITORING AGENCY NAME(S) AND ADDRESS(ES)
U.S. Army Medical Research and Materiel Command
Fort Detrick, Maryland 21702-5012

10. SPONSOR/MONITOR'S ACRONYM(S)

11. SPONSOR/MONITOR'S REPORT NUMBER(S)

12. DISTRIBUTION / AVAILABILITY STATEMENT
Approved for Public Release; Distribution Unlimited

13. SUPPLEMENTARY NOTES

14. ABSTRACT
We have made a significant progress toward our stated goals. Notable achievements for the past year of funding include comprehensive documentation that prostate cancer cell derived, secreted caveolin-1 is taken up by cancer cells and tumor associated endothelial cells (Tahir et al, Cancer Res 2008). This autocrine/paracrine activity of secreted caveolin-1 promotes malignant progression by stimulation of specific angiogenic activities. We have shown in cav-1 negative LP-LNCaP cells that adenoviral vector mediated expression of cav-1 stimulated VEGF mediated VEGFR2 autophosphorylation and activated downstream signaling. We are further exploring cav-1 mediated angiogenic signaling in endothelial cell models, including the possibility of direct interactions between cav-1 and VEGFR2. Our animal model studies have shown that systemic delivery of cav-1 antiserum suppresses primary tumor growth and lung metastasis in a pre-established metastasis prostate cancer model. Moreover, systemic treatment with cav-1 Ab increased survival in the mouse model of prostate cancer (see Fig 6-8). Our results indicate that cav-1 may be a clinically useful biomarker of prostate cancer progression and a potential therapeutic target.

15. SUBJECT TERMS
Prostate cancer, angiogenesis, caveolin-1

16. SECURITY CLASSIFICATION OF:			17. LIMITATION OF ABSTRACT	18. NUMBER OF PAGES	19a. NAME OF RESPONSIBLE PERSON
a. REPORT	b. ABSTRACT	c. THIS PAGE			USAMRMC
U	U	U	UU	41	19b. TELEPHONE NUMBER *(include area code)*

Table of Contents

INTRODUCTION

Background: Caveolin-1 (cav-1) is an important structural/regulatory molecule involved in many aspects of molecular transport and cell signaling. Cav-1 activities are dependent on protein level and cell context, yet an understanding of the biological consequences of inappropriate cav-1 expression in malignant cells has been elusive. We have shown previously that cav-1 up-regulation is associated with metastatic, androgen-insensitive prostate cancer. In studies funded by this grant we identified an underlying mechanism for the selection of cav-1 overexpression in prostate cancer cells during progression. We found that cav-1 binds to and inhibits the activities of PP1/PP2A serine / threonine phosphatases, preventing inactivation of Akt through dephosphorylation and thus sustaining levels of phospho-Akt and its oncogenic activities. Recently we have shown that cav-1 overexpression leads to increased levels of c-myc protein, and our preliminary data and the results of published studies lead us to speculate that the mechanisms for cav-1 mediated c-myc stabilization also involve PP1/PP2A inhibition and phospho-Akt stabilization. We have also shown that cav-1 overexpression leads to up-regulation and secretion of VEGF, FGF2 and TGF-β1, indicating that cav-1 stimulated molecular pathways can regulate these growth factors (GF) /angiogenic cytokines (AC). Importantly, we have also discovered that cav-1 itself is specifically secreted by prostate cancer cells and is taken up by prostate cancer cells and endothelial cells (EC).

Hypothesis: These results suggest that cells expressing cav-1 can function as "feeder cells" for local and potentially distant prostate cancer cells and tumor-associated EC through secretion of cav-1 and cav-1 stimulated GF/AC. In support of this concept we have shown that experimentally induced metastasis is potentiated in host transgenic mice that overexpress cav-1 in and secrete cav-1 from prostatic epithelium. In contrast experimental metastasis is suppressed in host *cav-1*$^{-/-}$ mice compared to *cav-1*$^{+/+}$ mice. We propose that prostate cancer cells secrete cav-1 which induces specific changes in EC that potentiate angiogenesis and metastatic activities.

Specific Aims: Using in vitro and in vivo models that involve novel genetically mutant mice we propose to resolve the molecular and cellular pathways that support these oncogenic activities through specific aims to: (1) to analyze the effects of cav-1 conditioned media on cav-1$^{-/-}$ endothelial cell gene expression and biological activity; (2) map the molecular pathways involved in EC angiogenesis stimulated by cav-1 protein alone or together with specific GF/AC; and (3) to correlate the effects of prostate cancer cell derived cav-1 uptake by TAEC with tumor growth activities.

Study Design: We have generated and characterized mice that have a deletion of the *cav-1* gene. These will be a source for isolation of EC that will be treated with conditioned media derived from prostate cancer cells with controlled levels of cav-1 protein (Aim 1) or with purified cav-1 protein (Aim 2). We will determine the molecular events that are induced by cav-1 in EC by analyzing expression of signaling molecules such as phosphorylated Akt, c-myc and relevant GF/AC (VEGF, FGF-2, and TGF-β1) at the transcription level by quantitative RT-PCR and at the protein level by western blotting. Additionally we will evaluate events further downstream of signaling such as nitric oxide (NO) production. Biological activities of the EC in response to cav-1 that we will examine will include proliferation, chemoattraction, motility and vasculogenesis. The validation of these activities will be accomplished by using specific molecular inhibitors of the signaling molecules. The final aim of the grant will focus on in vivo studies using a novel mouse metastatic prostate cancer cell line that overexpresses cav-1 and has a high level of metastasis to lung and to bone. We will inject this cell line orthotopically (prostate) into *cav-1*$^{-/-}$ mice and then analyze TAEC responses locally and at distant sites of metastasis by immunohistochemistry. Treatment of the mice with cav-1 specific antibody will directly test the effects of blocking cav-1 uptake in vivo on the growth and progression of experimental prostate cancer in this model.

Relevance: These studies could lead to the use of cav-1 positive TAEC as a potential prognostic/ predictive biomarker for prostate cancer in man. They will further serve to test the therapeutic potential of cav-1 antibody approaches for the treatment of prostate cancer.

BODY

Task 1. ***To analyze the effects of cav-1 conditioned media(CM) on cav1$^{-/-}$ endothelial cell gene expression and biological activity***

1. Prepare EC from aorta of 40 *cav-1$^{-/-}$* and 20 *cav-1$^{+/+}$* mice and CM from cav-1 (500ml) or pcDNA (500ml) transfected LP-LNCaP cells.
   (Months 1-3)
2. Perform western blotting and QRT-PCR on EC lysates treated with cav-1 CM.
   (Months 3-18)
3. Develop biological assays for the EC activity (Motility/invasion, migration, tubule formation, NO and PGI2 determination) and analyze the effect of soluble cav-1 on these activities.
   (Months 18-36)

Mutagenesis experiments have identified the cav-1 scaffolding domain (CSD) residues 82-101 as the region of cav-1 responsible for mediating the interaction with a number of signaling proteins including eNOS, platelet activating factor (PDGF) receptors, epidermal growth factor (EGF), the kinases Src and Fyn, heterotrimeric G-protein and cholesterol binding. Therefore we constructed cav-1 plasmid with deleted CSD termed phΔcav-1-V5-His, and prepared CM from phΔcav-1-V5-His transfected LNCaP cells. The use of recombinant protein with deleted CSD (rΔcav-1) as well as CM will be important to investigate the role of CSD in the secretion, uptake and angiogenic activities of ECs.
To determine the role of the CSD in exogenous rcav-1 membrane attachment and cellular uptake, we generated and purified the CSD deleted rcav-1 protein (Δrcav-1), treated EC and prostate cancer cells with different concentrations of FITC-Δrcav-1 over 1-6 h, and examined the cells for Δrcav-1 uptake using fluorescence microscopy. We did not detect internalized FITC-Δrcav-1 in cells incubated for as long as 6 h at concentrations of the mutant protein ranging to 5.0μg/ml. As expected, Δrcav-1 at concentrations up to 1.5 μg/ml failed to stimulate tubule formation and migration in *cav-1$^{-/-}$* EC (Fig 1), and eNOS phosphorylation at S1177 (Fig 2). These observations suggest that endocytosis of exogenous rcav-1 protein and its subsequent stimulation of angiogenic activities is mediated, in part, by CSD, which appears critical for cellular internalization of the protein.

Fig. 1: Rcav-1, but not Δrcav-1 stimulates angiogenic activities

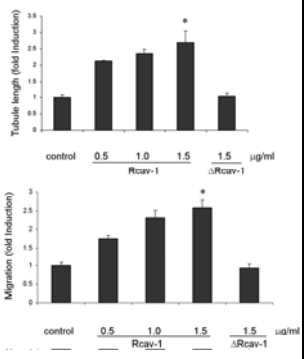

Fig. 2: Rcav-1, but not Δrcav-1 increase eNOS phosphorylation (S1177).

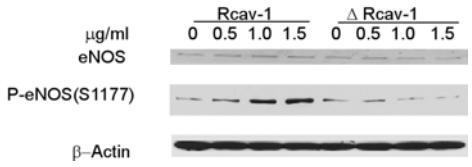

The study of protein expression using western blotting and gene expression using QRT-PCR in EC lysates treated with cav-1 CM is underway. We recognize that we are making slow progress in this area, and that is primarily due to the difficulties in producing large quantities of primary *cav-1$^{-/-}$* and *cav-1$^{+/+}$* EC sufficient for these studies.

Task 2. ***Map the molecular pathways involved in EC angiogenesis stimulated by cav-1 protein alone or together with specific GF/AC.***

1. Preparation/purchase of reagents, including recombinant cav-1, VEGF, FGF-2, TGF-β1, siRNA for VEGFR2, PI3-K, Akt, ERK1/2 and eNOS, chemical inhibitors for VEGFR2, PI3-K, ERK1/2 and eNOS.
   (Months 1-3)
2. Optimize conditions for siRNA transfection and for chemical inhibitions.
   (Months 1-6)

3. Analysis of gene knock down, including QRT-PCR analysis for mRNA and western analysis for protein. Analysis range covers target genes and their downstream components.
   (Months 7-24)
4. Biological function end points.
   (Months 25-36)

We are currently investigating different siRNA transfection protocols to find the highest transfection efficiency with primary mouse aortic endothelial cells. We tested transfection protocols from Santa Cruze Biotechnology, Ambion, and Lonza and we found that the Ambion amine transfection reagent produced the highest efficiency and we are currently developing procedures to further increase the efficiency to above 50% by changing the SiRNA concentrations, transfection reagents volume or the transfection time.

We have investigated the mechanism(s) that underlies rcav-1 stimulated eNOS activation by analyzing the effect of rcav-1 on the activities of two serine/threonine protein phosphatases PP1 and PP2A in *cav-1*$^{-/-}$ EC. These two phosphatases are known to regulate the phosphorylation of multiple protein targets including Akt and eNOS. We found that rcav-1 treatment significantly inhibited the activity of PP2A but had no effect on PP1 activity (P=0.0002 versus control, Fig 3) indicating that rcav-1 induces eNOS phosphorylation through Akt activation (previous progress report), and independently of Akt, through inhibition of PP2A which specifically dephosphorylates eNOS (S1177).

Fig. 3: Rcav-1 inhibits the activity of PP2A but not PP1 in *cav-1*$^{-/-}$ EC.

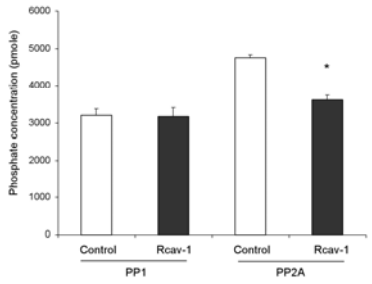

Fig. 4: Induction of eNOS/Akt association by rcav-1

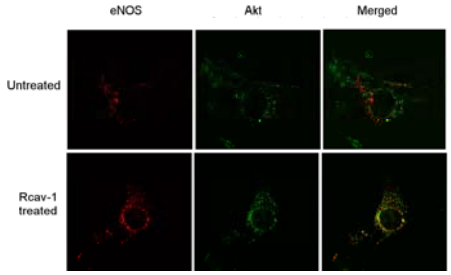

Additionally, we investigated the role played by cav-1 in compartmentalization of the PI-3-K-Akt-eNOS signaling pathway molecules in *cav-1*$^{-/-}$ EC, and found that Akt was not colocalized with eNOS in untreated cells, whereas significant colocalization of the two molecules was observed in the cells treated with rcav-1 (Fig 4).
To determine the role played by cav-1 in VEGF stimulated VEGFR2 autophosphorylation and down stream effects, we infected cav-1 negative LP-LNCaP cells with Adcav-1 or control AdRSV, and the cells were then treated with VEGF. Cav-1 overexpression significantly increased the phosphorylation of VEGFR2 (Y951) (Fig. 5). Increased phosphorylation of PLCγ1 (Y783) and Akt (S473) were also demonstrated with no change in the total protein in response to cav-1 overexpression. Treatment of the cells with VEGF had little or no effect on the above phosphorylations in the control AdRSV infected cell at all times 0, 5, and 15 min, while cav-1 overexpression further increased VEGF stimulated signaling. These results demonstrate that in the absence of cav-1, VEGF stimulation of VEGFR2 autophosphorylation and its downstream effects is minimal, and that cav-1 is required for optimal VEGF-dependent signaling (Fig. 5).
We will further investigate the mechanism and the role of cav-1 in VEGF stimulated angiogenic activities in EC by introducing cav-1 into *cav-1*$^{-/-}$ EC through infection of Adcav-1 or through treatment with rcav-1. Furthermore, analysis of the phosphorylation status of VEGF/VEGFR2 signaling pathway associated proteins will be performed. Additionally we will also investigate the role played by cav-1 in VEGF stimulated angiogenic activities in HUVEC.

Fig. 5: Cav-1 stimulates VEGF/VEGFR2 induced angiogenesis signaling in prostate cancer cells

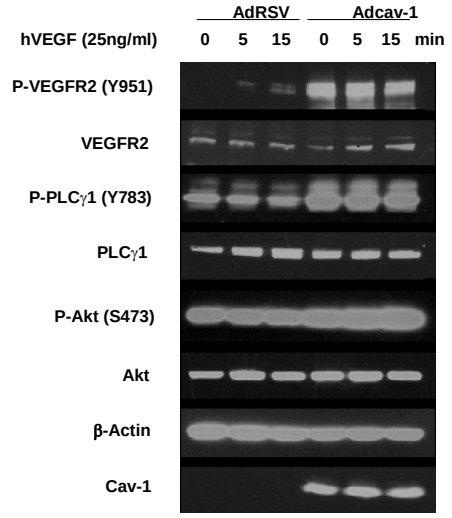

Task 3. ***To correlate the effects of prostate cancer cell derived cav-1 uptake by TAEC with tumor growth activities.***

1. Inject 178-2 BMAK cells into dorsolateral prostate of twenty *cav-1*$^{-/-}$ mice and analyze tumor weight and metastasis at 21 day, fixed time point. Analyze tissues by immunohistochemistry
   (Months 1-12)
2. Inject 178-2 BMAK cells into dorsolateral prostate of thirty nine *cav-1*$^{-/-}$ mice then treat with HBSS, rabbit IgG, or rabbit anti-cav-1 serum (thirteen per group) and analyze tumor weight and metastasis at 21 day, fixed time point (12-18 months). Analyze tissues by immunohistochemistry
   (Months 12-36)
3. Inject 178-2 BMAK cells into dorsolateral prostate of thirty *cav-1*$^{-/-}$ mice then treat with HBSS, rabbit IgG, or rabbit anti-cav-1 serum (ten per group) and analyze tumor weight and metastasis at survival time point (12-18 months). Analyze tissues by immunohistochemistry
   (Months 12-36)

As we explained in our previous report due to minor histocompatibility problems and poor "take" of 178-2BMAK cells in *cav1*$^{-/-}$mice we replaced 178-2BMAK cells with RM-9 prostate cancer cells that were originally isolated from C57/BL6 mice. We have previously demonstrated that RM-9 cells secrete cav-1 into conditioned media in vitro and can be used in the orthotopic mouse prostate cancer model in vivo.

Fig. 6: Anti-cav-1 antibody treatment significantly reduces the wet weight of orthotopic RM-9 tumors grown in cav-1$^{-/-}$ mice compare to control IgG or HBSS groups (* P < 0.05)

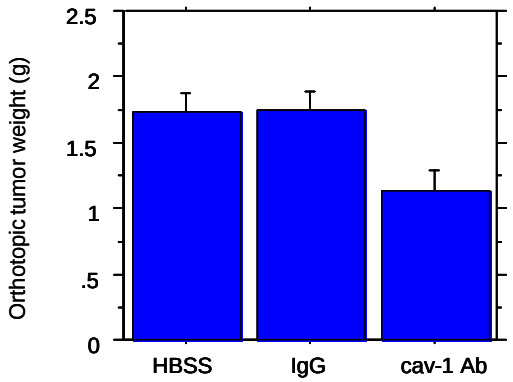

To test for anti-metastatic potential and the therapeutic effects of cav-1Ab in *cav-1*$^{-/-}$ mice, a mouse model of metastatic prostate cancer which involves simultaneous inoculation of RM-9 prostate cancer cells (preestablished metastasis model) via orthotopic prostate and tail vein injection was used as follow. A cohort of adult male *cav-1*$^{-/-}$ mice were injected with 5000 RM-9 cells into dorsolateral prostate to establish orthotopic prostate tumor and intravenously (tail vein) to establish experimental lung metastases. Two days after RM-9 cells injection mice were divided into 3 treatment groups and received IP injection (q.o.d) of cav-1 Ab, control IgG or HBSS. Mice were sacrificed at 21 days after initial tumor cells injection and prostate and lung tissues were collected for further analysis. Wet prostate tumor weight was significantly reduced in *cav-1*$^{-/-}$ mice that received cav-1 Ab compared to the mice treated with control IgG or HBSS only (Fig.6). Treatment with cav-1 Ab also had an anti-metastatic effect in *cav-1*$^{-/-}$ model and reduced number of lung metastasis compared to the control treatment groups (Fig. 7). Interestingly, in the same experimental setting the adult male *cav-1*$^{-/-}$ mice that received cav-1 Ab survived significantly longer then *cav-1*$^{-/-}$ littermate treated with control IgG or HBSS only (Fig.8). Thus, cav-1 Ab can significantly reduce local tumor growth as well as experimental metastasis most likely by reducing systemic cav-1 levels secreted by RM-9 prostate tumor cell. It is possible that high metastatic activity of *cav-1*$^{-/-}$ mice in HBSS and IgG groups are partially due to cav-1 secreted from the prostate tumor in Fig. 6. To eliminate the circulating cav-1 derived from the primary prostate tumor in the preestablished lung metastasis model (Figs 6,7,8) that potentially contributed to lung metastasis, another cohort of *cav-1*$^{-/-}$ mice were set up for RM-9 experimental metastasis analysis (i.e., without inoculation of a primary tumor- single experimental metastasis). These mice received 5000 cells of RM-9 cells through

Fig. 7: Anti-cav-1 antibody treatment significantly reduces the number of RM-9 experimental lung metastases tumors in cav-1$^{-/-}$mice compare to control IgG or HBSS groups (* P < 0.05)

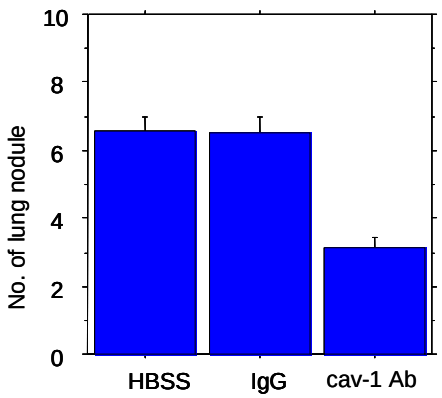

tail vein and two days later were divided into 3 treatment groups and received IP injection (q.o.d) of anti cav-1Ab, control IgG or HBSS. The mice were sacrificed at 21 days after initial tumor cells injection and lung tissues were collected for further analysis (Fig. 9). The number of lung metastasis generated in HBSS or IgG groups in this single experimental metastasis model were 30% less than the simultaneous injection of prostate and tail vein model discussed in Fig. 7. Furthermore, cav-1Ab treatment group of this single experimental metastasis had 50% less number of lung metastasis compared to the simultaneous injection group shown in Fig. 7. Reduced metastatic activity may be due to absence of secreted cav-1derived from the primary prostate tumor. The data supports our hypothesis that prostate cancer cells secrete cav-1 which potentiate angiogenesis and metastatic activities.

These experiments also suggest that cav-1 Ab can potentially be a novel systemic therapeutic modality for the treatment of metastatic prostate cancer. We will analyze collected tissues for any changes in GF/AC related to cav-1 Ab treatment.

Fig. 8: The cav-1$^{-/-}$ mice with orthotopic RM-9 tumor and lung metastases treated with anti-cav-1 antibody survive significantly longer compare to mice treated with control IgG or HBSS (Kaplan-Meier survival plot)

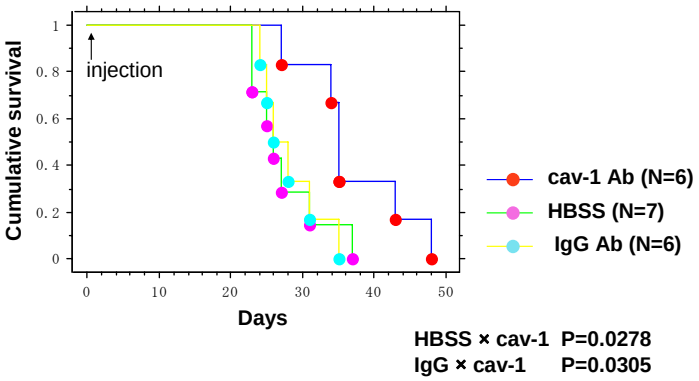

Fig. 9: Significant reduction in the number of lung metastasis in the single experimental metastasis model compared to the simultaneous prostate and metastasis model of Fig.6.

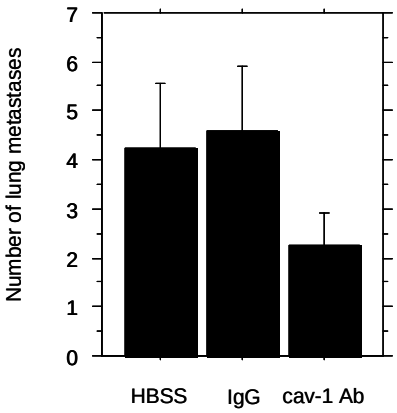

Significance

Thus far our new mechanistic data are consistent with the concept that angiogenic activities of prostate cancer cell derived, secreted cav-1 promotes tumor progression. In our view, this novel concept will lead to novel approaches for prostate cancer diagnosis and therapy.

Plans

In general our experiments are on track and yielding important and interesting results. Since last year we have published two important papers demonstrating cav-1 mediated angiogenic activity in prostate cancer. In the current year we anticipate to collect all the remaining experimental data to conclude the studies planned and supported by this grant.

Publications

1. Tahir SA, Frolov A, Hayes TG, Mims, MP, Miles BJ, Lerner SP, Wheeler TM, Ayala G, Wheeler TM, Thompson TC and Kadmon D**.** Preoperative serum caveolin-1 as a prognostic marker for recurrence in a radical prostatectomy cohort. Clin Can Res, 12(16):4872-4875, 2006.

2. Yang G, Addai J, Wheeler TM, Frolov A, Miles BJ, Kadmon D and Thompson TC. Correlative evidence that prostate cancer cell-derived caveolin-1 mediates angiogenesis. Hum Pathol. 2007 Nov;38 (11):1688-95.

3. Tahir SA, Yang G, Goltsov AA, Watanabe M, Tabata K, Addai J, Abdel Fattah E Kadmon D and Thompson TC. Tumor cell-secreted caveolin-1 has proangiogenic activities in prostate cancer. Cancer Res 68(3): 731-739, 2008.

4. Yang G, Timme TL, Naruishi K, Fujita T, Abdel Fattah E, Cao G, Rajocopolan K, Truong LD, and Thompson TC. Mice with *cav-1* gene disruption have benign stromal lesions and compromised epithelial differentiation. Experimental and Molecular Pathology, 84: 131-140, 2008

KEY RESEARCH ACCOMPLISHMENTS

1. Secreted cav-1 stimulates angiogenic activities in *cav-1*$^{-/-}$ mouse EC.

2. Akt (S473, T308) and eNOS (S1177) are significantly phosphorylated in rcav-1 treated *cav-1*$^{-/-}$ mouse EC.

3. Δrcav-1 did not stimulate the phosphorylation of eNOS on S1177 in *cav-1*$^{-/-}$ mouse EC

REPORTABLE OUTCOMES

Presentations

1. Tahir SA, Yang G, Goltsov A, Watanabe M, Tabata K, and Thompson TC. Caveolin-1 uptake by endothelial cells promotes angiogenic activities and is associated with prostate cancer progression. American Association for Cancer Research, 97th Annual Meeting, Washington DC, April 1-5, 2006.

2. Tahir SA, Yang G, Goltsov A, Watanabe M, Tabata K and Thompson TC. Caveolin-1 uptake by endothelial cells promotes angiogenic activities and is associated with prostate cancer progression. 4th Annual Cancer Center Symposium, Houston, TX, November 3, 2006.

3. Miles BJ, Yang G, Addai J, Wheeler TM, Frolov A, Kadmon D and Thompson TC. Correlative evidence that prostate cancer cell-derived caveolin-1 mediates angiogenesis. American Society of Clinical Oncology annual meeting, June 1 – 5, 2007, Chicago, IL.

4. Tahir SA, Park SH, and Thompson TC. Caveolin-1 regulates VEGF/VEGFR2 induced stimulation of angiogenesis. Submitted, 100th AACR Annual Meeting, Denver, Colorado, 2009

Manuscripts

1. Yang G, Addai J, Wheeler TM, Frolov A, Miles BJ, Kadmon D and Thompson TC. Correlative evidence that prostate cancer cell-derived caveolin-1 mediates angiogenesis. Hum Pathol. 2007 Nov;38(11):1688-95.

2. Tahir SA, Frolov A, Hayes TG, Mims, MP, Miles BJ, Lerner SP, Wheeler TM, Ayala G, Wheeler TM, Thompson TC and Kadmon D**.** Preoperative serum caveolin-1 as a prognostic marker for recurrence in a radical prostatectomy cohort. Clin Can Res, 12(16):4872-4875, 2006.

3. Tahir SA, Yang G, Goltsov AA, Watanabe M, Tabata K, Addai J, Abdel Fattah E Kadmon D and Thompson TC. Tumor cell-secreted caveolin-1 has proangiogenic activities in prostate cancer. Cancer Res 68(3): 731-739, 2008.

4. Watanabe M, Yang G, Cao G, Tahir SA, Naruishi K, Tabata K, Abdel Fattah E , Park SH, Demayo FJ, Goltsov AA and Thompson TC. Functional analysis of secreted caveolin-1 in mouse models of prostate cancer. In preparation

5. Li L, Ren C, Yang G, Goltsov AA, Tabata K, and Thompson TC. Caveolin-1 enhances malignant activities through auto regulatory, Akt-mediated maintanence of mRNA stabilities of cancer promoting growth factors. In preparation

6. Tahir SA, Park SH, and Thompson TC. Caveolin-1 regulates VEGF/VEGFR2 induced stimulation of angiogenesis. In preparation

CONCLUSIONS

Overall, we have made exceptional progress since the first year funding period of this project. Tasks 1-3 are on schedule and although, as is often the case, we have made some unanticipated and necessary adjustments (replacement of 178-2BMAK cells with RM-9 cells for Task 3) we are moving toward our stated goals. Importantly, our data thus far, are yielding important mechanistic insight into the angiogenic activities of prostate cancer cell derived, secreted cav-1. In addition the results of our studies using cav-1 Ab treatment raise the possibility of developing this approach toward therapeutic applications. In our view, after we further define these mechanisms we will be able to take the next important step, exploiting this new knowledge for prostate cancer diagnosis and therapy.

REFERENCES

None cited in text

APPENDICES

1. Tahir SA, Frolov A, Hayes TG, Mims, MP, Miles BJ, Lerner SP, Wheeler TM, Ayala G, Wheeler TM, Thompson TC and Kadmon D**.** Preoperative serum caveolin-1 as a prognostic marker for recurrence in a radical prostatectomy cohort. Clin Can Res, 12(16):4872-4875, 2006.

2. Yang G, Addai J, Wheeler TM, Frolov A, Miles BJ, Kadmon D and Thompson TC. Correlative evidence that prostate cancer cell-derived caveolin-1 mediates angiogenesis. Hum Pathol. 2007 Nov;38 (11):1688-1695.

3. Tahir SA, Yang G, Goltsov AA, Watanabe M, Tabata K, Addai J, Abdel Fattah E Kadmon D and Thompson TC. Tumor cell-secreted caveolin-1 has proangiogenic activities in prostate cancer. Cancer Res 68(3): 731-739, 2008.

4. Yang G, Timme TL, Naruishi K, Fujita T, Abdel Fattah E, Cao G, Rajocopolan K, Truong LD, and Thompson TC. Mice with *cav-1* gene disruption have benign stromal lesions and compromised epithelial differentiation. Experimental and Molecular Pathology, 84: 131-140, 2008.

Preoperative Serum Caveolin-1 as a Prognostic Marker for Recurrence in a Radical Prostatectomy Cohort

Salahaldin A. Tahir,[1] Anna Frolov,[1] Teresa G. Hayes,[4] Martha P. Mims,[4] Brian J. Miles,[1] Seth P. Lerner,[1] Thomas M. Wheeler,[2] Gustavo Ayala,[2] Timothy C. Thompson,[1,3,5] and Dov Kadmon[1]

Abstract

Purpose: Up-regulation of caveolin-1 (cav-1) is associated with virulent prostate cancer, and serum cav-1 levels are elevated in prostate cancer patients but not in benign prostatic hyperplasia. In this study, we evaluated the potential of high preoperative serum cav-1 levels to predict biochemical progression of prostate cancer. The value of the combined preoperative markers, prostate-specific antigen (PSA), biopsy Gleason score, and serum cav-1 for predicting biochemical recurrence was also investigated.

Experimental Design: Serum samples taken from 419 prostate cancer patients before radical prostatectomy were selected from our Specialized Programs of Research Excellence prostate cancer serum and tissue bank. Serum samples were obtained 0 to 180 days before surgery and all patients had complete data on age, sex, race, stage at enrollment, and follow-up for biochemical recurrence. Serum cav-1 levels were measured according to our previously reported ELISA protocol.

Results: Cav-1 levels were measured in the sera of 419 prostate cancer patients; the mean serum level was 4.52 ng/mL (median 1.01 ng/mL). Patients with high serum cav-1 levels had a 2.7-fold ($P = 0.0493$) greater risk of developing biochemical recurrence compared with those with low serum cav-1 levels. Importantly, patients with serum PSA $\geq$ 10 ng/mL and elevated levels of serum cav-1 had 2.44 times higher risk ($P = 0.0256$) of developing biochemical recurrence compared with patients with low levels of cav-1. In addition, high serum cav-1 levels combined with increasing biopsy Gleason score predicted much shorter recurrence-free survival in the group of patients with PSA $\geq$ 10 ng/mL ($P = 0.0353$). Cav-1 was also able to distinguish between high- and low- risk patients with biopsy Gleason score of seven, after adjusting, for patients PSA levels ($P = 0.0429$).

Conclusions: Overall, elevated preoperative levels of serum cav-1 predict decreased time to cancer recurrence. In the subset of patients with serum PSA of $\geq$10 ng/mL, the combination of serum cav-1 and biopsy Gleason score has the capacity to predict time to biochemical recurrence.

In 2005, ~90% of newly diagnosed prostate cancer patients had clinically localized disease (1). Consequently, the majority of patients are treated with curative intent by either radical prostatectomy or radiation therapy. It is well established, however, that 10% to 50% of patients who undergo radical prostatectomy will show biochemical evidence of disease recurrence [prostate-specific antigen (PSA) recurrence] within 5 years of surgery (2, 3). Various clinical variables have been used, singly and in combination (nomograms, tables, etc.), to predict, preoperatively, which patients are likely to fail definitive therapy (4). However, the predictive value of these variables has been thwarted by the vexing biological diversity of clinical prostate cancer. New markers are needed, preferably serum markers that have been mechanistically implicated in the progression of virulent disease. We believe that serum caveolin-1 (cav-1) may be such a marker.

Cav-1 is an important structural/regulatory molecule involved in many aspects of molecular transport and cell signaling (5, 6). Tissue cav-1 is overexpressed in metastatic and in hormone-resistant prostate cancer (7). Overexpression correlates with a shortened interval to disease recurrence following therapy for localized disease and tends to be associated with a high Gleason score pathologically (8–10). Interestingly, cav-1 is secreted by prostate cancer cells (11) and we have developed a sensitive ELISA immunoassay for the detection of cav-1 in the serum (12). In a preliminary study, we documented that prostate cancer patients have a higher serum cav-1 level when compared with age-matched controls with benign prostatic hyperplasia (12).

We report here the utility of a single preoperative measurement of serum cav-1 for predicting disease recurrence in a cohort of 419 prostate cancer patients undergoing radical prostatectomy at our institution.

Authors' Affiliations: [1]Scott Department of Urology and Departments of [2]Pathology, [3]Radiology, [4]Medicine, and [5]Molecular and Cellular Biology, Baylor College of Medicine, Houston, Texas

Received 2/21/06; revised 3/31/06; accepted 4/20/06.

Grant support: National Cancer Institute Specialized Programs of Research Excellence grants P50-58204 and RO1-68814.

The costs of publication of this article were defrayed in part by the payment of page charges. This article must therefore be hereby marked *advertisement* in accordance with 18 U.S.C. Section 1734 solely to indicate this fact.

Requests for reprints: Dov Kadmon, Scott Department of Urology, Baylor College of Medicine, 6560 Fannin, Suite 2100, Houston, TX 77030. E-mail: dkadmon@bcm.tmc.edu.

doi:10.1158/1078-0432.CCR-06-0417

Materials and Methods

Study population. The sera of 419 prostate cancer patients were obtained from the Specialized Programs of Research Excellence prostate cancer blood and tissue bank at Baylor College of Medicine. Entry into the study required availability of preoperative serum samples obtained within 6 months of surgery and complete data on age, race, stage at enrollment and follow-up, as well as availability of postoperative serum samples, as this is a part of a larger ongoing investigation. In addition, patients could have had no preoperative therapy. After completion of cav-1 measurements in the serum, it was discovered that seven patients were missing reliable data on their preoperative PSA and/or biopsy Gleason score and/or follow-up information. These patients were included in all analyses that did not require missing data. The preoperative serum collected from 355 patients was at a time period between prostate biopsy and surgery. No information was available in our database on the exact preoperative serum collection timing with respect to biopsy for 64 patients. The mean age of this patient group was 62.6 years (range 42.6-78.9 years); 91.4% were White males, with Hispanics, African-Americans, and Asians comprising 6.0%, 2.4%, and 0.2%, respectively. Mean follow-up time among this group of patients was 52 months, with a median follow-up time of 48 months. Biochemical recurrence is defined throughout this study as serum PSA level of $\geq$0.2 ng/mL on two consecutive measurements, using the first-generation postresection PSA assay (Hybritech, Beckman Coulter, Inc., Fullerton, CA). Patient data were gathered from the Informatics Core using the Specialized Programs of Research Excellence in Prostate Cancer Information System.

Determination of serum cav-1. Cav-1 was determined in the serum samples by the sandwich ELISA protocol developed in our laboratory (12). Briefly, Costar microplate wells were coated with 0.5 μg cav-1 polyclonal antibody (Transduction Laboratories, San Diego, CA) and blocked with TBS buffer containing 1.5% bovine serum albumin and 0.05% v/v Tween 20. Serum samples, calibrators, and controls (50 μL) were added to the well, and 50 μL TBS containing 0.5% v/v Tween 20 was added to each well. The plate was incubated at room temperature for 2 hours with shaking and after extensive washing, 100 μL horseradish peroxidase–conjugated cav-1 antibody (Santa Cruz Biotechnology, Santa Cruz, CA) diluted 1:200 in blocking buffer was added to each well. The microplate was incubated for 90 minutes at room temperature with shaking, the wells were then washed extensively, and 100 μL 3,3′,5,5′-tetramethylbenzidine substrate solution (Sigma-Aldrich, St. Louis, MO) was added and the blue color was allowed to develop for 20 minutes in the dark. The reaction was stopped by adding 50 μL of 2 N H_2SO_4, and the absorbance was read at 450 nm using a microplate reader (Sunrise Microplate Reader, Tecan US, Inc., Charlotte, NC).

Statistical analysis. Correlations of preoperative serum cav-1 levels with clinical and pathologic variables were evaluated using the Spearman correlation. The predictive value of cav-1 univariately and multivariately with other preoperative clinical and pathologic variables, such as preoperative PSA and biopsy Gleason score, as well as of the interactive terms, were analyzed using the Cox proportional hazards regression model. The minimum *P* value method was used to group patients into "low-level" and "high-level" cav-1 categories (13). The hazard ratio (HR) and 95% confidence intervals (95% CI) were computed for each marker. Kaplan-Meier survival curves were plotted for each risk category. $P < 0.05$ was considered statistically significant. All analyses were done using the SPSS 12.0 software package (SPSS, Inc., Chicago, IL)

Table 1. Preoperative serum cav-1 level correlation with clinical and pathologic variables

	n	Mean (range), %	r^2	*P*
Preoperative cav-1	419	4.5 (0.0-156.7)	—	—
Preoperative PSA (ng/mL)	415	8.6 (0.4-53.2)	0.01	0.9013
Age	419	62.6 (42.6-78.9)	0.02	0.6268
Biopsy Gleason score	412	6.1 (3-9)	−0.06	0.2051
Seminal vesicle invasion	419	7.6%	−0.01	0.8543
Lymph node involvement	419	3.8%	0.08	0.1024
Extraprostatic extension	419	32.7%	0.07	0.1378
Margin positive	419	11.9%	0.06	0.2425
Gleason score	419	6.5 (3-9)	−0.01	0.8342

Table 2. Preoperative serum cav-1 is a univariate and multivariate predictor of decreased biochemical recurrence-free survival

	HR (95% CI)	*P*
Univariate model		
Preoperative cav-1	2.78 (1.003-7.70)	0.0493
Multivariate model		
Preoperative cav-1	2.57 (0.92-7.12)	<0.0704
Ln(PSA)	2.31 (1.60-3.33)	<0.0001
Biopsy Gleason score	1.74 (1.32-2.30)	0.0001

Results

Serum cav-1 levels were measured in 419 prostate cancer patients. The mean cav-1 value was 4.52 ng/mL and the median level was 1.01 ng/mL (range 0.0-156.7 ng/mL). Serum cav-1 levels seemed to have a bimodal distribution, with positive values distributed log normally. The serum cav-1 levels were analyzed for correlation with other pathologic and clinical variables using the Spearman correlation. No statistically significant correlations with clinicopathologic variables were found (Table 1).

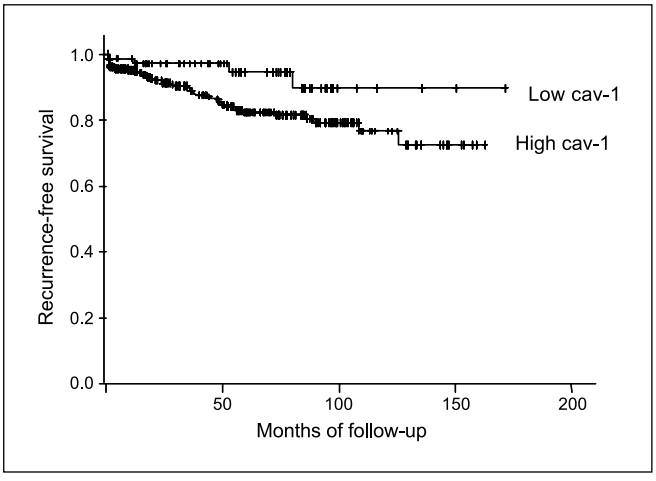

Fig. 1. High expression of cav-1 predicts decreased biochemical recurrence-free survival. This Kaplan-Meier plot illustrates the differences in recurrence-free survival between the low and high groups when separated by cav-1 cut point of 0.13 ng/mL. Patients with high level of cav-1 experienced significantly higher risk of recurrence than those with low levels ($P = 0.0493$).

There were 414 patients with complete follow-up information were included in the analysis of recurrence-free survival (mean follow-up 52.3 months, maximum 171.3 months); 54 patients had PSA recurrence during follow-up. Although it was clear that patients with no or very low levels of cav-1 had a better prognosis, the optimal cutoff was selected using the minimum *P* value method (13). This defined the low cav-1 group as patients with levels of <0.13 ng/mL and the high cav-1 group as those with >0.13 ng/mL. In univariate analysis, the risk of experiencing biochemical recurrence, estimated by HR, was 2.8 times higher ($P = 0.0493$) for the high cav-1 group compared with the low cav-1 group (Table 2). Kaplan-Meier plots illustrate the shorter time to biochemical recurrence following radical prostatectomy in the high cav-1 group compared with low cav-1 group. The 5- and 10-year recurrence-free survival rates were 94.4% and 90.5% for the low cav-1 group compared with 82.0% and 71.8% for the high cav-1 group. This corresponds to a consistent 12% to 21% increased progression-free survival for the low cav-1 group (Fig. 1). When the preoperative serum PSA level and the biopsy Gleason score were incorporated into the multivariate Cox proportional hazard model, the recurrence risk was 2.6 times higher for the high cav-1 group, but this effect was just below the level of significance ($P = 0.0704$; Table 2).

The effect of the serum cav-1 level on biochemical recurrence was further analyzed in patients with more advanced cancers, characterized by PSA of ≥10 ng/mL. The distribution shape remained the same and patients with low cav-1 levels continued to have a better prognosis. A new optimal cutoff of 2.86 ng/mL was identified for this subgroup of patients. Univariately, the estimated risk of recurrence was 2.44 times higher ($P = 0.0256$) in the high cav-1 group (serum cav-1 >2.86 ng/mL) than in its low cav-1 counterpart (serum cav-1 ≤ 2.86 ng/mL; Table 3). Kaplan-Meier plots illustrate that patients in the high cav-1 group had a much shorter time to recurrence than those in the low cav-1 group (Fig. 2). This figure also indicates a 10-year recurrence-free survival rate of 70.3% in the low cav-1 group compared with 47.4% in the high cav-1 group corresponding to a >20% decrease in progression-free survival in the low cav-1 group.

Incorporating the biopsy Gleason score into the Cox proportional hazard model (Table 3), we found that the interaction term between Gleason score and the cav-1 was the most predictive ($P = 0.0353$). This indicates that the biopsy Gleason score was an additional risk factor only in the high cav-1 group. The Kaplan-Meier plot (Fig. 3) illustrates this result by showing the highest recurrence risk in patients with high cav-1 and high biopsy Gleason score (7–9); and lower

Table 3. Preoperative serum cav-1 is a univariate and multivariate predictor of decreased biochemical recurrence-free survival among patients with preoperative PSA of ≥10

	HR (95% CI)	*P*
Univariate model		
Preoperative cav-1	2.44 (1.12-5.34)	0.0256
Multivariate model		
Preoperative Cav-1 × biopsy Gleason score	1.13 (1.01-1.27)	0.0353

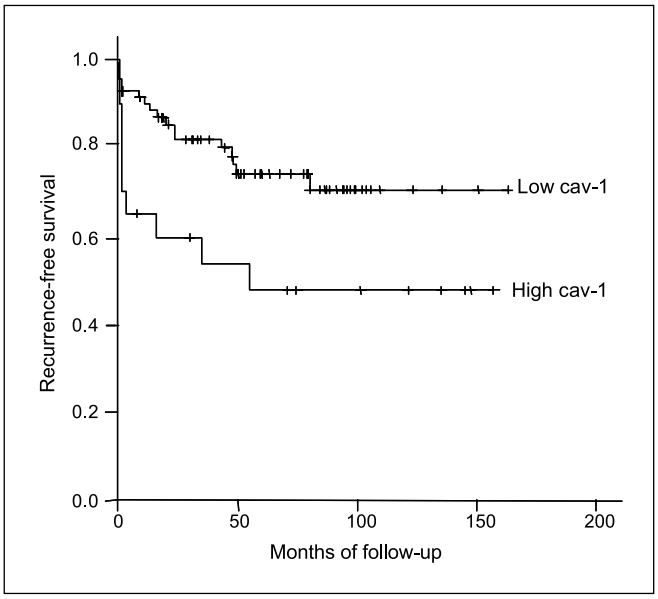

Fig. 2. For patients with PSA of ≥10, high expression of cav-1 is a strong predictor of decreased biochemical recurrence-free survival. For this high-risk patient subgroup, optimal cutoff was determined to be at 2.86 ng/mL. The Kaplan-Meier plot here shows the difference observed in the data.

recurrence risk in the high cav-1 and low biopsy Gleason score (<7) group, and those patients with low cav-1 regardless of the biopsy Gleason score. Recurrence-free survival curve for patients with low PSA (<10) was plotted for reference as well.

For biopsy Gleason 7 patients, the trend was the same: Higher cav-1 was observed in higher-risk patients. The difference in risk of recurrence, estimated by HR, between low and high cav-1 patients with cutoff defined at upper quartile of cav-1 (and confirmed by minimum *P* value method), was not statistically significant ($P = 0.0953$). However, after including preoperative PSA in the model, the

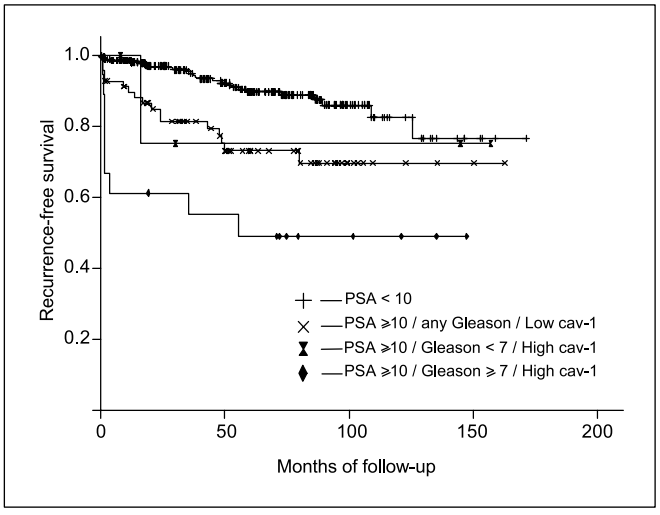

Fig. 3. Cav-1 works with biopsy Gleason score and preoperative PSA to predict biochemical recurrence-free survival. The interaction term between biopsy Gleason score and the cav-1, incorporated into the Cox proportional hazard, was the most predictive of recurrence-free survival among patients with PSA of ≥10 ($P = 0.0353$). This Kaplan-Meier plot illustrates how patients with both high cav-1 (>2.86 ng/mL) and biopsy Gleason score of ≥7 have the poorest prognosis. Curve for patients with PSA < 10 was plotted for reference.

difference became statistically significant (HR, 2.29; P = 0.0429). A patient with cav-1 in the upper quartile had over twice the risk of recurrence of one with cav-1 in the lower three quartiles if their preoperative PSA levels were the same.

Discussion

This study is part of our ongoing efforts to elucidate the biology and to define the clinical usefulness of serum cav-1 in prostate cancer. Although the factors modulating the serum levels of this biomarker remain largely unknown, the current study points out that a single preoperative serum cav-1 determination has prognostic value in a radical prostatectomy cohort. We observed the increase of the risk of biochemical recurrence with high levels of serum cav-1, and so we used the minimum P value method to segregate the patients into low-level and high-level groups. Remarkably, the risk of experiencing a PSA recurrence, estimated by HR, was 2.78 (95% CI, 1.003-7.70) times higher for the high-level cav-1 group (P = 0.0493), (see Fig. 1; Table 2). Incorporating the preoperative serum PSA level and the biopsy Gleason score into the model dropped the effect of cav-1 to just below the level of significance (HR, 2.57; P = 0.0704).

Interestingly, we found that the serum cav-1 levels are particularly important in predicting recurrence-free survival in patients with more advanced disease as defined by the preoperative serum PSA. When only patients with preoperative serum PSA levels of 10 ng/mL or higher were analyzed, cav-1 remained a significant predictor of recurrence-free survival (HR, 2.44; P = 0.0256). Additionally, the cav-1/biopsy Gleason score interaction term was a significant predictor (P = 0.0353). This implies that patients with both a high biopsy Gleason score and a high serum cav-1 level have a higher risk of biochemical recurrence than the remaining patients. Also, a subgroup of biopsy Gleason 7 prostate cancer patients, defined by the upper 25% of serum cav-1 levels, seems to harbor a biologically more aggressive prostate cancer after correction for individual PSA levels. All of these findings are consistent with our previous reports based on tissue up-regulation of cav-1 expression (8).

Notably, the distribution of the serum cav-1 values in the study population was not a normal distribution. About 10% of patients had undetectable serum levels by our sensitive ELISA essay. We can only speculate at this point as to the possible reason for this phenomenon. It is possible that the presence of any cav-1 in the serum is dictated by the genetic background of the individual and that, physiologically, there may be "secretors" and "nonsecretors." Within the secretor population, the specific makeup of the cancer may be contributing to the absolute serum level.

Surprisingly, we could not correlate the serum cav-1 levels with any of a large number of clinical and/or pathologic variables using the Spearman correlation (Table 1). We suggest that the reason is that cav-1 is an independent biomarker causally implicated in disease progression and not simply an epiphenomenon.

Many questions remain. For instance, we do not know the incidence of false-positive and/or false-negative elevated serum cav-1 values vis-à-vis the tumor tissue cav-1 expression. Only a correlative study of tissue and serum levels of cav-1 can answer this question. Likewise, the kinetics of the serum cav-1 has not been worked out, nor do we know what the stability of serum cav-1 is over extended periods of time. Clearly, we are at the beginning of the road leading to the establishment of serum cav-1 as a prognostic marker for prostate cancer. The data presented here suggest that this road is worth pursuing.

References

1. Cooperberg MR, Moul JW, Carroll PR. The changing face of prostate cancer. J Clin Oncol 2005;23:8146–51.
2. Shipley WU, Thames HD, Sandler HM, et al. Radiation therapy for clinically localized prostate cancer: a multi-institutional pooled analysis. JAMA 1999;281:1598–604.
3. Bracarda S, de Cobelli O, Greco C, et al. Cancer of the prostate. Crit Rev Oncol Hematol 2005;56:379–96.
4. Chin JL, Reiter RE. Molecular markers and prostate cancer prognosis. Clin Prostate Cancer 2004;3:157–64.
5. Shaul PW, Anderson RG. Role of plasmalemmal caveolae in signal transduction. Am J Physiol 1998;275:L843–51.
6. Ikonen E, Parton RG. Caveolins and cellular cholesterol balance. Traffic 2000;1:212–7.
7. Nasu Y, Timme TL, Yang G, et al. Suppression of caveolin expression induces androgen sensitivity in metastatic androgen-insensitive mouse prostate cancer cells. Nat Med 1998;4:1062–4.
8. Yang G, Truong LD, Wheeler TM, Thompson TC. Caveolin-1 expression in clinically confined human prostate cancer: a novel prognostic marker. Cancer Res 1999;59:5719–23.
9. Satoh T, Yang G, Egawa S, et al. Caveolin-1 expression is a predictor of recurrence-free survival in pT_2N_0 prostate carcinoma diagnosed in Japanese patients. Cancer 2003;97:1225–33.
10. Yang G, Addai J, Ittmann M, Wheeler TM, Thompson TC. Elevated caveolin-1 levels in African-American versus White-American prostate cancer. Clin Cancer Res 2000;6:3430–3.
11. Tahir SA, Yang G, Ebara S, et al. Secreted caveolin-1 stimulates cell survival/clonal growth and contributes to metastasis in androgen-insensitive prostate cancer. Cancer Res 2001;61:3882–5.
12. Tahir SA, Ren C, Timme TL, et al. Development of an immunoassay for serum caveolin-1: a novel biomarker for prostate cancer. Clin Cancer Res 2003;9:3653–9.
13. Mazumdar M, Glassman JR. Categorizing a prognostic variable: review of methods, code for easy implementation and applications to decision-making about cancer treatments. Stat Med 2000;19:113–32.

Human Pathology (2007) **38**, 1688–1695

ELSEVIER

Human PATHOLOGY

www.elsevier.com/locate/humpath

Original contribution

Correlative evidence that prostate cancer cell-derived caveolin-1 mediates angiogenesis☆

Guang Yang MD[a], Josephine Addai MS[a], Thomas M. Wheeler MD[b], Anna Frolov MS[a], Brian J. Miles MD[a], Dov Kadmon MD[a], Timothy C. Thompson PhD[a,c,d,*]

[a] *Department of Urology, Baylor College of Medicine, Houston, TX 77030, USA*
[b] *Department of Pathology, Baylor College of Medicine, Houston, TX 77030, USA*
[c] *Department of Molecular and Cellular Biology, Baylor College of Medicine, Houston, TX 77030, USA*
[d] *Department of Radiology, Baylor College of Medicine, Houston, TX 77030, USA*

Received 30 November 2006; revised 20 March 2007; accepted 23 March 2007

Keywords:
Prostate cancer;
Angiogenesis;
Caveolin-1

Summary Up-regulation of caveolin-1 (cav-1) has been implicated in human prostate cancer progression/metastasis and shown to promote cancer cell survival. It has also been shown that cav-1 is secreted by tumor cells and may regulate the growth, functional activities, and migration of vascular endothelial cells. However, the relationship of cav-1 expression in prostate cancer cells and tumor associated endothelial cells (TAEC) to tumor-associated angiogenesis remains to be investigated. Dual immunofluorescent labeling with antibodies to CD34 and cav-1 was performed on 56 prostate cancer specimens obtained by radical prostatectomy and stratified according to cav-1 positivity in cancer cells. The tumor microvessel densities (MVD) and cav-1 expression in TAEC within these specimens were measured and correlated with cav-1 expression in prostate cancer cells. The MVD values were significantly higher in cav-1-positive (n = 25) than in the cav-1-negative (n = 31) tumors (median of 44 versus 25 vessels/field, P = .0140). Additional studies showed that the cav-1 positivity in microvessels within tumor specimens was significantly less frequent than in the blood vessels of benign prostatic tissues (94.4% versus 98.6%, P = .0012). In contrast, the percentage of cav-1-positive TAEC in cav-1-positive tumors was significantly higher than in cav-1-negative tumors (95.8% versus 92.7%, P = .0024). This increased cav-1 positivity in TAEC was predominantly confined to regions with cav-1-positive tumor cells corresponding to the higher percentage of cav-1-positive microvessels within these regions in cav-1-positive, as opposed to cav-1-negative tumors (P = .0086). These positive correlations provide new evidence for the involvement of prostate cancer cell derived cav-1 in mediating angiogenesis during prostate cancer progression. They also establish a conceptual framework for further investigation of cav-1 proangiogenic activities.

1. Introduction

Caveolin-1 (cav-1) is an important structural/regulatory molecule involved in many aspects of molecular transport and normal cell signaling. The biologic consequences of inappropriate cav-1 expression in malignant cells depend

☆ This work was supported by NIH grants SPORE CA58204 and RO1 CA68814 and a grant from the Department of Defense.

* Corresponding author. Department of Urology, Baylor College of Medicine, Houston, TX 77030, USA.
E-mail address: timothyt@bcm.edu (T. C. Thompson).

0046-8177/$ – see front matter © 2007 Elsevier Inc. All rights reserved.
doi:10.1016/j.humpath.2007.03.024

on protein level and cell context (for review, see [1]). In contrast to studies that suggest a growth suppressor role for cav-1 in malignant cells [2-4], our research has documented overexpression of cav-1 in both mouse and human prostate cancer cells [5] and established its correlation with metastasis and androgen insensitivity of prostate cancer cells [6,7]. We have also shown that cav-1 overexpression is associated with an unfavorable clinical prognosis in men who have undergone radical prostatectomy [8]. A positive correlation between cav-1 overexpression and clinicopathologic markers of cancer progression has been reported for other malignancies, including colon cancer [9], renal cancer [10,11], bladder cancer [12,13], oral squamous cancer [14], esophageal squamous cancer [15,16], papillary carcinoma of the thyroid [17], lung cancer [18-20], pancreatic cancer [21,22], ovarian cancer [23], and some types of breast cancer [24].

The molecular mechanism(s) that underlie the role of increased cav-1 expression in promoting prostate cancer cell progression are unclear. However, we have recently shown that cav-1 protein binds to and inhibits the activities of PP1/PP2A serine/threonine phosphatases, preventing inactivation of Akt through dephosphorylation and thus sustaining levels of phospho-Akt and its activity in procancer cells survival [25,26]. We have also demonstrated that metastatic prostate cancer cells secrete biologically active cav-1 in a steroid-regulated fashion [27]. Using an in vivo mouse prostate cancer model, we showed that antibody to cav-1 protein may inhibit prostate cancer metastasis, whereas cav-1 derived from cancer cells may function as a paracrine/endocrine factor [27]. This clearly indicates that the function of cav-1 in prostate cancer progression/metastasis may involve a complex series of cell/cell interactions, some with cancer cells exclusively, some with stromal cells, and others with vascular endothelial cell (EC).

Accumulating evidence suggests that cav-1 can regulate the growth, differentiation, and functional activities of vascular EC [28-30]. In cultured human EC, cav-1 up-regulation enhances EC tubule formation [31] and stimulates the migration of cultured human EC [32]. In an experimental tumor model based on a melanoma cell line, B16-F10, angiogenesis is impaired in *cav-1*$^{-/-}$ compared to *cav-1*$^{+/+}$ mice, indicating a critical role for this regulatory protein in tumor angiogenesis [33].

We therefore analyzed the role of cav-1 expression in angiogenesis in human prostate cancer specimens with close attention to the potential interaction between cancer cells and tumor-associated EC (TAEC). Using a dual immunofluorescent technique that detects colocalization of cav-1 protein and CD34 antigen, an EC marker [34], in situ, we compared measurements of cav-1expression in prostate cancer cells with tumor microvessel densities (MVDs) or cav-1 positivity in TAEC. Results indicate an important role for prostate cancer cell-derived cav-1 in tumor angiogenesis and thus in the promotion of tumor progression/metastasis.

2. Materials and methods

2.1. Patients and tissue processing

For this study, prostate cancer specimens were obtained from Baylor College of Medicine Prostate Cancer Specialized Programs of Research Excellence Tissue Core, and collected from fresh radical prostatectomy specimens after informed consent was obtained under an institutional review board-approved protocol. Fifty-six specimens derived from a patient cohort (n = 189) that had been previously selected in a consecutive manner by an independent statistician and had been characterized for cav-1 expression using ABC immunostaining as described [8] were included in this study. All patients had undergone radical prostatectomy for moderate to poorly differentiated prostate adenocarcinoma (Gleason score, 5-9) that was clinically localized to the prostate (cT1/T2, NX, M0) as determined by physical examination and transrectal ultrasound imaging in each case. The dominant focus of tumor cells within the radical prostatectomy specimen was representative of the overall grade ascribed to that tumor using the method of Gleason. The 56 specimens, based on cav-1 immunostaining result, were categorized into the following 2 groups: those with (n = 25) or without (n = 31) cav-1-positive cancer cells. Eight benign prostate specimens from cystoprostatectomies were used as controls.

2.2. Immunohistochemistry

Double immunofluorecence staining was performed on formalin-fixed, paraffin-embedded, 5-μm sections derived from punch biopsies of archived blocks of prostate tumor specimens. The rabbit polyclonal anti-cav-1 antibody (Santa Cruz Biotechnology Inc, Santa Cruz, CA) and mouse monoclonal anti-CD34 antibody (QBEnd/10; Neo-Markers, Fremont, CA) were used to identify cav-1 protein accumulation in vascular EC. Briefly, after tissue sections were deparaffinized and rehydrated through graded alcohol, they were heated in 0.01 mol/L citrate buffer at pH 6.0 by microwave for 10 minutes to enhance antigen retrieval. After a 20-minute blocking step with 3% normal horse or goat serum, the sections were sequentially incubated with cav-1 antibody diluted 1:200 for 90 minutes, and then in biotinylated antirabbit IgG and in streptavidin-FITC for 30 minutes each. The sections were reblocked in 1.5% normal horse serum for 20 minutes and incubated in CD34 antibody diluted 1:80, followed by incubation in Cy-3 conjugated antimouse IgG. Positive and negative controls were included in each experiment. The specificity of immunoreactions was verified by replacing the primary antibodies with phosphate-buffered saline or with normal rabbit or mouse serum. In addition, double labeling with cav-1 and PCNA (DaKo, Glostrup, Denmark), or cav-1 and vascular endothelial growth factor

receptor 2 (VEGFR2) (Santa Cruz Biotechnology Inc) as well as VEGFR2 and factor VIII (Dako) antibodies were performed by using similar protocols on some specimens. The labeled specimens were evaluated with a Zeiss fluorescent microscope (Carl Zeiss Inc, Jena, Germany) equipped with a video camera that captured and digitized the images from each fluorophore (red for CD34 and green for cav-1). Each complete section was viewed systematically field-by-field over the entire cancer area, with each measured field corresponding to a real tissue area of 0.0625 mm^2. The densities of microvessels labeled by CD34 and the percentages of the cav-1-negative microvessels were measured on individually acquired images for each fluorophore and on superimposed images of both fluorophores with the aid of OPTIMAS (6.0) software. The percentage of cav-1-positive microvessels was calculated by the formula, 100 × (total number of CD34-positive vessels − cav-1-negative vessels) / total number of CD34-positive vessels. The percentage of VEGFR2-positive microvessels was also measured by using a similar procedure.

2.3. Statistical methods

Mann-Whitney rank analysis was used to compare MVD values, the percentages of cav-1-positive microvessels, and the percentages of VEGFR2-positive microvessels. Wilcoxon signed-rank test was used to analyze paired comparisons of cav-1 positivity in the TAEC of cav-1-positive versus cav-1-negative tumor regions. A *t* test for independent samples and Mann-Whitney rank test were used to compare covariates distributions between groups. Logistic regression analysis was used to verify the significance of the observed differences among covariates. *P* values of less than .05 were considered statistically significant. All analyses were performed with the SPSS 12.0 software package (SPSS Inc, Chicago, IL).

3. Results

Immunohistochemical analyses were conducted on the adjacent sections of a subset of prostate cancer specimens that had been analyzed for cav-1 expression and in which positive correlations between cancer cell cav-1 expression and adverse clinicopathologic features, as well as a poor clinical outcome, had been found [8]. The specimens were then stratified as cav-1-positive (n = 25) or cav-1-negative (n = 31) based on the detection of cav-1 expression in cancer cells by the ABC immunohistochemical analysis with confirmation by immunofluorescence staining (100% concurrence between the 2 procedures). The 2 groups of patients represented by the stratified specimens were comparable in age, pathologic and clinical staging, and Gleason score. CD34 antigen and cav-1 were expressed simultaneously in the vascular EC of these specimens; hence, specific expression of cav-1 in EC could be recognized on the superimposed images derived from dual labeling (Fig. 1). The specificity of each antibody reaction was confirmed by the loss of staining after the primary antibody was replaced with nonspecific IgG or phosphate-buffered saline (data not shown).

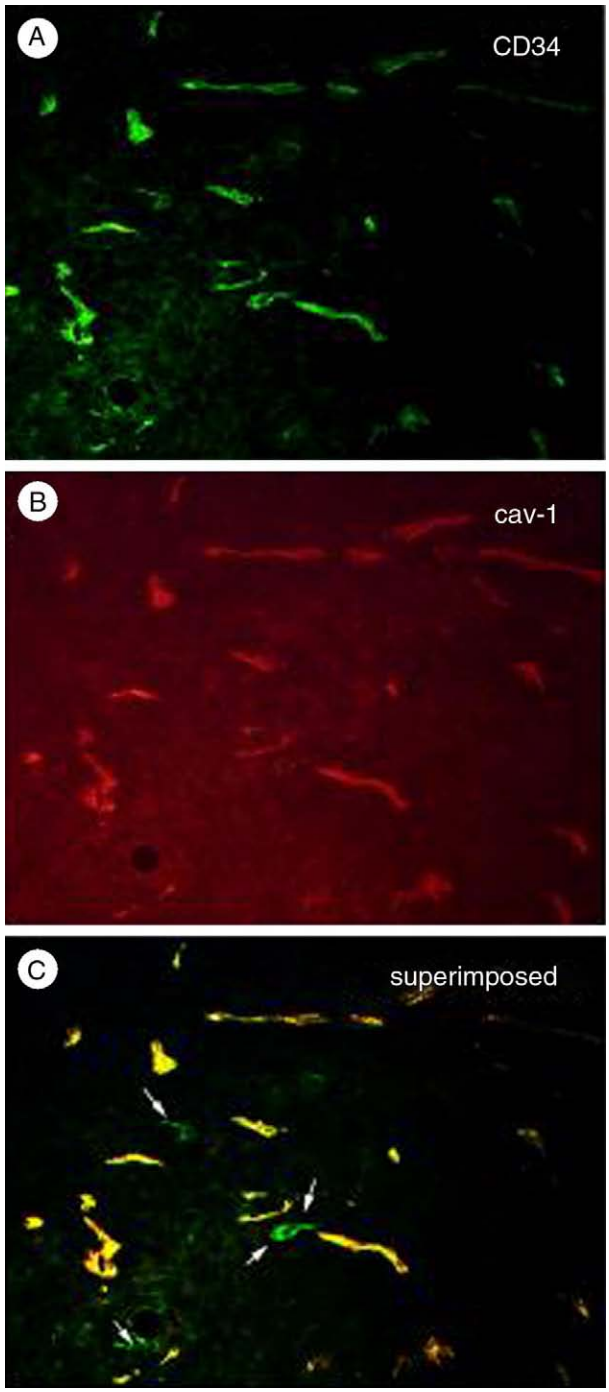

Fig. 1 Analysis of cav-1 positivity in human prostate cancer specimens using cav-1 and CD34 double immunofluorescence labeling. A, $CD34^+$ cells; B, $cav\text{-}1^+$ cells; C, superimposed $CD34^+$ and $cav\text{-}1^+$ cells (arrows indicate cav-1-negative EC).

3.1. Higher MVDs in cav-1-positive tumors

Microvessels labeled with CD34 antibody were quantified within systemically sampled regions of prostate tumor specimens. The MVDs were first assessed according to the cav-1 status of the samples. The MVD value for all cav-1-positive tumors was significantly higher than that for the cav-1-negative tumors (median density, 44 versus 25 microvessels/field; $P = .0140$) (Fig. 2). This difference remained significant ($P = .038$) after adjusting for patients' ages, clinicopathologic tumor stage, and total Gleason score (data not shown).

3.2. Cav-1-positive tumors demonstrate a higher percentage of cav-1-positive microvessels

Most CD34-positive microvessels (>90%) were positively labeled by the cav-1 antibody (Fig. 1A, B); however, a small fraction of the EC aggregates lacked detectable cav-1 protein by immunohistochemistry (Fig. 1C) and tended to form smaller microvessel fragments or to extend via single cell "sprouts" (arrows in Fig. 1C). To calculate the percentage of cav-1-positive microvessels, we used the formula: 100 × (total number of CD34-positive vessels − cav-1-negative, CD-34-positive vessels) / total number of CD34-positive vessels. Thus, the median proportion of cav-1-positive blood vessels in benign prostate specimens was 98.61% (range, 93.19%-100%), compared with 94.41% (range 71.32%-98.76%) in the tumor specimens ($P = .0012$, Fig. 3). After stratification of the samples into cav-1-positive and cav-1-negative groups (n = 25 and 31, respectively), a significantly higher percentage of cav-1-positive microvessels (median, 95.78%; range, 80%-98.76%) was found in cav-1-positive compared with cav-1-negative specimens (median, 92.65%; range71.32%-97.32%) ($P = .0024$; Fig. 4). This difference remained significant ($P = .0280$) after adjustment for patients' ages, clinicopathologic tumor stage, and total Gleason score. Moreover, both the cav-1-negative and the cav-1-positive tumors had a significantly lower percentage of cav-1-positive vessels than the benign prostates specimens ($P = .0004$ or $P = .0148$, respectively) (Fig. 4).

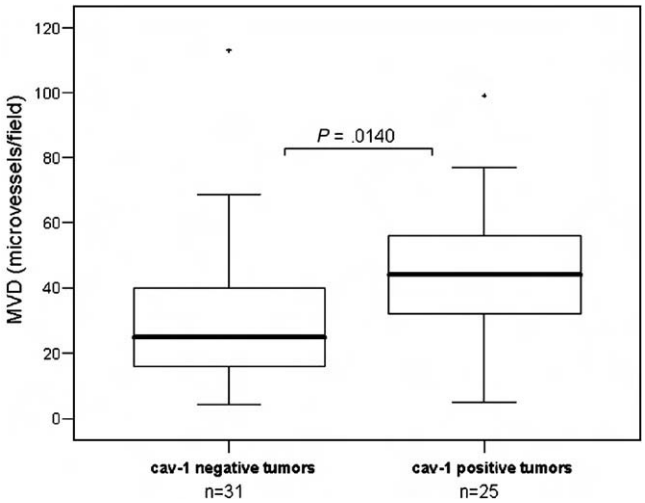

Fig. 2 Comparisons of MVDs between cav-1^+ and cav-1^- tumor specimens as demonstrated by box plots. Top and bottom lines of each box denote 75th and 25 percentile values, whereas the middle line shows the median value. Vertical bars extend to 90th and 10th percentiles, outliers are indicated by crosses.

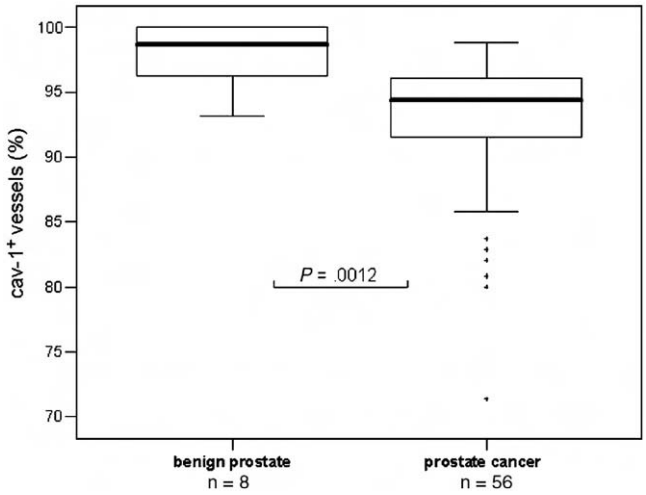

Fig. 3 Cav-1 positivity in vascular EC of benign prostate specimens (n = 8) was compared with that of prostate cancer specimens in box plots. Top and bottom lines of each box denote 75th and 25 percentile values, whereas the middle line shows the median value. Vertical bars extend to 90th and 10th percentiles, outliers are indicated by crosses.

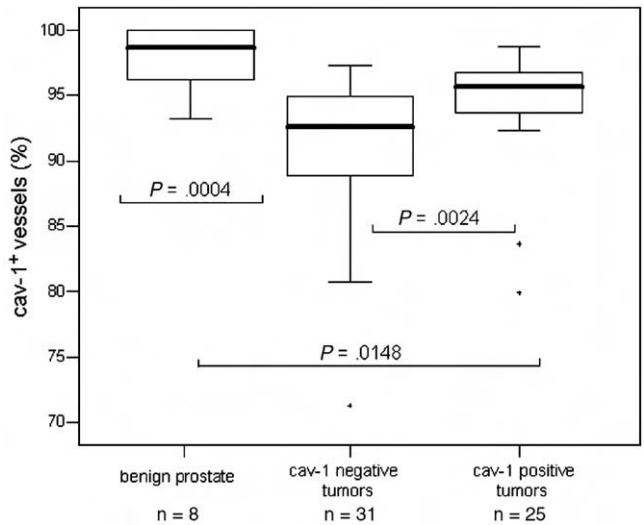

Fig. 4 Comparison of the percentages of cav-1^+ blood vessels between cav-1^+ and cav-1^- tumor specimens as well as benign prostate tissues. In the box plots, top and bottom lines of each box denote 75th and 25 percentile values, whereas the middle line shows the median value. Vertical bars extend to 90th and 10th percentiles, outliers are indicated by crosses.

3.3. Increased percentage of cav-1-positive microvessels surrounding cav-1-positive cancer cells

To further analyze the effect of prostate cancer cell-associated cav-1 expression on angiogenesis, we examined cav-1 positivity in EC within regions of cav-1-positive tumors containing cav-1-positive cancer cells versus that in regions lacking such cells. Results (Fig. 5) showed a higher percentage of cav-1-positive microvessels within cav-1-positive regions (median, 96.30%; range, 79.75%-100%) than in regions comprising cav-1-negative tumor cells (median, 93.55%; range, 72.45%-98.76%) (P = .0102). Further comparison showed that the percentage of cav-1-positive microvessels in tumor regions positive for cav-1 was also significantly higher than in cav-1-negative tumors (P = .0086; Fig. 5).

3.4. Similar proliferative rates in cav-1-positive and cav-1-negative TAEC

The possibility that differences in cav-1 expression in TAEC might be related to cell proliferative rate led us to double-label 12 cav-1-negative tumors with cav-1 and PCNA antibodies and the nuclear dye DAPI to measure proliferative index. The median PCNA labeling index was 0.26 (range, 0.14 -1.27) for cav-1-negative TAEC and 0.40 (range, 0-2.45) for cav-1-positive TAEC (P = .51), suggesting that our cav-1 findings were not significantly influenced by the EC proliferative rate.

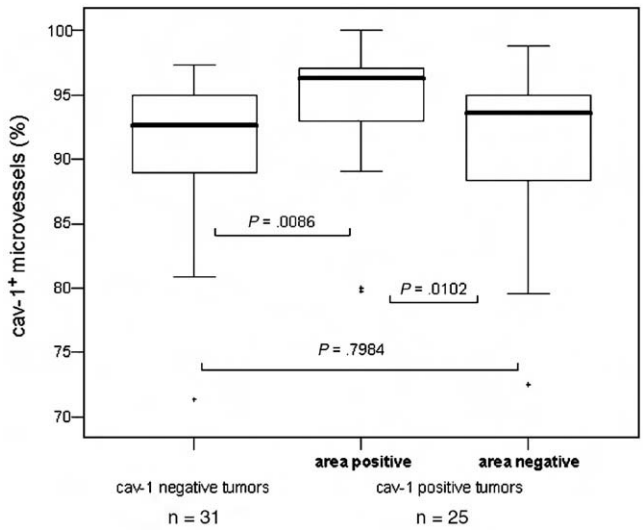

Fig. 5 Comparisons of microvessel cav-1 positivity within cav-1^+ tumor specimens (areas with cav-1^- versus cav-1^+ cancer cells) and between areas with cav-1^- or cav-1^+ cancer cells in cav-1^+ tumor species with cav-1^- cancer specimens. Top and bottom lines of each box denote 75th and 25 percentile values, whereas the middle line shows the median value. Vertical bars extend to 90th and 10th percentiles, outliers are indicated by crosses.

3.5. Higher percentage of VEGFR2-positive microvessels is associated with cav-1-positive tumors

To explore a possible mechanism for the cav-1 effect on angiogenesis, VEGFR2 expression was analyzed on prostate cancer samples double-labeled with VEGFR2 and cav-1 or factor VIII antibodies. We demonstrated that VEGFR2 was present in both prostate cancer cells and some TAEC, and that VEGFR2 tended to be colocalized with cav-1 in TAEC (Fig. 6A). Quantitative analysis indicated that the percentage of microvessels containing VEGFR2-positive TAEC was significantly higher in the cav-1-positive than the cav-1-negative tumors (P = .002, Fig. 6B).

4. Discussion

In a previous study we demonstrated that cav-1 is overexpressed in focal clusters of prostate cancer cells in approximately 30% human prostate cancers, and that the presence of cav-1-positive tumor cells is associated with a poor survival [8]. The relationship of cav-1 overexpression in cancer cells to cancer progression/metastasis has been suggested to involve multiple mechanisms, including the promotion of cancer cells survival [35] and migration [18]. The quantitative immunohistochemical analyses reported here demonstrate a positive correlation of cav-1 expression in prostate cancer cells with MVD, suggesting that cav-1 may play a proangiogenic role in human prostate cancer. In experimental cancer models, cav-1 has been suggested both as an antiangiogenic [36] and as a proangiogenic factor [33], depending on the model system used. Most in vitro studies, however, have shown that cav-1 can exert direct effects on cultured human EC, regulate EC growth and differentiation [28,29], and stimulate capillary tubule formation and EC migration [30,31]. Positive association of cav-1 levels and MVDs has been reported in clear cell renal carcinoma [11]. Consistent with these data, our findings support a proangiogenic role for cav-1 in human prostate cancer. Because increased angiogenesis has been implicated in the development of prostate cancer progression [37], we suggest that the proangiogenic activity of cav-1 may, in part, underlie prostate cancer progression/metastasis.

Our dual labeling technique enabled specific analysis of cav-1 expression in TAEC. By using this technique, we demonstrate that vascular EC in healthy prostate specimens almost invariably express high levels of cav-1 protein. In prostate cancer specimens, however, a small but increased percentage of TAEC does not express cav-1 at a level detectable by immunohistochemical staining. Consequently, the percentage of the cav-1-positive TAEC was significantly lower in malignant as compared with benign prostate specimens. This finding agrees with a recent study

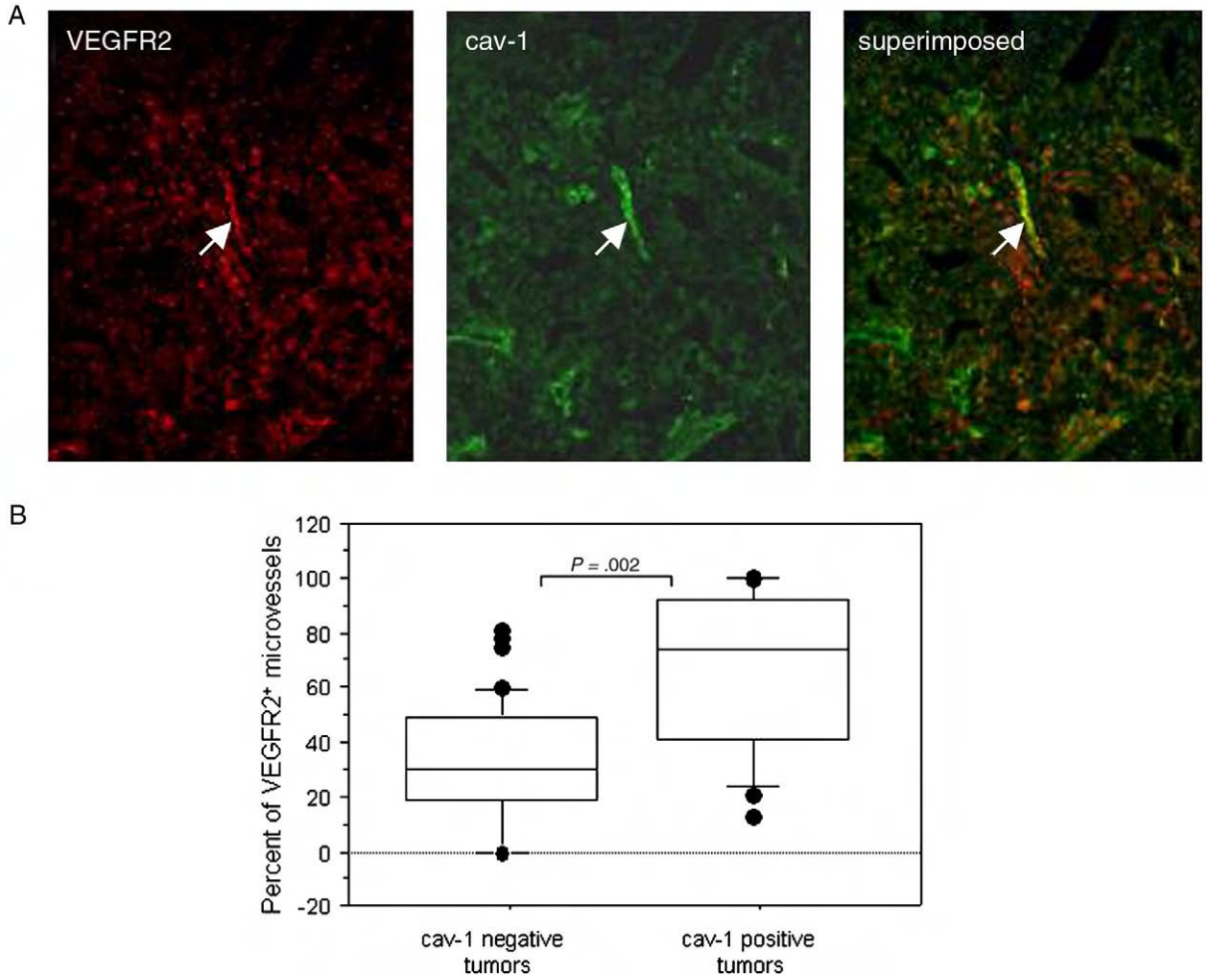

Fig. 6 A, Double immunofluorescence of VEGFR2 and cav-1 expression in a cav-1-positive cancer specimen showed VEGFR2 was present in some EC (indicated by arrows) in addition to cancer cells. The VEGFR2 (red) immunoreactivity was colocalized with cav-1 immunoreactivity (green) in these cells (see merged image). B, Comparisons in the percentages of VEGFR2-positive microvessels between cav-1-positive and cav-1-negative tumor specimens.

demonstrating a tumor-associated cav-1 deficiency in liver EC [38].

Although they account for only a small fraction of the vasculature of a prostate cancer, the cav-1-negative microvessels might represent the most functionally active tumor vasculature. Validation of this hypothesis will require additional studies. However, this concept is supported by the observation that the intratumoral cav-1-negative microvessels often appear as single cell "sprouts," suggesting that these formations are new microvessels. Notably, cav-1 deficiency in some TAEC does not appear to be directly related to EC proliferation, as the proliferative activity of these cells (as indicated by PCNA labeling), was not significantly different from that of cav-1-positive EC. The factors leading to cav-1 reduction in some TAEC remain to be identified. They may involve molecular events associated with EC sprouting/migration in response to certain proangiogenic growth factors (Fig. 7), such as VEGFs, which is known to be produced by prostate cancer cells and has been reported to inhibit cav-1 expression in cultured human EC [32].

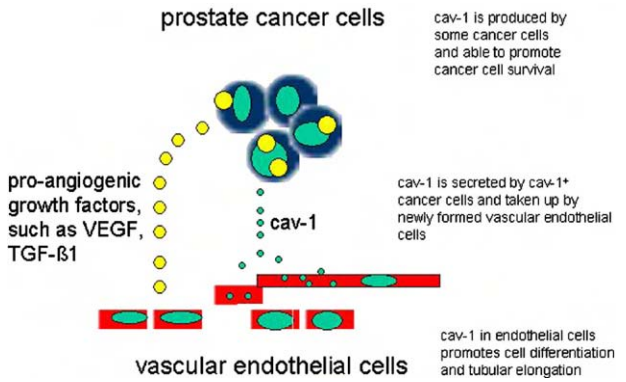

Fig. 7 Schematic layout of the possible mechanisms for cav-1-mediated interaction between cancer cells and adjacent vascular EC. Cav-1 is overexpressed in some prostate cancer cells and may be secreted into their microenvironment. In collaboration with other angiogenic growth factors (such as VEGF, transforming growth factor-β1, etc) also secreted by cancer cells, cav-1 is taken up by newly formed vascular EC that otherwise have very low levels of cav-1. The tumor cells associated cav-1 may thus regulate the formation, differentiation, and extension of the new microvessels.

Another important finding of this study is the association of cav-1 expression in cancer cells with cav-1 positivity in TAEC. In cav-1-positive tumors, there were fewer cav-1-negative TAEC than in the cav-1-negative tumors. Moreover, within the cav-1-positive tumors, TAEC in the regions containing cav-1-positive tumor cells have higher levels of cav-1 than TAEC in regions where cancer cells lacked cav-1 expression. We previously demonstrated that prostate cancer cells can secrete cav-1 and that the secreted protein can promote prostate cancer cell viability and clonal growth under serum-free conditions by inhibiting apoptosis in prostate cancer cells [27]. This activity is similar to that elicited by enforced expression of cav-1 within cells [25,26]. Interestingly, we also detected higher levels of cav-1 in the sera of patients with prostate cancer than in the sera of healthy controls or men with benign prostatic hyperplasia [39], another line of evidence that cancer cells secrete cav-1 into their microenvironment and blood circulation. More recently, we showed that recombinant cav-1 protein is taken up by mouse EC lacking the *cav-1* gene, and that cav-1 protein uptake may enhance the migration of EC (Tahir et al, unpublished results). Thus, the reduction of cav-1-negative TAEC surrounding cav-1-positive cancer cells is likely due, in part, to EC uptake of cav-1 protein secreted by cancer cells into the microenvironment or general circulation (Fig. 7). Thus, cancer cell–derived cav-1 may affect cav-1 levels in TAEC. Through the provision of cav-1 to the small fraction of highly active TAEC that are cav-1 deficient, the cav-1-positive tumors may have an advantage over their cav-1-negative counterparts in facilitating some aspects of tumor associated angiogenesis, and thereby, tumor progression/metastasis.

The molecular mechanism for the cav-1 effect in promoting angiogenesis remains to be investigated. It has been reported that VEGFR2 is a critical mediator of VEGF [40] one of the most potent proangiogenic growth factors in many types of cancer including prostate cancer [41,42]. The stimulation of VEGFR2 by tumor-derived VEGF represents a key event in the initiation of tumor-associated angiogenesis and VEGFR2 is localized in endothelial caveolae and associated with cav-1 [43]. To test for a possible role of VEGFR2 in cav-1-mediated angiogenesis, we analyzed VEGFR2/cav-1 coexpression in prostate cancer specimens by using double antibody labeling techniques. Our data show that VEGFR2 is colocalized with cav-1 protein in TAEC. We further demonstrated that there is a significantly higher percentage of VEGFR2-positive microvessels in the cav-1-positive tumors than in cav-1-negative tumors (Fig. 6). These results suggest that cav-1 may promote angiogenesis via interaction with VEGFR2. It has been reported that cav-1 interacts with VEGFR2 in endothelial caveolae and plays multiple roles in the VEGF-induced signaling cascade [43]. A further study of cav-1 interaction with the VEGF signaling pathway in prostate cancer is warranted.

The findings reported here suggest an important biologic mechanism through which cav-1 promotes prostate cancer progression. The use of our results for clinical application will require additional studies.

References

[1] Thompson TC. Metastasis-related genes in prostate cancer: the role of caveolin-1. Cancer Metastasis Rev 1998;17:439-42.

[2] Williams TM, Lisanti MP. The caveolin genes: from cell biology to medicine. Ann Med 2004;36:584-95.

[3] Galbiati F, Volonte D, Engelman JA, et al. Targeted downregulation of caveolin-1 is sufficient to drive cell transformation and hyperactivate the p42/44 MAP kinase cascade. EMBO J 1998;17:6633-48.

[4] Engelman JA, Zhang XL, Lisanti MP. Genes encoding human caveolin-1 and -2 are co-localized to the D7S522 locus (7q31.1), a known fragile site (FRA7G) that is frequently deleted in human cancers. FEBS Lett 1998;436:403-10.

[5] Yang G, Truong LD, Timme TL, et al. Elevated expression of caveolin is associated with prostate and breast cancer. Clin Cancer Res 1998;4: 1873-80.

[6] Satoh T, Yang G, Egawa S, et al. Caveolin-1 expression is a predictor of recurrence-free survival in pT2N0 prostate carcinoma diagnosed in Japanese patients. Cancer 2003;97:1225-33.

[7] Nasu Y, Timme TL, Yang G, et al. Suppression of caveolin expression induces androgen sensitivity in metastatic androgen-insensitive mouse prostate cancer cells. Nat Med 1998;4:1062-4.

[8] Yang G, Truong LD, Wheeler TM, Thompson TC. Caveolin-1 expression in clinically confined human prostate cancer: a novel prognostic marker. Cancer Res 1999;59:5719-23.

[9] Patlolla JM, Swamy MV, Raju J, Rao CV. Overexpression of caveolin-1 in experimental colon adenocarcinomas and human colon cancer cell lines. Oncol Rep 2004;11:957-63.

[10] Horiguchi A, Asano T, Asakuma J, Asano T, Sumitomo M, Hayakawa M. Impact of caveolin-1 expression on clinicopathological parameters in renal cell carcinoma. J Urol 2004;172:718-22.

[11] Joo HJ, Oh DK, Kim YS, Lee KB, Kim SJ. Increased expression of caveolin-1 and microvessel density correlates with metastasis and poor prognosis in clear cell renal cell carcinoma. BJU Int 2004;93:291-6.

[12] Rajjayabun PH, Garg S, Durkan GC, Charlton R, Robinson MC, Mellon JK. Caveolin-1 expression is associated with high-grade bladder cancer. Urology 2001;58:811-4.

[13] Sanchez-Carbayo M, Socci ND, Charytonowicz E, et al. Molecular profiling of bladder cancer using cDNA microarrays: defining histogenesis and biological phenotypes. Cancer Res 2002;62: 6973-80.

[14] Hung KF, Lin SC, Liu CJ, Chang CS, Chang KW, Kao SY. The biphasic differential expression of the cellular membrane protein, caveolin-1, in oral carcinogenesis. J Oral Pathol Med 2003;32:461-7.

[15] Hu YC, Lam KY, Law S, Wong J, Srivastava G. Profiling of differentially expressed cancer-related genes in esophageal squamous cell carcinoma (ESCC) using human cancer cDNA arrays: over-expression of oncogene MET correlates with tumor differentiation in ESCC. Clin Cancer Res 2001;7:3519-25.

[16] Kato K, Hida Y, Miyamoto M, et al. Overexpression of caveolin-1 in esophageal squamous cell carcinoma correlates with lymph node metastasis and pathologic stage. Cancer 2002;94:929-33.

[17] Ito Y, Yoshida H, Nakano K, et al. Caveolin-1 overexpression is an early event in the progression of papillary carcinoma of the thyroid. Br J Cancer 2002;86:912-6.

[18] Ho CC, Huang PH, Huang HY, Chen YH, Yang PC, Hsu SM. Up-regulated caveolin-1 accentuates the metastasis capability of lung adenocarcinoma by inducing filopodia formation. Am J Pathol 2002;161:1647-56.

[19] Yoo SH, Park YS, Kim HR, et al. Expression of caveolin-1 is associated with poor prognosis of patients with squamous cell carcinoma of the lung. Lung Cancer 2003;42:195-202.

[20] Sunaga N, Miyajima K, Suzuki M, et al. Different roles for caveolin-1 in the development of non-small cell lung cancer versus small cell lung cancer. Cancer Res 2004;64:4277-85.

[21] Suzuoki M, Miyamoto M, Kato K, et al. Impact of caveolin-1 expression on prognosis of pancreatic ductal adenocarcinoma. Br J Cancer 2002;87:1140-4.

[22] Terris B, Blaveri E, Crnogorac-Jurcevic T, et al. Characterization of gene expression profiles in intraductal papillary-mucinous tumors of the pancreas. Am J Pathol 2002;160:1745-54.

[23] Davidson B, Goldberg I, Givant-Horwitz V, et al. Caveolin-1 expression in ovarian carcinoma is MDR1 independent. Am J Clin Pathol 2002;117:225-34.

[24] Van den Eynden GG, Van Laere SJ, Van der Auwera I, et al. Overexpression of caveolin-1 and -2 in cell lines and in human samples of inflammatory breast cancer. Breast Cancer Res Treat 2006;95:219-28 [Epub 2005 Oct 22].

[25] Li L, Ren CH, Tahir SA, Ren C, Thompson TC. Caveolin-1 maintains activated Akt in prostate cancer cells through scaffolding domain binding site interactions with and inhibition of serine/threonine protein phosphatases PP1 and PP2A. Mol Cell Biol 2003;23:9389-404.

[26] Li L, Yang G, Ebara S, et al. Caveolin-1 mediates testosterone-stimulated survival/clonal growth and promotes metastatic activities in prostate cancer cells. Cancer Res 2001;61:4386-92.

[27] Tahir SA, Yang G, Ebara S, et al. Secreted caveolin-1 stimulates cell survival/clonal growth and contributes to metastasis in androgen-insensitive prostate cancer. Cancer Res 2001;61:3882-5.

[28] Carver LA, Schnitzer JE. Caveolae: mining little caves for new cancer targets. Nat Rev Cancer 2003;3:571-81.

[29] Massimino ML, Griffoni C, Spisni E, Toni M, Tomasi V. Involvement of caveolae and caveolae-like domains in signalling, cell survival and angiogenesis. Cell Signal 2002;14:93-8.

[30] Frank PG, Woodman SE, Park DS, Lisanti MP. Caveolin, caveolae, and endothelial cell function. Arterioscler Thromb Vasc Biol 2003;23:1161-8 [Epub 2003 Apr 10].

[31] Sonveaux P, Martinive P, DeWever J, et al. Caveolin-1 expression is critical for vascular endothelial growth factor-induced ischemic hindlimb collateralization and nitric oxide-mediated angiogenesis. Circ Res 2004;95:154-61 [Epub 2004 Jun 17].

[32] Liu J, Razani B, Tang S, Terman BI, Ware JA, Lisanti MP. Angiogenesis activators and inhibitors differentially regulate caveolin-1 expression and caveolae formation in vascular endothelial cells. Angiogenesis inhibitors block vascular endothelial growth factor-induced down-regulation of caveolin-1. J Biol Chem 1999;274:15781-5.

[33] Woodman SE, Ashton AW, Schubert W, et al. Caveolin-1 knockout mice show an impaired angiogenic response to exogenous stimuli. Am J Pathol 2003;162:2059-68.

[34] Vermeulen PB, Gasparini G, Fox SB, et al. Second international consensus on the methodology and criteria of evaluation of angiogenesis quantification in solid human tumours. Eur J Cancer 2002;38:1564-79.

[35] Thompson TC, Timme TL, Li L, Goltsov A. Caveolin-1—a metastasis-related gene that promotes cell survival in prostate cancer. Apoptosis 1999;4:233-7.

[36] Lin MI, Yu J, Murata T, Sessa WC. Caveolin-1-deficient mice have increased tumor microvascular permeability, angiogenesis, and growth. Cancer Res 2007;67:2849-56.

[37] Weidner N, Carroll PR, Flax J, Blumenfeld W, Folkman J. Tumor angiogenesis correlates with metastasis in invasive prostate carcinoma. Am J Pathol 1993;143:401-9.

[38] Yerian LM, Anders RA, Tretiakova M, Hart J. Caveolin and thrombospondin expression during hepatocellular carcinogenesis. Am J Surg Pathol 2004;28:357-64.

[39] Tahir SA, Ren C, Timme TL, et al. Development of an immunoassay for serum caveolin-1: a novel biomarker for prostate cancer. Clin Cancer Res 2003;9:3653-9.

[40] Waltenberger J, Claesson-Welsh L, Siegbahn A, Shibuya M, Heldin CH. Different signal transduction properties of KDR and Flt1, two receptors for vascular endothelial growth factor. J Biol Chem 1994;269:26988-95.

[41] Borre M, Nerstrom B, Overgaard J. Association between immunohistochemical expression of vascular endothelial growth factor (VEGF), VEGF-expressing neuroendocrine-differentiated tumor cells, and outcome in prostate cancer patients subjected to watchful waiting. Clin Cancer Res 2000;6:1882-90.

[42] Ferrer FA, Miller LJ, Andrawis RI, et al. Vascular endothelial growth factor (VEGF) expression in human prostate cancer: in situ and in vitro expression of VEGF by human prostate cancer cells. J Urol 1997;157:2329-33.

[43] Labrecque L, Royal I, Surprenant DS, Patterson C, Gingras D, Beliveau R. Regulation of vascular endothelial growth factor receptor-2 activity by caveolin-1 and plasma membrane cholesterol. Mol Biol Cell 2003;14:334-47.

Tumor Cell–Secreted Caveolin-1 Has Proangiogenic Activities in Prostate Cancer

Salahaldin A. Tahir,[1] Guang Yang,[1] Alexei A. Goltsov,[1] Masami Watanabe,[1] Ken-ichi Tabata,[1] Josephine Addai,[1] El Moataz Abdel Fattah,[1] Dov Kadmon,[1] and Timothy C. Thompson[1,2,3]

[1]Scott Department of Urology, Departments of [2]Molecular and Cellular Biology and [3]Radiology, Baylor College of Medicine, Houston, Texas

Abstract

Caveolin, a major structural component of specialized plasma membrane invaginations (caveolae) that participate in diverse cellular activities, has been implicated in the pathogenesis of several human diseases, including cancer. We showed in earlier studies that caveolin-1 (cav-1) is consistently and strongly overexpressed in metastatic prostate cancer and is secreted in a biologically active form by virulent prostate cancer cells. Using both *in vitro* and *in vivo* model systems, we now present evidence supporting a proangiogenic role for cav-1 in prostate cancer development and progression. Recombinant cav-1 (rcav-1) was taken up by cav-1$^{-/-}$ endothelial cells through either a lipid raft/caveolae- or clathrin-dependent mechanism, leading to specific angiogenic activities (tubule formation, cell migration, and nitric oxide production) that were mediated by rcav-1 stimulation of the PI3K-Akt-eNOS signaling module. Pathologic angiogenesis induced by cav-1 in prostate cancer–bearing mice correlated with an increased frequency, number, and size of lung metastases. We propose that in addition to its antiapoptotic role, cav-1 secreted by prostate cancer cells functions critically as a proangiogenic factor in metastatic progression of this tumor. These new insights into cav-1 function in prostate cancer may provide a base for the design of clinically applicable therapeutic strategies. [Cancer Res 2008;68(3):731–9]

Introduction

As essential components of caveolae, caveolin proteins help to generate and maintain these highly ordered structures at the cell surface. They also mediated endocytosis and transcytosis of molecules attached to the cell surface and organize signaling proteins involved in cell proliferation, adhesion, and migration, among numerous other biological processes (1). This functional versatility has focused increasing attention on the possible role of caveolins in cancer development and progression. Findings to date clearly indicate that caveolin-1 (cav-1), the first of several caveolin family members that differ in structure and tissue distribution, can influence both tumorigenesis and metastatic spread in certain types of cancer (2–6), although the mechanisms of these effects are largely unknown. We showed in earlier studies that cav-1 is consistently and strongly overexpressed in metastatic prostate cancer and is secreted in a biologically active form by virulent prostate cancer cells (2, 3, 7). Interestingly, we detected significantly increased serum cav-1 levels in prostate cancer patients compared with control men or men with benign prostatic hyperplasia, and showed that preoperative serum cav-1 is a potential prognostic marker for recurrence in radical prostatectomy cohort (8, 9). The ability of some prostate cancer cells to secrete biologically active cav-1 (7, 8), and the demonstration that loss of cav-1 function in the TRAMP transgenic mouse prostate cancer model results in highly significant reductions of prostate cancer growth and metastasis (10), led us to suspect that tumor cell–secreted cav-1 may function as a paracrine factor during prostate cancer development, possibly as a regulator of pathologic angiogenesis. The studies described here substantiate this role and suggest a paradigm that may be applicable to other tumors that secrete cav-1.

Materials and Methods

Endothelial cell isolation. Endothelial cells from *cav-1*$^{-/-}$ mice (11) were isolated from mouse aorta according to the primary explant procedure and used throughout the study. Briefly, the aorta was removed from the anaesthetized mice, placed in PBS, and carefully cleaned of periadventitial fat and connective tissue. The vessel was then cut into 1-mm pieces, opened longitudinally, and placed with the intima side down on Matrigel-coated (BD Biosciences) 12-well plates in endothelial cell growth medium (EGM; Cambrex) to generate endothelial outgrowth. The aortic pieces were removed after 4 to 7 days, and the cells were allowed to grow to confluence. After recovery with dispase, the cells were plated on a 12-well plate and then subcultured twice. The confluent monolayers showed the typical cobblestone pattern of endothelial cells stained positively for uptake of Dil-Ac-LDL (Biomedical Technologies).

Western blotting. Protein aliquots from cell lysates were separated by 10% or 12% SDS-PAGE and transferred to nitrocellulose membranes. The membranes were probed with antibodies to cav-1 (Santa Cruz Biotechnology), eNOS, Erk1/2, Akt (BD Biosciences), P-Akt, P-eNOS, or P-Erk1/2 (Cell Signaling Technology).

Recombinant cav-1 and Δrecombinant cav-1 purification. phCav-1V5 and phΔcav-1V5His plasmids were constructed as described previously (8), whereas recombinant cav-1 (rcav-1) and Δrcav-1 were purified by our modified procedure. Briefly, transfected 293PE cells were washed with PBS and lysed with 10 mL of ice-cold buffer A [50 mmol/L phosphate buffer, 300 mmol/L NaCl, 10 mmol/L imidazole, and 5 mmol/L mercaptoethanol (pH.8)] containing 0.5% Triton X-100 and 0.7% octylβ-D-glucopyranoside (OGP). The lysate was centrifuged for 15 min at 4°C, 12,000 × *g*, and the supernatant was mixed and incubated with 1 mL of Ni-NTA agarose slurry for 3 h. The resultant mixture was loaded on to a 10 mL polyprep column (Bio-Rad), and the resin was washed with 10 volumes of buffer A containing 500 mmol/L NaCl, 50 mmol/L imidazole, and 0.2% OGP. The bound cav-1-V5-His was eluted with 3 mL of elution buffer (buffer A containing 300 mmol/L imidazole, 300 mmol/L NaCl, and 0.1% OGP). For Western blot analysis, the crude supernatant as well as unbound and eluted fractions were subjected to SDS-PAGE. FITC labeling of recombinant cav-1 proteins was prepared with the EZ-label FITC

Requests for reprints: Timothy C. Thompson, The University of Texas M. D. Anderson Cancer Center, Department of Genitourinary Medical Oncology, Unit 1374, 1515 Holcombe Boulevard, Houston, TX 77030. Phone: 713-792-9955; Fax: 713-792-9956; E-mail: timthomp@mdanderson.org.

doi:10.1158/0008-5472.CAN-07-2668

protein labeling kit (Pierce Biotechnology, Inc.) according to the manufacturer's instructions.

Tubule formation assay. The *in vitro* tubule formation assay was used as described previously (12). Briefly, endothelial cells were incubated in growth factor–reduced Matrigel-coated 24-well plates in 0.5 mL of endothelial basement medium (EBM; Cambrex) in the presence or absence of rcav-1 or Δrcav-1. Images of tubule structures that formed after 18 to 24 h were captured by phase contrast microscopy, and the length of the endothelial network was quantified by image analysis of five low-power fields using free object quantification software (NucleoTech Corp.).

Wound-healing migration assay. Endothelial cells were cultured in 24-well plates to 70% to 80% confluency in EGM, and a straight longitudinal incision was made on the monolayer. After a wash with EBM and incubation with rcav-1 or Δrcav-1 in EBM containing 0.1% bovine serum albumin (BSA) for 4 h followed by an additional 48 h of incubation in EBM containing 2% of fetal bovine serum (FBS), the cells were stained with the Protocol HEMA3 stain set (Biochemical Sciences, Inc.), and the number of cells migrating into the cleared area were counted with a microscope, using advanced colony counting software (NucleoTech Corp.).

Cell proliferation and [^{3}H]-thymidine incorporation. Endothelial cells were seeded into 12-well plates (5×10^4 cells per well) and incubated overnight. After the medium was removed, the cells were treated with rcav-1 in EBM for 4 h and incubated for an additional 48 h in EBM containing 2% FBS, after which they were trypsinized and counted with a coulter counter. For [^{3}H]-thymidine uptake, the endothelial cells were seeded into 96-well plates (2.5×10^3 cells per well) in EGM then treated with rcav-1 and incubated for 48 h in EGM. [^{3}H]-thymidine (5 μCi/mL) was then added, the cells were incubated for 24 h, and the cell lysate-associated radioactivity was counted.

Nitric oxide determination. The basal and rcav-1 stimulated NO derived from endothelial cells that had accumulated in EBM over a 24-h period was measured with the Nitric Oxide Colorimetric Assay (Roche Diagnostics).

PP1 and PP2A activities. Endothelial cells were treated with rcav-1 and incubated in EBM containing 0.1% BSA for 24 h at 37°C and 5.5% CO_2. The cells were lysed with ice-cold phosphatase lysis buffer, and PP1 and PP2A activities were measured after immunoprecipitation as described previously (13).

Animal models. Orthotopic RM-9 tumors were generated by injecting 5×10^3 cells directly into the dorsolateral prostates of *cav-1*$^{+/+}$ or *cav-1*$^{-/-}$ male mice. The resultant tumors were removed at necroscopy on day 21 postinjection, and their wet weight were determined; all tumors were processed for specific immunostaining protocols (see below).

To generate the LNCaP cav-1 tet-on system, we transfected *cav-1*$^{-/-}$ low passage (LP)-LNCaP cells with pTetOn vector (Clontech), isolated stable G418-resistant clones, and screened them in a transient trasfection reporter assay with pTRE2Luc vector according to the manufacturer's protocol with or without 1 μg/mL doxycycline. Clone LNT36, which had the highest induction level, was chosen for the second cotransfection, in which a pTRECav-1 vector containing full-length human *cav-1* cDNA and the pBabeHygro plasmid were used. Double stable G418- and hygromycin-resistant clones were isolated and tested for cav-1 induction in response to the doxycycline (1.0 μg/mL). Clone LNTB25cav, which showed strong induction of cav-1 after addition of doxycycline to the medium and the lowest endogenous expression in the absence of the drug *in vitro*, was used for further *in vivo* studies.

To establish xenografts, we inoculated male nude mice with LNTB25cav cells that were suspended in Matrigel matrix and injected s.c. Tumors were present 21 days after inoculation, and tumor-bearing mice were divided into two groups that were normalized for tumor size. One group was treated with drinking water containing doxycycline (2 mg/mL) and 5% sucrose, whereas the other (control group) was treated with drinking water containing only 5% sucrose. After 21 days, the animals were sacrificed, and the tumor tissues were harvested and either snap frozen in liquid nitrogen or fixed in 10% neutral formalin.

For the *in vivo* metastasis assay, 1×10^6 LNTB25cav cells were injected into the tail veins of male nude mice to establish experimental metastases. Two months after the initial injection, the mice were divided into two groups: one was treated with drinking water containing doxycycline (2 mg/mL) and 5% sucrose and the other (control group) with drinking water containing only 5% sucrose. After a 42-day treatment, the animals were sacrificed and lung tissue was collected, fixed, and analyzed for tumor foci.

Immunohistochemistry and deconvolution microscopy. Depending on the fluorescent protein treatment, LNCaP, PC-3, and TSU-Pr1 tumor cells or endothelial cells were placed on glass coverslips in 24-well plates and incubated overnight in RPMI 1640 or EGM, respectively. After removal of the medium, the cells were washed twice with PBS buffer, then FITC-rcav-1, FITC-Δrcav-1, Alexa fluor 594–labeled cholera toxin B, and transferrin (Invitrogen) were added to medium that contained 0.1% BSA. The cells were incubated for 5 h, rinsed twice with PBS buffer, and fixed in 4% formaldehyde for 5 min at room temperature.

For immunostaining, fixed cells were permeabilized for 5 min with 0.1% Triton X-100 in PBS buffer and blocked with 3% normal horse or goat serum. They were then incubated with primary antibody followed by biotinylated anti-rabbit IgG (Vector Labs) and rhodamine-conjugated streptavidin or FITC-streptavidin (Jackson Immuno Research). Reactions were evaluated with the Delta Vision Deconvolution Microscopy System (Applied Precision, Inc.), in which a Z-series of optical sections (0.15-μm steps) were digitally imaged and deconvolved with the Delta Vision–constrained iterative algorithm to generate high-resolution images.

Mouse model–derived tumor specimens were stained for CD31 (BD Biosciences) using the avidin-biotin-peroxidase complex technique (ABC kit; Vector Lab) as previously described (14). Quantitative analysis of microvessel density was performed on the stained sections. The vascular "hot region" was first identified by low-power screening (magnification, ×40). Vascular counting was then performed on at least five 200× measuring fields (each with a real area of 0.198 mm^2). For each sample, the highest count per field was used.

Dual-immunofluorescence staining was also performed on these tissues. Briefly, after tissue sections were deparaffinized and rehydrated through graded alcohol, they were heated in 0.01 mol/L citrate buffer at pH 6.0 by microwave for 10 min to enhance antigen retrieval. After a 20-min blocking step with 1.5% normal goat serum, the sections were sequentially incubated with polyclonal cav-1 antibody diluted 1:200 for 90 min, followed by biotinylated anti-rabbit IgG and streptavidin-FITC for 30 min each. The sections were rinsed and reblocked in 1.5% normal horse serum for 20 min and incubated in CD31 rat monoclonal antibody followed by Cy-3–conjugated anti-rat IgG for 30 min. The specificity of immunoreactions was verified by replacing the primary antibodies with PBS or with corresponding normal serum. The labeled specimens were evaluated using a Zeiss fluorescence microscope equipped with a video camera (Hamamatsu). Each section was analyzed systematically, field-by-field (300×400 μm^2), over the area of cancer cells. The percentages of cav-1–positive CD31 microvessels were determined for each field for each fluorophore and on superimposed images of both fluorophores with the aid of OPTIMAS (6.0) software.

Statistical analysis. The Mann-Whitney rank test was used to analyze differences in microvessel density within mouse prostate cancer tissues; comparisons of *in vitro* tubule formation, cell migration, phosphatase activity assay, NO release assay, and RM-9 tumor wet weights relied on the unpaired two-sided *t* test. Fisher's exact test was used for the comparison of the metastasis frequency in LNTB25cav-injected mice. All statistical analyses were performed with Statview software (Version 5.0; SAS Institute).

Results

Cav-1 uptake by prostate cancer cells and endothelial cells. We have shown that prostate cancer cells secrete cav-1 possessing antiapoptotic activity that can be suppressed by cav-1–specific antiserum *in vitro* (7). Such antiserum also suppressed metastasis *in vivo*, raising the possibility that secreted cav-1 is taken up by tumor cells or tumor-associated endothelial cells or both. Thus, we treated cav-1–negative LP-LNCaP tumor cells or primary

endothelial cells, isolated from *cav-1*$^{-/-}$ mouse aorta, with conditioned medium collected from cav-1–transfected LP-LNCaP cells or with rcav-1 alone. Western blot analysis showed that cav-1 contained in conditioned medium was taken up by LP-LNCaP cells in a dose- and time-dependent manner, as indicated by the appearance of cav-1 in cell lysates within 1 h and the achievement of maximal intracellular levels 3 h posttreatment (Fig. 1*A*). Rcav-1 protein was also taken up by the LP-LNCaP cells and *cav-1*$^{-/-}$ endothelial cells in a dose-dependent fashion over a 24-h incubation period (Fig. 1*B* and *C*). Rcav-1 uptake by tumor cells (LP-LNCaP, TSU-Pr1, and PC-3) and endothelial cells [human umbilical vascular endothelial cell (HUVEC), and mouse *cav-1*$^{-/-}$ and *cav-1*$^{+/+}$] was further shown by fluorescence and deconvolution microscopy. FITC-rcav-1 uptake by these cells was temperature dependent, with 5 h of incubation at 0°C, abolishing uptake altogether (data not shown). Internalized FITC-rcav-1 was distributed throughout the cytoplasm (Fig. 1*D*).

Lipid raft/caveolae-dependent and clathrin-dependent endocytic pathways are involved in rcav-1 internalization in endothelial cells. To determine the endocytic pathways responsible for rcav-1 internalization, we pretreated HUVEC and *cav-1*$^{+/+}$ or *cav-1*$^{-/-}$ mouse endothelial cells with methyl-β-cyclodextrin (MCD) or chlorpromazine to disrupt the formation of cholesterol-rich raft microdomains or clathrin-coated pits, respectively. Fluorescence microscopy revealed that MCD effectively inhibited FITC-rcav-1 uptake in both types of endothelial cells, whereas chlorpromazine inhibited FITC-rcav-1 uptake effectively in mouse endothelial cells but only marginally in HUVEC (Fig. 2*A*). Under the same conditions, MCD effectively reduced the uptake of cholera toxin B, whereas chlorpromazine reduced the uptake of transferrin substances known to penetrate cells through cholesterol-rich lipid raft and clathrin endocytic pathways, respectively (Fig. 2*B*). These results indicate that internalization of exogenous rcav-1 proceeds through lipid raft/caveolae and clathrin pathways in both HUVEC and mouse endothelial cells, with the former pathway dominant in HUVEC (Fig. 2*A, left*). To directly show that rcav-1 associates with internalized lipid rafts/caveolae to enter endothelial cells, we incubated HUVEC for 5 h with a mixture of FITC-rcav-1 and cholera toxin B and tested for their cellular colocalization. We found that a majority (76%) of the FITC-rcav-1–positive endosomes also contained cholera toxin B (Fig. 2*C*), indicative of a requirement for caveolae and ganglioside G_{M1} lipid rafts in cav-1 penetration of human endothelial cells.

Internalization of rcav-1 is mediated by cav-1 scaffolding domain. Mutagenesis experiments have identified cav-1 scaffolding domain (CSD) residues 82 to 101 as the region responsible for mediating interactions with a number of signaling proteins including the endothelial form of nitric oxide synthase (eNOS), platelet-activating factor receptors, epidermal growth factor, the kinases Src and Fyn, heterotrimeric G protein,

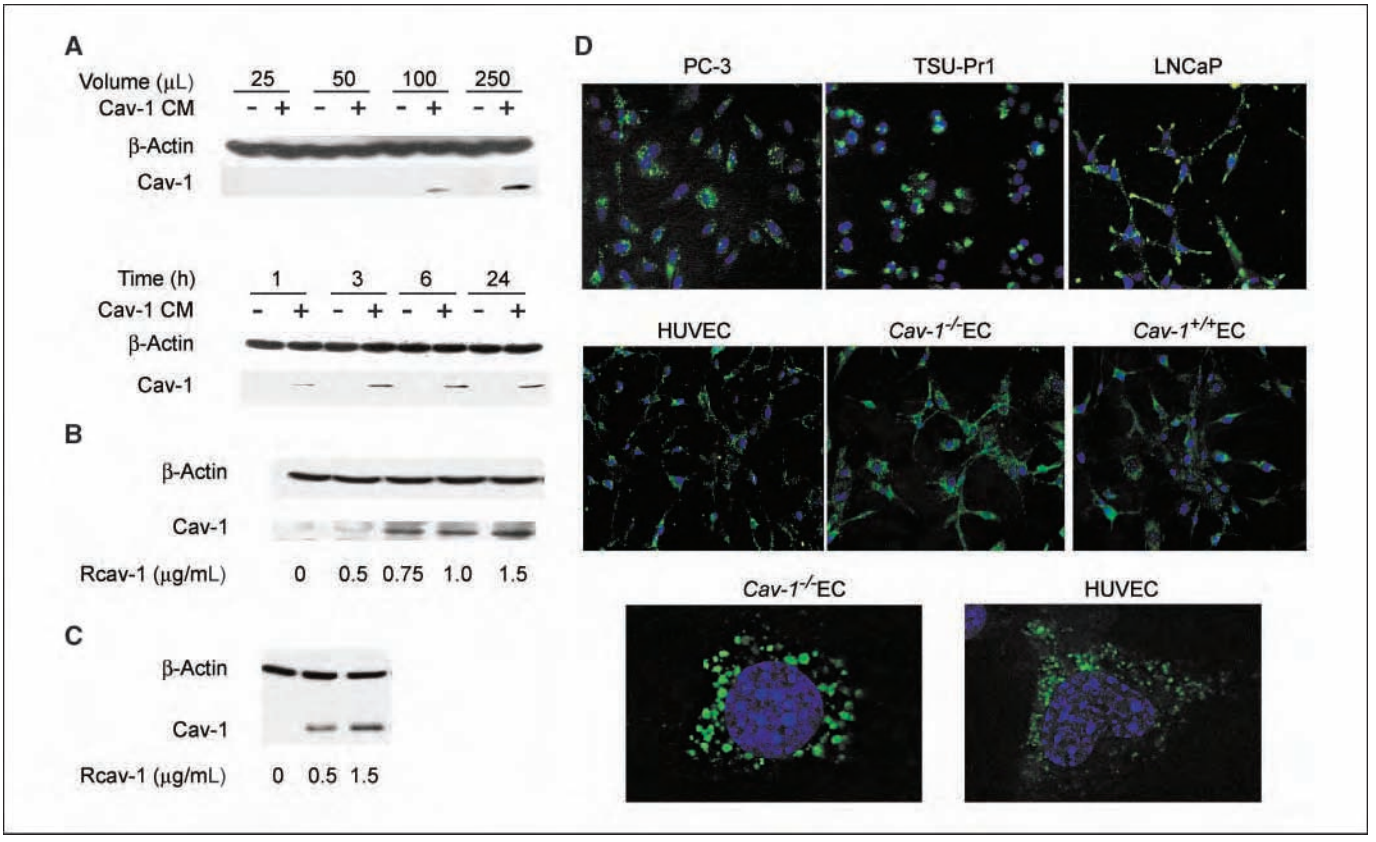

Figure 1. Cav-1 uptake by prostate cancer and bladder cancer cells and endothelial cells. *A,* dose- and time-dependent uptake of cav-1 from *cav-1*–transfected (+) or control-transfected (−) conditioned medium (*CM*) by LP-LNCaP cells. *Top,* detection of cav-1 after a 24-h treatment with conditioned medium over a range of volumes; *bottom,* detection after 1 to 24 h of treatment with 250 μL conditioned medium. *B* and *C,* dose-dependent rcav-1 uptake by LP-LNCaP tumor cells (*B*) and *cav-1*$^{-/-}$ endothelial cells (*EC*; *C*) treated for 24 h. *D,* internalization of FITC-rcav-1 by cancer cells (*top*) and endothelial cells (*middle*) treated with 3.0 μg/mL of FITC-rcav-1 for 5 h. Uptake by endothelial cells (*cav-1*$^{-/-}$ endothelial cells and HUVEC) were imaged by deconvolution microscopy after treatment with FITC-rcav-1 (*bottom*); nuclei were visualized by Hoechst 33342 staining.

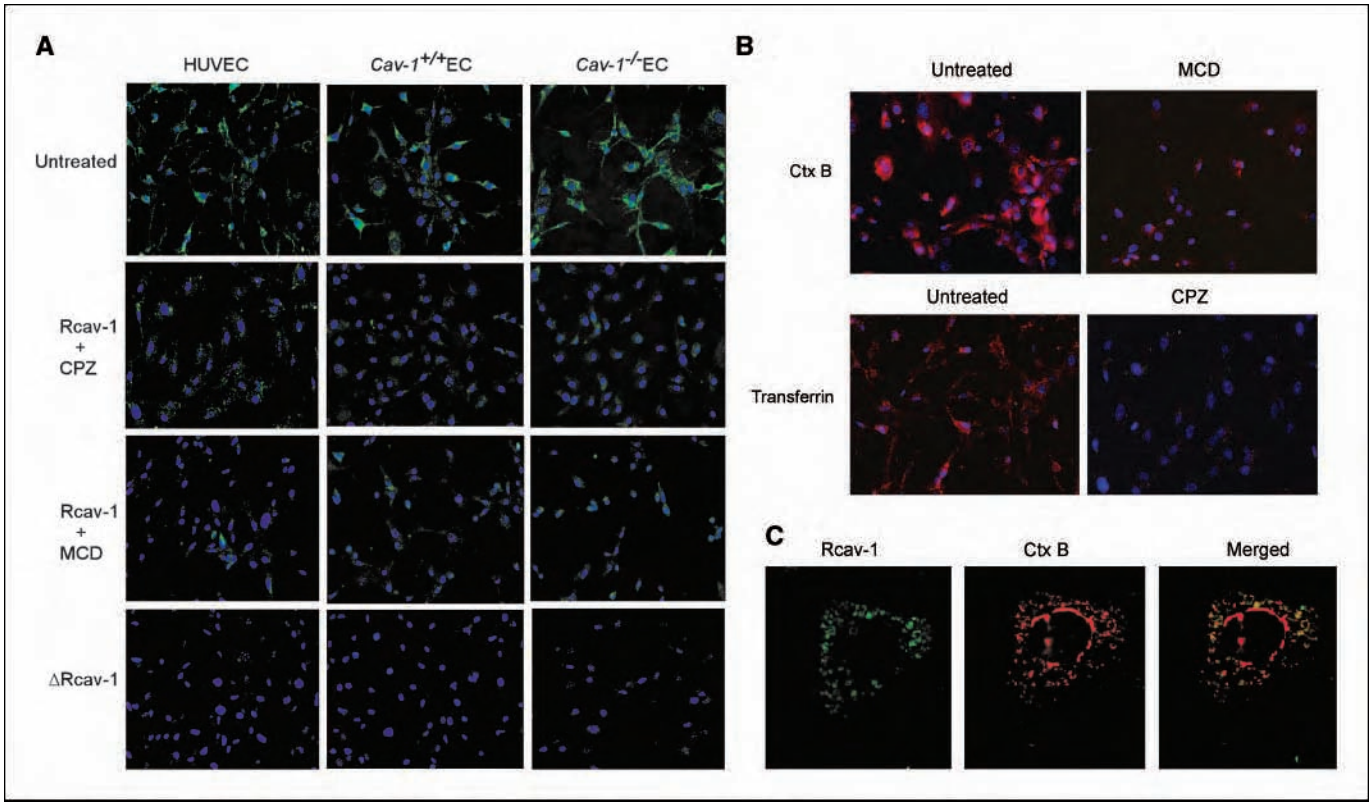

Figure 2. Internalization of rcav-1 by lipid raft/caveolae-dependent and clathrin-dependent endocytic pathways. *A,* cells were incubated with FITC-rcav-1 (3.0 μg/mL) in the presence or absence of 7.5 μg/mL of chlorpromazine (*CPZ*) or 7 mmol/L MCD for 5 h and analyzed by fluorescence microscopy. *B,* cholera toxin B (*Ctx B*) and transferrin internalization are blocked by MCD and chlorpromazine, respectively. HUVEC cells were incubated with Alexa fluor 594–labeled cholera toxin B and transferrin containing the same MCD and chlorpromazine concentrations as in *A* for 5 h and analyzed by fluorescence microscopy. Cholera toxin B internalization was impaired by cholesterol depletion (MCD treatment), whereas transferrin uptake was blocked by disruption of clathrin-coated pits (chlorpromazine treatment). *C,* colocalization of internalized FITC-rcav-1 with cholera toxin B, a ganglioside G_{M1} lipid raft/caveolae marker, as detected by deconvolution microscopy of HUVEC cells after the incubation for 5 h with FITC-rcav-1 and Alexa fluor 594–labeled cholera toxin B; nuclei were visualized by Hoechst 33342 staining.

and cholesterol-binding protein (15). This domain also targets the full-length endogenous cav-1 to lipid rafts/caveolae and cell membranes (16). To determine the role of the CSD in exogenous rcav-1 membrane attachment and cellular uptake, we generated and purified the CSD-deleted rcav-1 protein (Δrcav-1), treated endothelial cells and prostate cancer cells with different concentrations of FITC-Δrcav-1 over 1 to 6 h, and examined the cells for Δrcav-1 uptake using fluorescence microscopy. We did not detect internalized FITC-Δrcav-1 in cells incubated for as long as 6 h at concentrations of the mutant protein ranging to 5.0 μg/mL (Fig. 2*A*). In separate coincubation experiments, we showed uptake of cholera toxin B or transferrin under the same conditions (data not shown). These observations suggest that endocytosis of exogenous rcav-1 protein and its subsequent stimulation of angiogenic activities is mediated, in part, by CSD, which seems critical for cellular internalization of the protein.

Rcav-1 stimulates differentiation and migration of *cav-1*$^{-/-}$ endothelial cells. We initially analyzed the formation of tubules by endothelial cells, isolated from *cav-1*$^{+/+}$ or *cav-1*$^{-/-}$ aorta, on growth factor–reduced Matrigel. Compared with *cav-1*$^{+/+}$ endothelial cells, cells lacking this gene showed significantly reduced tubule formation in the absence of rcav-1 stimulation (Fig. 3*A*; micrographs). However, treatment with rcav-1 stimulated tubule formation in *cav-1*$^{-/-}$ endothelial cells in a dose-dependent manner with a >2-fold increase in tubule length observed with use of 1.5 μg/mL rcav-1 compared with untreated controls (P = 0.021). Importantly, Δrcav-1 at this concentration failed to stimulate tubule formation (Fig. 3*A*). To determine the effects of rcav-1 on *cav-1*$^{-/-}$ endothelial cell migration, we used the *in vitro* wound-healing assay. Rcav-1 treatment stimulated *cav-1*$^{-/-}$ endothelial cell migration in a dose-dependent fashion with a 2-fold increase in the number of migratory cells at a rcav-1 concentration of 1.5 μg/mL (P = 0.019), whereas Δrcav-1 at this concentration failed to increase migration/motility of the endothelial cells (Fig. 3*B*). This enhancement of tubule formation and the number of migratory/motile cells by rcav-1 treatment did not result from increased cell proliferation, as the numbers of cells or levels of thymidine uptake posttreatment were similar to the results for untreated controls (data not shown).

Rcav-1 stimulates the angiogenic activities in *cav-1*$^{-/-}$ endothelial cells through the activation of eNOS. Caveolae and cav-1 play critical roles in ensuring the coupling between vascular endothelial growth factor (VEGF) receptors and downstream mediators of angiogenesis, such as VEGF, which activates Erk and eNOS via the phosphatidylinositol-3-kinase (PI3-K)-Akt signaling pathway (17–19). Thus, to assess the contribution of this signaling module to the angiogenic activities of rcav-1, we tested the effects of inhibitors of PI3 kinase (LY294002), eNOS (L-NAME), and Erk (PD98059) in *cav-1*$^{-/-}$ endothelial cells. Figure 3*C* and *D* shows that both LY294002 and L-NAME, but not PD98059, significantly suppressed rcav-1–stimulated angiogenesis, implicating PI3-K-Akt-eNOS signaling in the pathologic angiogenic effects

of cav-1 in prostate cancer cells. To investigate this possibility further, we measured the levels of accumulated NO (NO_2^- + NO_3^-) at 24 h after rcav-1 treatment of *cav-1*$^{-/-}$ endothelial cells. NO release by these cells was significantly increased by rcav-1 in a dose-dependent manner (P = 0.029 versus untreated control; Fig. 4*A, left*). Analysis of the effects of rcav-1 on the phosphorylation status of Akt and its downstream target protein eNOS in *cav-1*$^{-/-}$ endothelial cells showed a dose-dependent increase in Akt phosphorylation on S473 and T308 with no change in total Akt. Rcav-1 treatment also led to increased eNOS phosphorylation on S1177 but not T495 (Fig. 4*A, right*). The CSD-deleted rcav-1 failed to stimulate eNOS S1177 phosphorylation, as expected (Fig. 4*B, top*). We also tested the effect of LY294002 on the rcav-1–induced phosphorylation of Akt (T308) and eNOS (S1177) in *cav-1*$^{-/-}$ endothelial cells. As expected, LY294002 treatment of the cells diminished the observed Akt phosphorylation induction by rcav-1. Interestingly, the phosphorylation of eNOS (S1177) induced by rcav-1 was reduced but not completely diminished as a result of LY294002 treatment (Fig. 4*B, bottom*).

To further investigate the mechanism(s) that underlies rcav-1–stimulated eNOS activation, we tested the effect of rcav-1 on the activities of serine/threonine protein phosphatases PP1 and PP2A in *cav-1*$^{-/-}$ endothelial cells. These two phosphatases are known to regulate the phosphorylation of multiple protein targets including Akt and eNOS (20, 21) and are inhibited by cav-1 overexpression in prostate cancer cells (13). The activation of eNOS by a number of stimuli including VEGF involves a transient increase in the phosphorylation of S1177 with a decrease in T495 phosphorylation, alternatively, protein kinase C signaling inhibits eNOS activity by phosphorylating T495 and dephosphorylating S1177. Both PP1 and PP2A are associated with eNOS phosphorylation. PP1 is specific for dephosphorylation of T495, whereas PP2A is specific for S1177

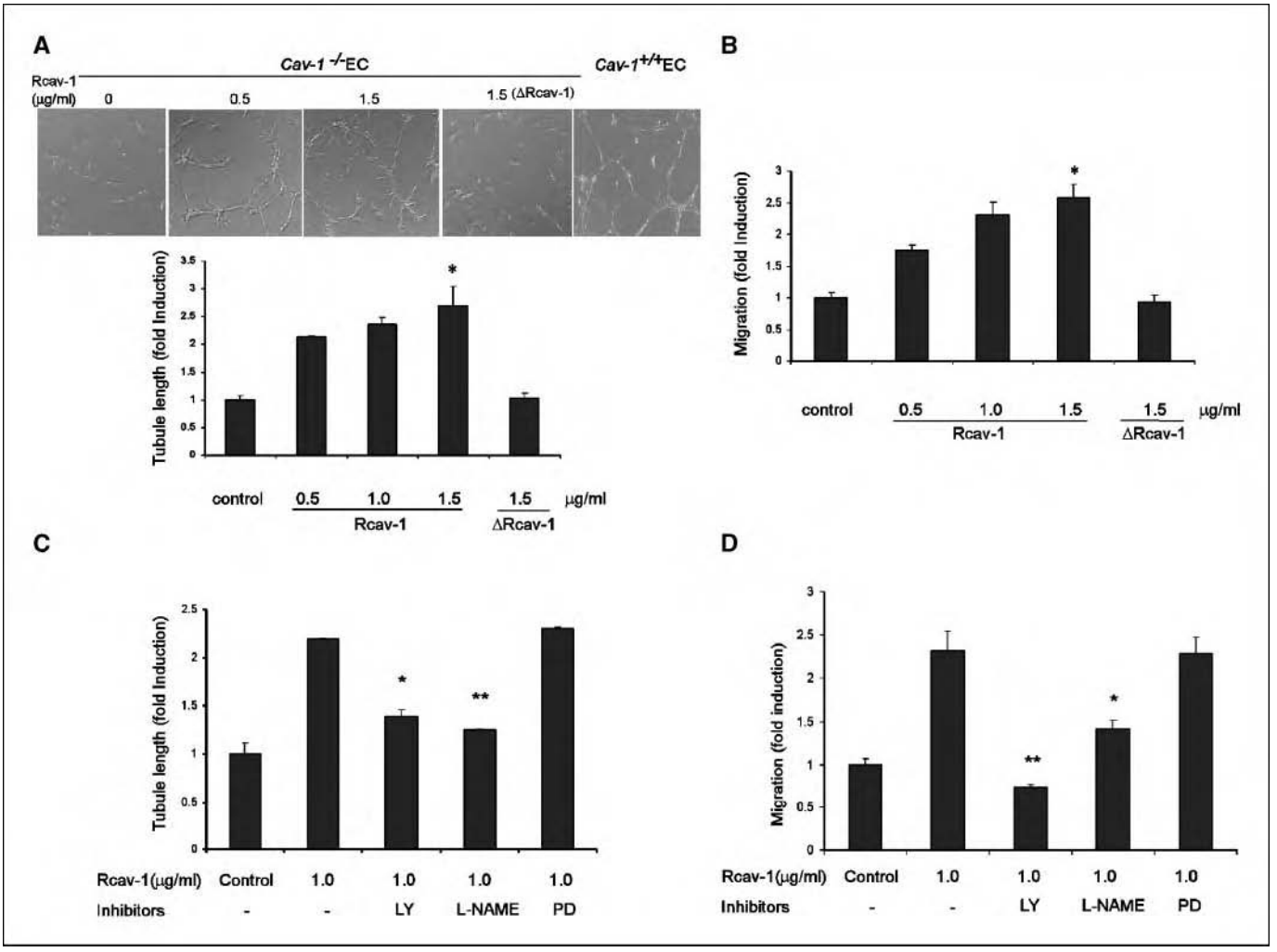

Figure 3. Rcav-1 stimulates tubule formation and cell migration in *cav-1*$^{-/-}$ endothelial cells. *A,* representative micrographs showing newly formed tubules of *cav-1*$^{+/+}$ and *cav-1*$^{-/-}$ endothelial cells cultured on growth factor–reduced Matrigel under basal conditions or after treatment with 0.5 to 1.5 μg/mL of rcav-1 and 1.5 μg/mL Δrcav-1 for 18 h. Bar graph depicts dose-dependent rcav-1 or Δrcav-1 stimulation of tubule formation in *cav-1*$^{-/-}$ endothelial cells. The values are folds of induction relative to untreated control ± SD of three independent experiments. *, P = 0.02 versus untreated control by two-sided t test. *B,* dose-dependent rcav-1 or Δrcav-1 stimulation of *cav-1*$^{-/-}$ endothelial cell migration in a wound-healing assay. The values are folds of induction relative to untreated control ± SD of three independent experiments. *, P = 0.0193 versus untreated control by two-sided t test. *C,* inhibition of rcav-1–stimulated tubule formation by LY294002 (*LY*; 3.0 μmol/L) or L-NAME (1.0 mmol/L) but not by PD98059 (*PD*; 50 μmol/L) in *cav-1*$^{-/-}$ endothelial cells. *, P = 0.008; **, P = 0.003 versus rcav-1 treated only. *D,* inhibition of rcav-1–stimulated wound-healing assay cell migration by LY294002 (3.0 μmol/L) or L-NAME (1.0 mmol/L), but not by PD98059 (50 μmol/L) in *cav-1*$^{-/-}$ endothelial cells. *, P = 0.011; **, P = 0.005 versus rcav-1 treated only, by-two sided t test. Bar graphs in *C* and *D* represent tubule length relative to untreated controls and the number of migratory cells relative to untreated controls, respectively. *Columns,* mean; *bars,* SD.

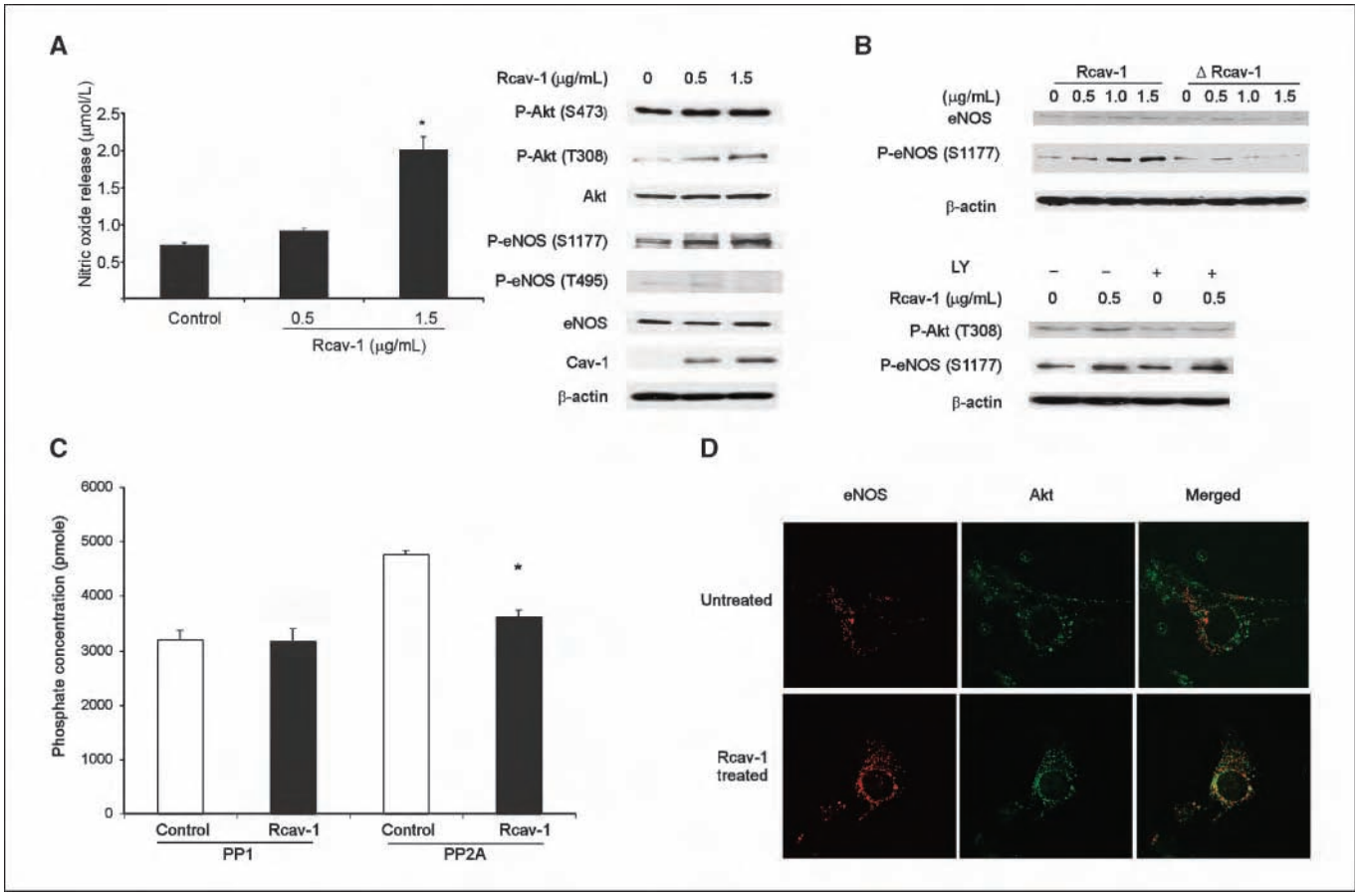

Figure 4. Rcav-1 is involved in PI3-K-Akt-eNOS–mediated stimulation of angiogenic activities in *cav-1*$^{-/-}$ endothelial cells. *A,* dose-dependent NO release by *cav-1*$^{-/-}$ endothelial cells after rcav-1 treatment. *Columns,* mean; *bars,* SD. *, $P = 0.029$ versus untreated control, by two-sided *t* test (*left*). Increased phosphorylation of Akt on S473 and T308, and of eNOS on S1177 by Western blot analysis of *cav-1*$^{-/-}$ endothelial cells lysates treated for 24 h with different concentrations of rcav-1 (*right*). *B,* Δrcav-1 treatment of *cav-1*$^{-/-}$ endothelial cells for 24 h does not affect the phosphorylation status of eNOS on S1177, but rcav-1 increases eNOS phosphorylation on S1177 in a dose-dependent fashion (*top*). Treatment of *cav-1*$^{-/-}$ endothelial cells with LY29400 abolishes the rcav-1–induced Akt phosphorylation on T308 and reduces, but does not completely eliminate, the eNOS phosphorylation on S1177 induced by rcav-1 (*bottom*). *C,* rcav-1 inhibits the activity of PP2A but not PP1 in *cav-1*$^{-/-}$ endothelial cells. PP1-C or PP2A-C immunprecipitation complexes from rcav-1–treated *cav-1*$^{-/-}$ endothelial cells or untreated controls were used to determine phosphatase activities with the serine/threonine protein phosphatase assay. *Columns,* mean; *bars,* SD. *, $P = 0.0002$ by two-sided *t* test. *D*, induction of eNOS/Akt association by rcav-1. *Cav-1*$^{-/-}$ endothelial cells were cultured for 6 h in the presence or absence of rcav-1. After fixation, the cells were double-labeled with anti-eNOS and anti-Akt immunofluorecence. In untreated cells, eNOS (*red*) and Akt (*green*) were localized to separate compartments (*top*), whereas rcav-1 protein treatment of the cells for 6 h induced eNOS (*red*) and Akt (*green*) colocalization in cytoplasmic vesicles (*bottom*), as visualized by deconvolution microscopy.

dephosphorylation (21). The results showed that rcav-1 treatment significantly inhibited the activity of PP2A but had no effect on PP1 activity ($P = 0.0002$ versus control; Fig. 4*C*). These data provide evidence that rcav-1 induces eNOS phosphorylation through Akt activation, and independently of Akt, through inhibition of PP2A, which specifically dephosphorylates eNOS (S1177).

A number of studies have shown that both eNOS and PI3 kinase are colocalized within the caveolar region of the plasma membrane (22, 23); therefore, we investigated the role played by cav-1 in compartmentalization of the PI3-K-Akt-eNOS signaling pathway molecules in *cav-1*$^{-/-}$ endothelial cells. We incubated the cells with or without rcav-1 for 5 h and visualized the cells by deconvolution microscopy for colocalization of Akt with eNOS. We found that Akt was not colocalized with eNOS in untreated cells, whereas significant colocalization of the two molecules was observed in the cells treated with rcav-1 (Fig. 4*D*).

Rcav-1 uptake in tumor-associated endothelial cells and proangiogenic activities in prostate cancer animal models. To investigate the effects of endothelial cells–localized cav-1 on microvessel density and tumor growth *in vivo*, we used an orthotopic RM-9 mouse prostate cancer model (24), in which cav-1 expressing and secreting RM-9 prostate cancer cells are injected directly into the dorsolateral prostate of male *cav-1*$^{+/+}$ or *cav-1*$^{-/-}$ mice. In this model, the mean (1.85 ± 0.167) tumor wet weight was significantly higher in *cav-1*$^{+/+}$ versus *cav-1*$^{-/-}$ mice ($P = 0.045$; Fig. 5*A*). Moreover, immunohistochemical analysis of tumor sections collected from sacrificed mice showed that RM-9 tumors had significantly higher microvessel densities in *cav-1*$^{+/+}$ compared with *cav-1*$^{-/-}$ hosts [median, 21.5 (range, 15.6–36.1) versus 13.3 (range, 8.2–22.8; $P = 0.0078$); Fig. 5*B* and *C*]. Interestingly, >70% of the CD31^{+} microvessels in the *cav-1*$^{-/-}$ mouse tumor sections were positive for cav-1 staining, indicating uptake of RM-9 cell–derived cav-1 by tumor-associated endothelial cells (Fig. 5*D, arrows*).

We examined the association between cav-1 expression and prostate tumor–associated angiogenesis more closely by generating an LNCaP tet-on cav-1 stable cell line (LNTB25cav) in which the expression of cav-1 can be regulated by manipulating doxycycline. In the absence of doxycycline, the level of cav-1 protein in lysate is low, whereas the addition of doxycycline to the culture medium

leads to a rapid induction of cav-1 protein *in vitro* (Fig. 6*A*). LNTB25cav tumors were established as s.c. growing xenografts in adult male nude mice; tumor-bearing mice were then treated with either doxycycline or control sucrose solution added to the drinking water. Tumor volumes in the doxycycline-treated group were significantly greater than those in the control group on days 12, 15, and 18 after treatment ($P = 0.0195$, $P = 0.035$, $P = 0.019$, respectively; Fig. 6*A*). Further immunohistochemical analysis showed increased cav-1 levels in the cytoplasm of tumor cells in doxycycline-treated compared with control mice (Fig. 6*B, top*). Microvessel densities determined by CD31 labeling were greater in cav-1–induced tumors compared with controls ($P = 0.039$; Fig. 6*B, bottom*; Fig. 6*C*). In separate experiments, we injected 1×10^6 LNTB25cav cells into the tail veins of nude mice to establish experimental lung metastases. After 42 days of continuous treatment, the number and frequency of lung metastases in doxycycline-treated animals significantly exceeded results in the control group ($P = 0.008$ and 0.04, respectively; Fig. 6*D*) and their average size was clearly larger in doxycycline-treated mice (data not shown).

Discussion

The establishment of prostate cancer metastases involves the successful negotiation of multiple endogenous physiologic barriers, survival during transit through the blood or lymphatic stream, and colonization at distant sites. The growth and metastasis of prostate cancer and other tumors is dependent on the induction of new blood vessels from preexisting ones through angiogenesis (25, 26). Cav-1 has been implicated in the regulation of endothelial cells proliferation, differentiation, and stabilization (6, 17, 27, 28). In a study using Lewis lung carcinoma cells animal cancer model, cav-1 was found to be antiangiogenic factor (29). In contrast, the results of a number of studies including this report have shown a proangiogenic function for cav-1. In an experimental melanoma model, impairment of pathologic angiogenesis was reported in *cav-1*$^{-/-}$ compared with *cav-1*$^{+/+}$ (30). Increased expression of cav-1 and microvessel density was found to be associated with metastasis and a worse prognosis in human clear cell renal cell carcinoma, suggesting a proangiogenic role for cav-1 (31). We also presented correlative evidence for a proangiogenic role of cav-1 in human prostate cancer (4). Endogenous levels of cav-1 expression in endothelial cells may provide an explanation for this controversy. C*av-1*$^{-/-}$ endothelial cells showed abrogated tubule formation and reduced NO production with or without VEGF treatment. Enforced expression of relatively low levels of cav-1 in cav-1$^{-/-}$ endothelial cells produced increased eNOS phosphorylation (S1177) and NO production in response to VEGF treatment, yet expression of higher levels of cav-1 blocked this process (17).

Apparently, without cav-1, endothelial cells do not undergo proper maturation and maintain a hyperproliferative state. This

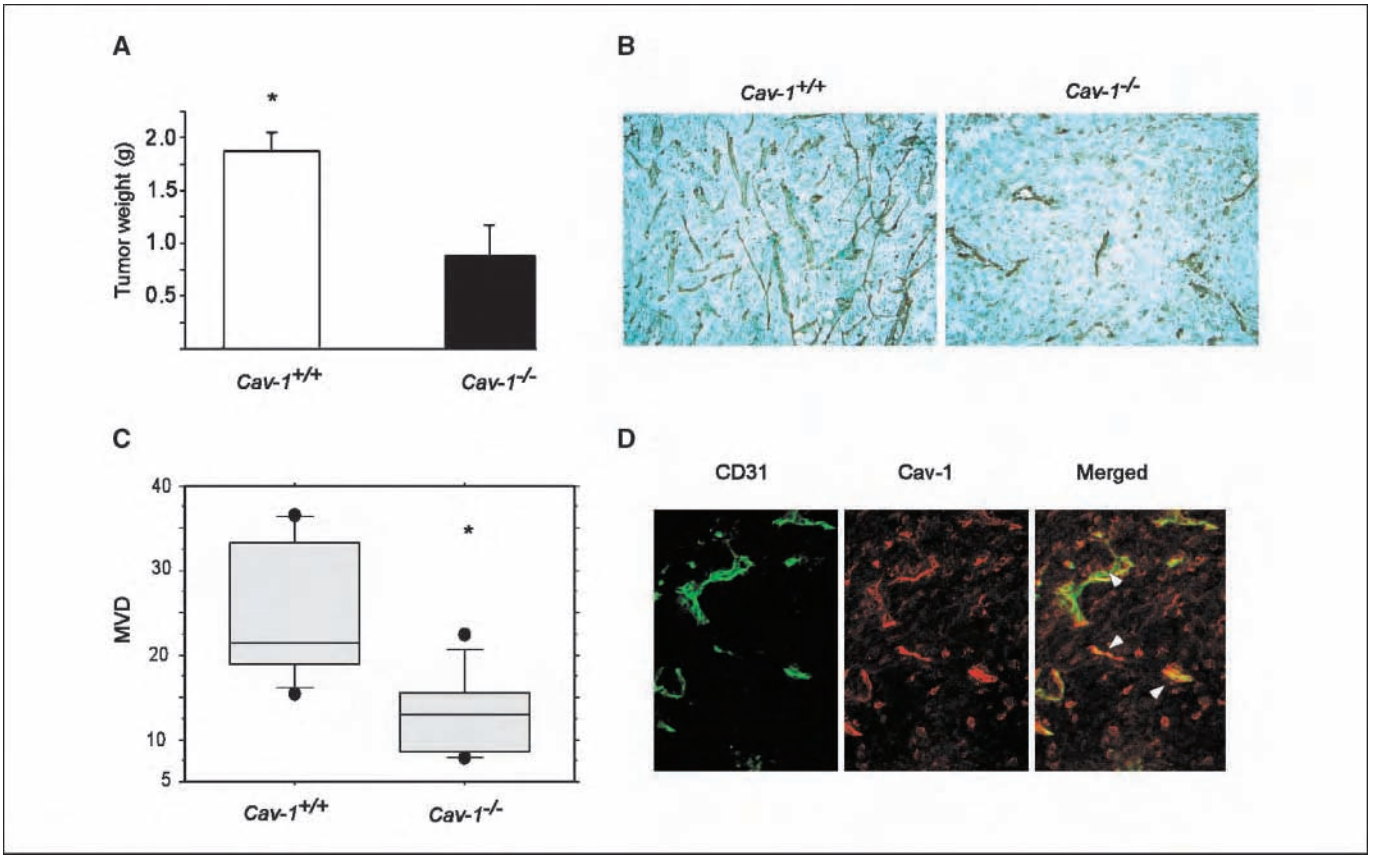

Figure 5. Secreted cav-1 promotes growth and angiogenesis in orthotopic RM-9 mouse prostate cancer model. *A,* increased RM-9 tumor wet weight in *cav-1*$^{+/+}$ hosts ($n = 7$) compared with *cav-1*$^{-/-}$ hosts ($n = 7$). *Columns,* mean; *bars,* SE. *, $P = 0.045$ by two-sided *t* test. *B,* immunohistochemical staining for CD31 in RM-9 tumors shows increased microvessel density in *cav-1*$^{+/+}$ hosts compared with *cav-1*$^{-/-}$ hosts. *C,* quantitative box plot analysis of the microvessel density (*MVD*) in RM-9 tumors from *cav-1*$^{+/+}$ versus *cav-1*$^{-/-}$ hosts. *Top lines,* 10th percentile; *bottom lines,* 90th percentile; *middle lines,* median value. *, $P = 0.0078$ by Mann-Whitney rank test. *D,* images of double immunostaining for CD31 (*green*) and cav-1 (*red*) in a tissue section of an RM-9 tumor from a *cav-1*$^{-/-}$ host. Arrows in the merged image (*yellow*) indicate the uptake by microvessels of cav-1 secreted by RM-9 tumors.

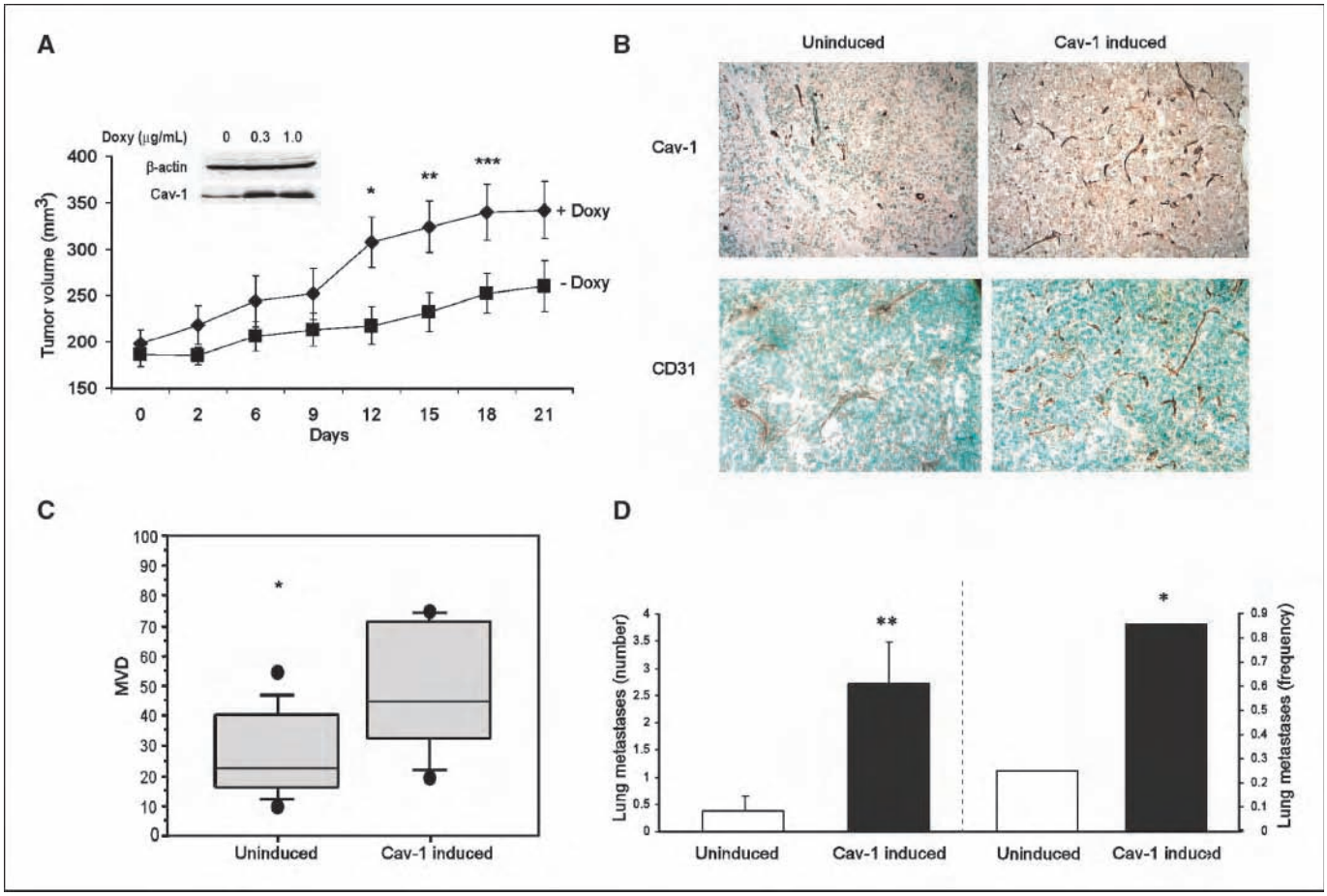

Figure 6. Secreted cav-1 promotes growth and angiogenesis in LNTB25cav tumors. *A,* Cav-1 induction by doxycycline (*Doxy*) leads to increased tumor volume in LNTB25cav s.c xenograft tumors growing s.c. Two groups of mice (n = 8 each) normalized for tumor volume were treated with either doxycycline (2 mg/mL) or control sucrose in drinking water for 21 d. *Points,* mean; *bars,* SE. *, P = 0.0195; **, P = 0.035; ***, P = 0.019 by two-sided t test. *B,* representative immunohistochemical staining for cav-1 and CD31 shows increased cytoplasmic cav-1 in cancer cells (*top*), and increased numbers of microvessels (*bottom*) in cav-1–induced LNTB25cav tumors compared with uninduced LNTB25cav tumors. *C,* quantitative box plot analysis of microvessel density in cav-1–induced (n = 8) and uninduced (n = 11) tumors. *Top lines,* 10th percentile; *bottom lines,* 90th percentiles; *middle lines,* median value. *, P = 0.039 by Mann-Whitney rank test. *D,* increased number and frequency of lung metastases in cav-1–induced compared with uninduced tumors. Lung metastases were established by injecting LNTB25cav cells into the tail veins of nude mice that were subsequently treated with doxycycline (n = 7) or sucrose (n = 8) in drinking water for 42 d. *Columns,* mean; *bars,* SE. *, P = 0.040 by Fisher's exact test; **, P = 0.008 by two-sided t test.

leads to a lack of polarization and a failure to form intercellular junctions (32), which may compromise selective transport mechanisms for specific macromolecules. Similarly, in tumor-associated endothelial cells a certain basal level of cav-1 may be required for minimal functional capacity. We have recently shown that cav-1 low/negative endothelial cells are relevant to prostate cancer. We reported significant reduction in the density of cav-1 positive microvessels in cav-1–negative human prostate cancer tissue compared with benign prostate tissues, clarifying the existence and possible significance of cav-1–negative microvessels in these malignancies (4).

We show that endocytosis of extracellular rcav-1 occurs in cancer cells (TSU-Pr1, DU145, and PC-3) and endothelial cells (HUVEC, *cav-1*$^{-/-}$ endothelial cells, and *cav-1*$^{+/+}$ endothelial cells), and that endothelial cells take up rcav-1 through lipid rafts/caveolae and clathrin-dependent pathways. Our results also show that rcav-1 uptake does not have an absolute cellular requirement for caveolae. The involvement of multiple endocytic pathways is not unique to cav-1 internalization, as these mechanisms have been described for the internalization of a number of proteins such as protein-specific membrane antigen (33), insulin growth factor binding protein-3 (34), transforming growth factor β receptor (35), and decorin (36). A possible explanation for the internalization of cav-1 through multiple pathways is its ability to interact with and bind to a large number of signaling proteins including multiple membrane receptors (15), which places it in proximity to endosome-forming activities of various pathways.

We show that CSD is necessary but may not be sufficient for cav-1 uptake, which leads to tubule formation, cell migration, and NO production in *cav-1*$^{-/-}$ endothelial cells. These data are supported by the results of a study that identified a highly conserved region of the engrailed homeoproteins that bears a high degree of homology with the CSD and are responsible for oligopeptide or oligonucleotide transmembrane, and cellular transport (37). The CSD was also found to have the ability to direct endogeneous cav-1 to cell membranes (16).

We show that cav-1 angiogenic activities involve the PI3-K-Akt-eNOS pathway but not Erk1/2. Indeed, rcav-1 treatment increases phosphorylation of Akt (S473 and T308) and, hence, eNOS phosphorylation (S1177 but not T495), leading to NO production.

Because previous studies show that Akt phosphorylates eNOS on the S1177 site, leading to eNOS activation, our results are consistent with a straight forward molecular pathway through which cav-1 uptake activates Akt, which in turn activates eNOS. However, Akt inhibitor studies indicated that Akt signaling is not the only pathway culminating in eNOS phosphorylation on S1177. That is, rcav-1–stimulated Akt activation was accompanied by inhibition of PP2A, a specific serine/threonine kinase that dephosphorylates S473 and T308 on Akt, and S1177 and T495 on eNOS (13, 21, 38). It is of interest that rcav-1 did not inhibit PP1, a serine/threonine kinase whose substrate specificity is similar to that of PP2A. Because PP1 may have selective activity for the T495 site on eNOS, which unlike the S1177 site leads to inhibition of eNOS activity, the absence of cav-1–mediated inhibition of PP1 could further contribute to eNOS activation (21). This notion is supported by the absence of increased phosphorylation of T495 on eNOS in response to rcav-1 (Fig. 4*A, right*). Because we previously showed that cav-1–stimulated PP1, and PP2A inhibition is mediated through direct interaction between the cav-1 CSD and PP1/PP2A binding sites in prostate cancer cells, (13) it seems reasonable to suggest that this specific interaction also applies to rcav-1–mediated inhibition of PP2A in *cav-1*$^{-/-}$ endothelial cells.

Studies with two complementary animal model systems (i.e., the RM-9-*cav-1*$^{-/-}$ host orthotopic model and the LNTB25cav xenograft model) substantiate our *in vitro* findings that tumor-associated endothelial cells internalize tumor-secreted cav-1, which is associated with tumor growth, and that overexpression of cav-1 in prostate cancer cells promotes angiogenesis and tumor growth.

Overall, our data show that prostate cancer cell–derived and prostate cancer cell–secreted cav-1 has autocrine (tumor cell uptake) and paracrine (tumor-associated endothelial cells uptake) activities that can contribute to angiogenesis, tumor progression, and metastasis. We propose that prostate cancer and potentially other malignancies that overexpress and secrete cav-1, may benefit from anti–cav-1 therapy that could involve cav-1 antibodies or peptide inhibitors of CSD.

Acknowledgments

Received 7/13/2007; revised 9/27/2007; accepted 11/12/2007.

Grant support: NIH grants RO1 CA68814 and Specialized Programs of Research Excellence P50 58204 and DAMD PC051247 from the Department of Defense.

The costs of publication of this article were defrayed in part by the payment of page charges. This article must therefore be hereby marked *advertisement* in accordance with 18 U.S.C. Section 1734 solely to indicate this fact.

References

1. Shaul PW, Anderson RG. Role of plasmalemmal caveolae in signal transduction. Am J Physiol 1998;275: L843–51.

2. Nasu Y, Timme TL, Yang G, et al. Suppression of caveolin expression induces androgen sensitivity in metastatic androgen-insensitive mouse prostate cancer cells. Nat Med 1998;4:1062–4.

3. Yang G, Truong LD, Timme TL, et al. Elevated expression of caveolin is associated with prostate and breast cancer. Clin Cancer Res 1998;4:1873–80.

4. Yang G, Addai J, Ayala G, et al. Correlative evidence that prostate cancer cell-derived caveolin-1 mediated angiogenesis. Hum Pathol 2007;38:1688–95.

5. Williams TM, Lisanti MP. The Caveolin genes: from cell biology to medicine. Ann Med 2004;36:584–95.

6. Carver LA, Schnitzer JE. Caveolae: mining little caves for new cancer targets. Nat Rev Cancer 2003;3: 571–81.

7. Tahir SA, Yang G, Ebara S, et al. Secreted caveolin-1 stimulates cell survival/clonal growth and contributes to metastasis in androgen-insensitive prostate cancer. Cancer Res 2001;61:3882–5.

8. Tahir SA, Ren C, Timme TL, et al. Development of an immunoassay for serum caveolin-1: a novel biomarker for prostate cancer. Clin Cancer Res 2003;9:3653–9.

9. Tahir SA, Frolov A, Hayes TG, et al. Preoperative serum caveolin-1 as a prognostic marker for recurrence in a radical prostatectomy cohort. Clin Cancer Res 2006;12: 4872–5.

10. Williams TM, Hassan GS, Li J, et al. Caveolin-1 promotes tumor progression in an autochthonous mouse model of prostate cancer: genetic ablation of Cav-1 delays advanced prostate tumor development in TRAMP mice. J Biol Chem 2005;10:1074.

11. Cao G, Yang G, Timme TL, et al. Disruption of the caveolin-1 gene impairs renal calcium reabsorption and leads to hypercalciuria and urolithiasis. Am J Pathol 2003;162:1241–8.

12. Brouet A, Sonveaux P, Dessy C, et al. Hsp90 and caveolin are key targets for the proangiogenic nitric oxide-mediated effects of statins. Circ Res 2001;89: 866–73.

13. Li L, Ren CH, Tahir SA, Thompson TC. Caveolin-1 maintains activated Akt in prostate cancer cells through scaffolding domain binding site interactions with and inhibition of serine/threonine protein phosphatases PP1 and PP2A. Mol Cell Biol 2003;23:9389–404.

14. Vermeulen PB, Gasparini G, Fox SB, et al. Second international consensus on the methodology and criteria of evaluation of angiogenesis quantification in solid human tumours. Eur J Cancer 2002;38:1564–79.

15. Smart EJ, Graf GA, McNiven MA, et al. Caveolins, liquid-ordered domains, and signal transduction. Mol Cell Biol 1999;19:7289–304.

16. Schlegel A, Lisanti MP. A molecular dissection of caveolin-1 membrane attachment and oligomerization. Two separate regions of the caveolin-1 C-terminal domain mediate membrane binding and oligomer/oligomer interactions *in vivo*. J Biol Chem 2000;275: 21605–17.

17. Sonveaux P, Martinive P, DeWever J, et al. Caveolin-1 expression is critical for vascular endothelial growth factor-induced ischemic hindlimb collateralization and nitric oxide-mediated angiogenesis. Circ Res 2004;95: 154–61.

18. Labrecque L, Royal I, Surprenant DS, et al. Regulation of vascular endothelial growth factor receptor-2 activity by caveolin-1 and plasma membrane cholesterol. Mol Biol Cell 2003;14:334–47.

19. Liu J, Wang XB, Park DS, Lisanti MP. Caveolin-1 expression enhances endothelial capillary tubule formation. J Biol Chem 2002;277:10661–8.

20. Cohen PT. Protein phosphatase 1-targeted in many directions. J Cell Sci 2002;115:241–56.

21. Michell BJ, Chen Z, Tiganis T, et al. Coordinated control of endothelial nitric-oxide synthase phosphorylation by protein kinase C and the cAMP-dependent protein kinase. J Biol Chem 2001;276:17625–8.

22. Chambliss KL, Shaul PW. Rapid activation of endothelial NO synthase by estrogen: evidence for a steroid receptor fast-action complex (SRFC) in caveolae. Steroids 2002;67:413–9.

23. Stirone C, Boroujerdi A, Duckles SP, Krause DN. Estrogen receptor activation of phosphoinositide-3 kinase, akt, and nitric oxide signaling in cerebral blood vessels: rapid and long-term effects. Mol Pharmacol 2005;67:105–13.

24. Nasu Y, Bangma C, Hull G, et al. Combination gene therapy with adenoviral vector-mediated HSV-tk+GCV and IL-12 in an orthotopic mouse model for prostate cancer. Prostate Cancer Prostatic Diseases 2001;4:44–55.

25. Hanahan D, Folkman J. Patterns and emerging mechanisms of the angiogenic switch during tumorigenesis. Cell 1996;86:353–64.

26. Carmeliet P, Jain RK. Angiogenesis in cancer and other diseases. Nature 2000;407:249–57.

27. Frank PG, Woodman SE, Park DS, Lisanti MP. Caveolin, caveolae, and endothelial cell function. Arterioscler Thromb Vasc Biol 2003;23:1161–8.

28. Massimino ML, Griffoni C, Spisni E, Toni M, Tomasi V. Involvement of caveolae and caveolae-like domains in signalling, cell survival and angiogenesis. Cell Signal 2002;14:93–8.

29. Lin MI, Yu J, Murata T, Sessa WC. Caveolin-1-deficient mice have increased tumor microvascular permeability, angiogenesis, and growth. Cancer Res 2007;67:2849–56.

30. Woodman SE, Ashton AW, Schubert W, et al. Caveolin-1 knockout mice show an impaired angiogenic response to exogenous stimuli. Am J Pathol 2003;162: 2059–68.

31. Joo HJ, Oh DK, Kim YS, Lee KB, Kim SJ. Increased expression of caveolin-1 and microvessel density correlates with metastasis and poor prognosis in clear cell renal cell carcinoma. BJU Int 2004;93:291–6.

32. Razani B, Engelman JA, Wang XB, et al. Caveolin-1 null mice are viable but show evidence of hyperproliferative and vascular abnormalities. J Biol Chem 2001;276:38121–38.

33. Anilkumar G, Barwe SP, Christiansen JJ, et al. Association of prostate-specific membrane antigen with caveolin-1 and its caveolae-dependent internalization in microvascular endothelial cells: implications for targeting to tumor vasculature. Microvasc Res 2006; 72:54–61.

34. Lee KW, Liu B, Ma L, et al. Cellular internalization of insulin-like growth factor binding protein-3: distinct endocytic pathways facilitate re-uptake and nuclear localization. J Biol Chem 2004;279:469–76.

35. Di Guglielmo GM, Le Roy C, Goodfellow AF, Wrana JL. Distinct endocytic pathways regulate TGF-β receptor signalling and turnover. Nat Cell Biol 2003;5:410–21.

36. Feugaing DD, Tammi R, Echtermeyer FG, et al. Endocytosis of the dermatan sulfate proteoglycan decorin utilizes multiple pathways and is modulated by epidermal growth factor receptor signaling. Biochimie 2007;89:637–57.

37. Joliot A, Trembleau A, Raposo G, et al. Association of engrailed homeoproteins with vesicles presenting caveolae-like properties. Development 1997;124: 1865–75.

38. Urbich C, Reissner A, Chavakis E, et al. Dephosphorylation of endothelial nitric oxide synthase contributes to the anti-angiogenic effects of endostatin. FASEB J 2002;16:706–8.

Available online at www.sciencedirect.com
ScienceDirect
Experimental and Molecular Pathology 84 (2008) 131–140
Experimental and Molecular Pathology
www.elsevier.com/locate/yexmp

Mice with *cav-1* gene disruption have benign stromal lesions and compromised epithelial differentiation

Guang Yang [a], Terry L. Timme [a,b], Koji Naruishi [a], Tetsuo Fujita [a], El Moataz Abdel Fattah [a], Guangwen Cao [a], Kartik Rajocopolan [a], Luan D. Troung [c], Timothy C. Thompson [a,b,d,e,*]

[a] *Scott Department of Urology, Baylor College of Medicine, Houston, TX, USA*
[b] *Michael E DeBakey Veterans Affairs Medical Center, Houston, TX, USA*
[c] *Research Institute, The Methodist Hospital, Houston, TX, USA*
[d] *Department of Cellular and Molecular Biology, Baylor College of Medicine, Houston, TX, USA*
[e] *Department of Radiology, Baylor College of Medicine, Houston, TX, USA*

Received 24 July 2007
Available online 31 August 2007

Abstract

Caveolin-1 (cav-1) is a major structural protein of caveolae, small invaginations of the plasma membrane that integrate and regulate signaling pathways involved in cell growth and differentiation. We previously generated a genetically engineered mice that are homozygous for a null mutation in exon 2 of *cav-1* and documented increased incidence of urolithiasis in young male *cav-1*$^{-/-}$ mice. We attributed this, in part, to improper localization of plasma membrane calcium/calmodulin-dependent calcium ATPase in the distal convoluted tubules of the kidney. To document pathologies related to cav-1 function, we maintained *cav-1*$^{-/-}$ and control *cav-1*$^{+/+}$ mice for an extended time period. We report here that *cav-1*$^{-/-}$ mice demonstrate organ-specific growth-related disorders in stromal cells that normally have high levels of cav-1 expression. In many of these organs, epithelial cell growth/differentiation abnormalities were also observed, yet in most of these sites the epithelial cells normally express low to non-detectable levels of cav-1. We propose that loss of cav-1 function in stromal cells of various organs directly leads to a disorganized stromal compartment that, in turn, indirectly promotes abnormal growth and differentiation of adjacent epithelium.

Introduction

Caveolin-1 (cav-1) protein was originally isolated as a structural component of caveolae in endothelial cells (Rothberg et al., 1992) and epithelial cells (Kurzchalia et al., 1992). Subsequently cav-1 expression has been observed in multiple cell types and was shown to play an important role in signal transduction and molecular transport in a cell and context-specific fashion (Fielding and Fielding, 2001; Massimino et al., 2002; Parton, 2003; Shaul and Anderson, 1998; Smart et al., 1999). The role of cav-1 in human disease has been the subject of considerable debate especially with regard to the development and progression of various malignancies. To develop model systems that provide insight into the role of cav-1 in human disease, multiple investigators generated cav-1 gene knockout mice.

There are currently three independent reports of the generation of cav-1 knockout mice (Drab et al., 2001; Razani et al., 2001a; Cao et al., 2003) and one of a cav-2 knockout mouse (Razani et al., 2002). Unexpectedly, *cav-1*$^{-/-}$ mice were viable and apparently healthy despite the absence of cav-1 (Parton, 2001). However, pathologic analysis revealed abnormalities in specific cell types. Pulmonary and cardiac defects were consistently reported for all *cav-1*$^{-/-}$ mice (Drab et al., 2001; Razani et al., 2001a; Cao et al., 2003). We also reported that young *cav-1*$^{-/-}$ male mice demonstrate an increased incidence of urolithiasis that likely results in part from improper localization of plasma membrane calcium/calmodulin-dependent calcium ATPase in the distal convoluted tubules of the kidney (Cao et al., 2003). These studies confirmed a functional role for cav-1 in specific tissues or cell types. Additional studies using *cav-1*$^{-/-}$ mice have focused on the role of cav-1 in

* Corresponding author. 6560 Fannin, Suite 2100, Houston, TX 77030. Fax: +1 713 794 7983.
E-mail address: timothyt@bcm.edu (T.C. Thompson).

0014-4800/$ - see front matter © 2007 Elsevier Inc. All rights reserved.
doi:10.1016/j.yexmp.2007.08.004

malignancy, and early reports suggested that cav-1 was a tumor suppressor. Unambiguous functional evidence for a tumor suppressor gene is the demonstration of tumorigenesis in a knockout mouse model (Hakem and Mak, 2001). The absence of *cav-1* has not been reported to increase the incidence of spontaneous malignancies; however, loss of cav-1 function has been shown to increase the incidence of carcinogen-induced hyperplasia and tumorigenesis following application of dimethylbenzanthracene to the skin (Capozza et al., 2003). The development of epithelial cell hyperplasia but not overt dysplasia in the mammary glands of *cav-1*$^{-/-}$ mice was also reported (Lee et al., 2002). In addition, an increased incidence of dysplastic lesions was observed in *cav-1*$^{-/-}$ mice compared to *cav-1*$^{+/+}$ when the mice were bred with transgenic mice expressing a dominant transforming oncogene, polyoma middle T (PyMT), in breast tissue permissive for MMTV promoter activities (Williams et al., 2003). In older MMTV-PyMT mice, breast cancer lesions appeared sooner and with increased multifocality in female mice in a *cav-1*$^{-/-}$ background than in *cav-1*$^{+/+}$ or *cav-1*$^{+/-}$ mice, and there were more metastatic lesions in the lungs (Williams et al., 2004).

Some reports document down-regulation of cav-1 in various malignancies (Aldred et al., 2003; Bagnoli et al., 2000; Bender et al., 2000; Davidson et al., 2001; Kato et al., 2004; Racine et al., 1999; Sagara et al., 2004; Sunaga et al., 2004; Wiechen et al., 2001; Wikman et al., 2004). However, with regard to prostate cancer, in a recently published study, it was shown that TRAMP (transgenic mouse prostate);*cav-1*$^{-/-}$ mice demonstrate significantly reduced numbers of primary tumors and metastatic lesions compared to TRAMP;*cav-1*$^{+/+}$ mice (Williams et al., 2005). These data are consistent with numerous studies that have clearly documented overexpression of cav-1 is associated with unfavorable clinical prognosis in various adenocarcinomas (reviewed in Bender et al., 2000; Carrion et al., 2003; Davidson et al., 2002; Ho et al., 2002; Horiguchi et al., 2004; Hu et al., 2001; Hung et al., 2003; Ito et al., 2002; Joo et al., 2004; Kato et al., 2002; Mouraviev et al., 2002; Patlolla et al., 2004; Rajjayabun et al., 2001; Sanchez-Carbayo et al., 2002; Satoh et al., 2003; Sunaga et al., 2004; Suzuoki et al., 2002; Terris et al., 2002; Yang et al., 2000, 1998, 1999; Yoo et al., 2003). To provide additional insight into the role of cav-1 in abnormal cellular growth, we further analyzed *cav-1*$^{-/-}$ mice.

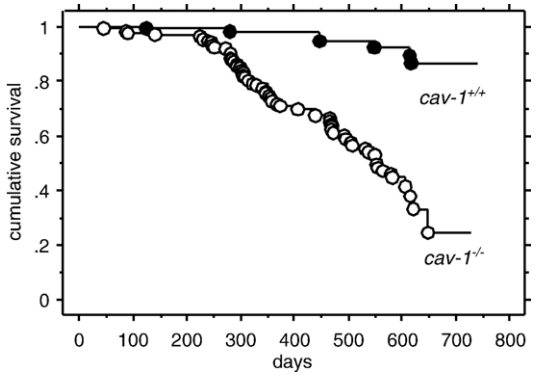

Fig. 1. Kaplan–Meyer survival plot of *cav-1*$^{+/+}$ and *cav-1*$^{-/-}$ mice.

Table 1
Organ wet weight in adult *cav-1*$^{+/+}$ and *cav-1*$^{-/-}$ mice at two time points

	Male				Female			
	cav-1$^{+/+}$		*cav-1*$^{-/-}$		*cav-1*$^{+/+}$		*cav-1*$^{-/-}$	
Age (months)	10	19	10	19	10	19	10	19
N	7	55	15	30	6	37	10	16
Body weight (g)	32.08	31.44	30.38	31.35	23.99	27.71	24.96	27.30
Kidney (mg)	247	302	278	290	187	208	232	206
Spleen (mg)	146	170	445	188	206	176	450	346
Liver (mg)	1506	1700	1710	1657	1179	1501	1586	1533
Lung (mg)	181		385		172		293	
Pancreas (mg)	145		143		165		122	
Prostate (mg)		89		67				

We report here our long-term observations of a cohort of *cav-1*$^{+/+}$ and *cav-1*$^{-/-}$ mice. In agreement with previous observations, *cav-1*$^{-/-}$ have a decreased lifespan (Park et al., 2003). We did not detect any increase in overt cancer development. We document stromal cell growth abnormalities in *cav-1*$^{-/-}$ mice compared to *cav-1*$^{+/+}$ mice. Specifically, these abnormalities were seen in endothelial cells and smooth muscle cells of specific organs that normally express high levels of cav-1. Interestingly, in many of these organs epithelial/parenchymal cells that normally do not express significant levels of cav-1 also demonstrated growth and differentiation abnormalities including glandular malfunction and reduced cytokeratin staining.

Materials and methods

Mice

Using *Lox*P/Cre technology, we generated genetically engineered mice that were homozygous for a deletion of exon 2 of the *cav-1* gene (Cao et al., 2003). The mice were kept in a mixed strain background of C57/BL6 and129/Sv by interbreeding. They had access to food, Harlan TekLab 22/5 Rodent Diet (W), and water *ad libitum*. They were maintained in facilities accredited by the American Association for Accreditation of Laboratory Animal Care and all experiments conducted in accordance with the principles and procedures outlined in the National Institutes of Health's Guide for the Care and Use of Laboratory Animals.

Histopathology and immunohistochemistry

Animals were euthanized and after careful observation for gross changes, selected organs were removed by dissection and weighed. Tissue samples were fresh frozen in OCT (Optimal Cutting Temperature) compound or fixed in 10%

Table 2
Organ confined pathologies in adult (>18 months) *cav-1*$^{+/+}$ and *cav-1*$^{-/-}$ mice

Phenotype	*cav-1*$^{+/+}$	*cav-1*$^{-/-}$
Thickening of alveolar septa in lung	3/44 (7%)	13/23 (56%)
Breast epithelial hyperplasia	2/31 (6%)	6/13 (46%)†
Prostate epithelial cell hyperplasia	3/13 (23%)	2/9 (22%)
Seminal vesicle enlargement	1/12 (8%)	6/9 (67%)‡
Ovarian cysts	1/31 (3%)	3/13 (23%)
Hepatic carcinoma	4/44 (9%)	0/23 (0%)
Lymphoma in spleen	4/44 (9%)	2/23 (9%)
Lymphoma in uterus	2/31 (6%)	0/13 (0%)

$^{\dagger}P=0.0072$ or $^{\ddagger}P=0.0182$; Fisher's exact test.

buffered formalin and embedded in paraffin for sectioning. Sections (4–5 μm) were stained with hematoxylin and eosin (H&E) according to standard protocols and were evaluated histologically. Immunohistochemical (IHC) analysis using standard ABC detection was performed as previously described (Yang et al., 1998). Antibodies used included rabbit polyclonal anti-cav-1 (N-20, Santa Cruz Biotech, Inc., Santa Cruz, CA), goat polyclonal anti-CD31 (M-20, Santa Cruz), rabbit polyclonal anti-cytokeratin (Z0575, Dako, Carpinteria, CA), mouse monoclonal anti-proliferative cell nuclear antigen (PCNA) (PC-10, Dako), mouse monoclonal anti-alpha smooth muscle-specific actin (1A4, Dako), rabbit polyclonal anti-desmin (D8281, Sigma-Aldrich, St. Louis, MO) and goat polyclonal anti-vimentin (V4630, Sigma) and rat monoclonal anti-CD11b (Clone M1/70, Pharmingen, San Diego, CA). The TUNEL technique (Gavrieli et al., 1992) was used to label apoptotic splenocytes as previously described (Yang et al., 1996). IHC quantitation of PCNA-positive and apoptotic splenocytes were conducted on 30 randomly selected measuring fields (0.198 μm^2 each) for each specimen. The number of positively labeled cells per unit spleen area was recorded and the statistical significance of the differences in proliferative and apoptotic activities was evaluated by the Mann–Whitney rank test.

Results

We observed a large cohort of *cav-1*$^{+/+}$ and *cav-1*$^{-/-}$ mice for more than 2 years. The *cav-1*$^{+/+}$ mice had significantly longer overall survival times than their *cav-1*$^{-/-}$ littermates (Fig. 1).

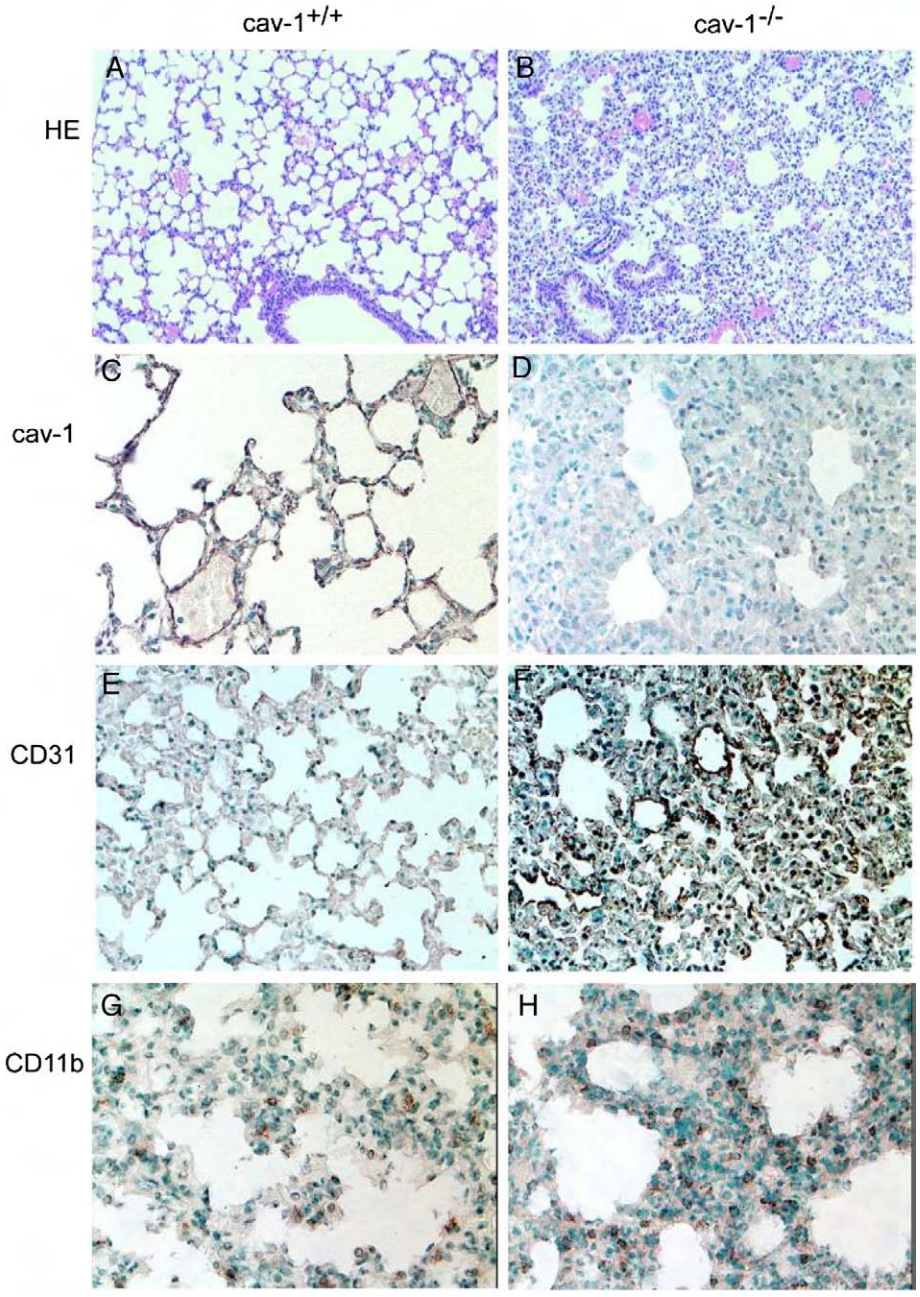

Fig. 2. Histological and IHC characterization of lung tissues from *cav-1*$^{+/+}$ (A, C, E and G) and *cav-1*$^{-/-}$ (B, D, F and H) mice. (A and B) H&E staining; (C and D) cav-1 staining; (E and F) CD31 staining; (G and H) CD11b staining. Original magnification: A and B, 100×; C–F, 200×; G and H, 400×.

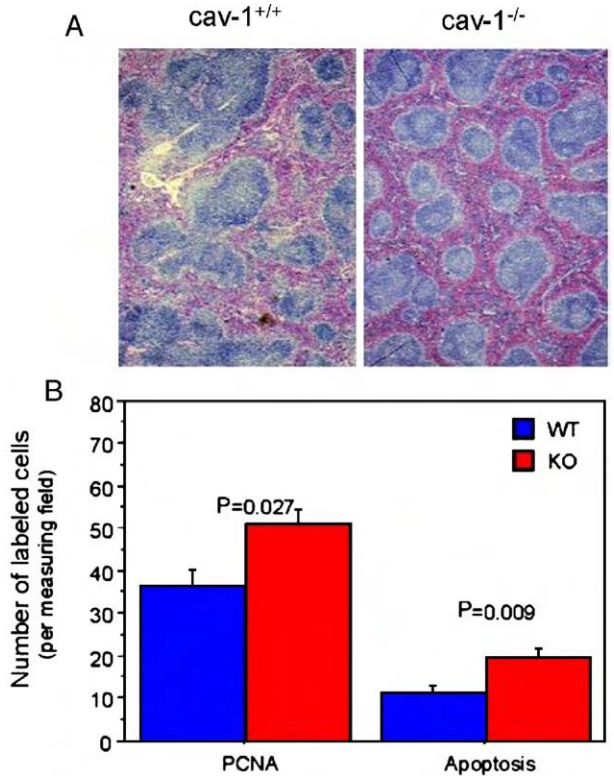

Fig. 3. H&E-stained sections of spleen (A) depicting the morphological difference between 3-month-old *cav-1*$^{+/+}$ and *cav-1*$^{-/-}$ mice. Original magnification: 200×. Quantitation of PCNA and apoptosis labeling (B) in the spleen. The densities of PCNA-positive cells and apoptotic bodies in spleen from *cav-1*$^{-/-}$ mice were significantly higher than in the *cav-1*$^{+/+}$ mice ($P=0.027$ and $P=0.009$, respectively).

The mean survival for the *cav-1*$^{+/+}$ mice was 602±6 days compared with 500±15 days for the *cav-1*$^{-/-}$ mice ($P<0.001$, Mantel-Cox Rank test). A smaller group of heterozygous mice ($n=30$) was also observed to have an intermediate survival time of 537±29 days. There was no difference in survival between male and female mice (data not shown). In most cases no obvious cause of death was apparent. At gross necropsy the most commonly observed abnormalities in older mice were swollen and purulent lymph nodes in the head and neck. One specific abnormality noted in several *cav-1*$^{-/-}$ mice was anal exstrophy.

We sacrificed two cohorts of mice at approximately 10 or 19 months of age and obtained the weight of selected organs (Table 1). The overall body weight was similar for mice of the same sex independent of genotype. However, the wet weights of specific organs including lungs, liver, kidney and spleen were increased in both male and female *cav-1*$^{-/-}$ mice at 10 months compared to *cav-1*$^{+/+}$ of the same sex. These differences achieved statistical significance in the spleen (males $P=0.0026$, females $P=0.0323$) and in the liver of females ($P=0.0164$). In mice evaluated at an age of 19 months these differences largely resolved, except the spleen weight from the *cav-1*$^{-/-}$ females remained significantly increased ($P=0.0404$).

The general gross anatomical and microscopic features based on evaluation of H&E-stained sections from selected organs of both cohorts of the *cav-1*$^{+/+}$ and *cav-1*$^{-/-}$ animals are summarized in Table 2. The penetrance of each abnormal phenotype as well as the incidence of spontaneous tumors in the mice is also compared in Table 2. Hepatocarcinoma and lymphoma were observed in a few animals with no statistical difference in incidence between *cav-1*$^{+/+}$ and *cav-1*$^{-/-}$ mice.

The lungs of *cav-1*$^{-/-}$ mice demonstrated thickened alveolar septa and hypercellularity. The alveolar lumens appeared smaller or constricted, as a result of the hypercellularity as compared to *cav-1*$^{+/+}$ mice (Fig. 2). In *cav-1*$^{-/-}$ mice, immunostaining with CD31 (PECAM) (Fig. 2) demonstrated significantly increased numbers of endothelial cells, whereas vimentin staining failed to show increased fibroblasts in the thickened septa (data not shown). Significantly increased numbers of infiltrating macrophages as demonstrated by CD11b staining were also seen in the thickened alveolar walls of *cav-1*$^{-/-}$ lung (Fig. 2). These lung abnormalities were observed most dramatically in 3- to 4-month-old *cav-1*$^{-/-}$ mice. They persisted in the aged animals with the incidence of the lung abnormalities in *cav-1*$^{-/-}$ significantly higher than that in the *cav-1*$^{+/+}$ mice at 18 months (Table 2).

Tissue sections of the spleen from 3-month-old mice revealed that the red pulp compartment represented a larger percentage of the area in *cav-1*$^{-/-}$ mice compared to *cav-1*$^{+/+}$ mice (Fig. 3A). However, this difference became less dramatic as the mice aged. The proliferative rate of splenocytes as demonstrated by the

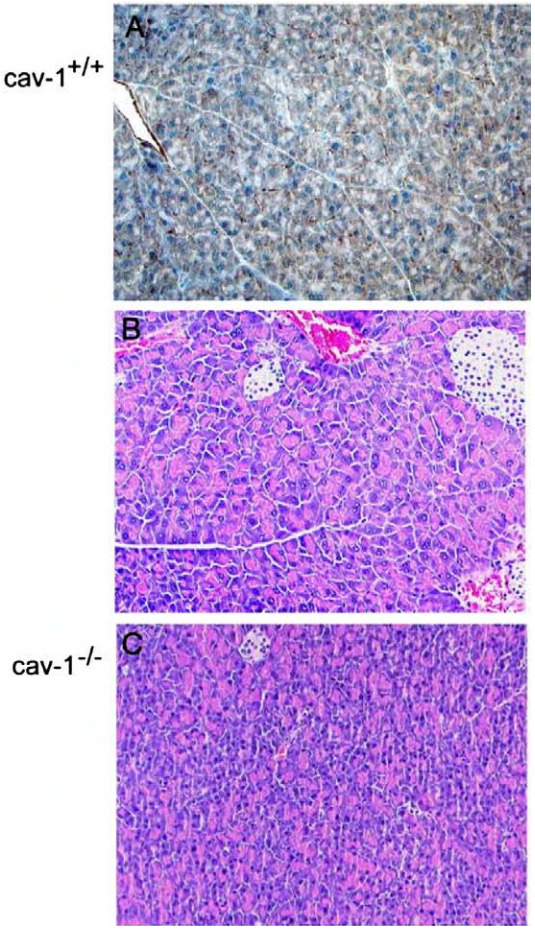

Fig. 4. H&E-stained sections of the pancreas of 3-month-old (A) *cav-1*$^{+/+}$ and (B) *cav-1*$^{-/-}$ mice demonstrating a higher density of exocrine secretory cells in *cav-1*$^{-/-}$ mice versus *cav-1*$^{+/+}$ mice. Original magnification: 200×.

number of PCNA-positive splenocytes per microscopic measuring field was also significantly higher in the *cav-1*$^{-/-}$ mice compared to the *cav-1*$^{+/+}$ mice ($P=0.027$, Mann–Whitney rank test, Fig. 3B). The apoptotic rate of splenocytes was also significantly higher in the *cav-1*$^{-/-}$ mice ($n=12$) compared to the *cav-1*$^{+/+}$ mice ($n=14$, $P=0.009$, Mann–Whitney rank test, Fig. 3B).

In the exocrine pancreas, there was a significant hypercellularity in glandular acini and ductal epithelia in the *cav-1*$^{-/-}$ animals compared to the *cav-1*$^{+/+}$ mice (Fig. 4). In the *cav-1*$^{-/-}$ pancreas, the pyramidal epithelial cells in the acini appeared to have a smaller size than those in the *cav-1*$^{+/+}$ pancreas. These cells tended to form fewer apically oriented zymogen granules and this made the exocrine pancreas appear more basophilic on H&E-stained sections The endocrine pancreas showed no significant difference between *cav-1*$^{+/+}$ and *cav-1*$^{-/-}$ animals.

We previously noted that in mice under 6 months of age soft urinary calculi were seen in the bladders of more than 60% of the *cav-1*$^{-/-}$ male mice and frank stone formation was observed in 13% of *cav-1*$^{-/-}$ males whereas this was not seen in *cav-1*$^{+/+}$ mice (Cao et al., 2003). In the older mice evaluated in the present study soft calculi and calcified deposits were also frequently observed at the juxtaposition of the bladder neck and urethra. Although no hypercellularity was demonstrated in the bladder wall of *cav-1*$^{-/-}$ animals on H&E-stained sections the smooth muscle layer in the bladder wall appeared to be disorganized (Fig. 5). Smooth muscle actin (SMA)-positive staining tended to be less abundant in the bladder wall of *cav-1*$^{-/-}$ mice relative to *cav-1*$^{+/+}$ mice (Fig. 5).

In mice that were over 18 months old, focal epithelial hyperplasia was occasionally seen in the dorsal lobe of prostate (data not shown). The incidence of these lesions did not differ between c*av-1*$^{+/+}$ and *cav-1*$^{-/-}$ mice (Table 2). The cav-1-positive abundant fibromuscular stroma that surrounded the prostatic glandular epithelia appeared slightly thicker in the older mice compared to younger adults (data not shown). No differences in the thickness of the stroma fibromuscular sheath were detected by SMA staining of prostate tissue from *cav-1*$^{-/-}$ and *cav-1*$^{+/+}$ (Figs. 6C and D). Interestingly, in the prostate of *cav-1*$^{-/-}$ mice, there was reduced cytokeratin staining in the glandular epithelia (Figs. 6E and F).

In the urogenital tract, we noted that *cav-1*$^{-/-}$ female mice had profoundly weaker cytokeratin staining in the uterine epithelium (Figs. 6G and H). There was an increase in the

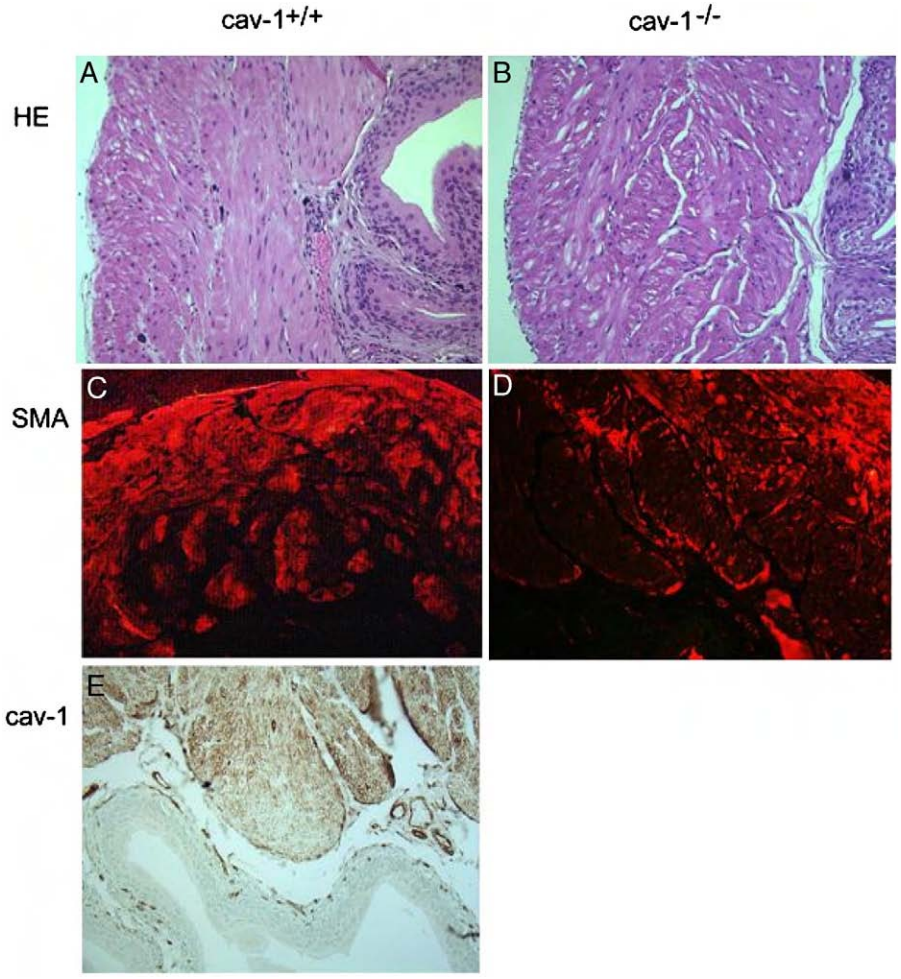

Fig. 5. H&E-stained sections of urinary bladder wall from 10-month-old (A) *cav-1*$^{+/+}$ and (B) *cav-1*$^{-/-}$ mice. SMA staining revealed more intense reactivity in the muscle layer of *cav-1*$^{+/+}$ mice (C) compared to the disorientated appearance in the *cav-1*$^{-/-}$ mice (D). Cav-1 immunostaining in *cav-1*$^{+/+}$ mice is shown in panel E. Original magnification: 200×.

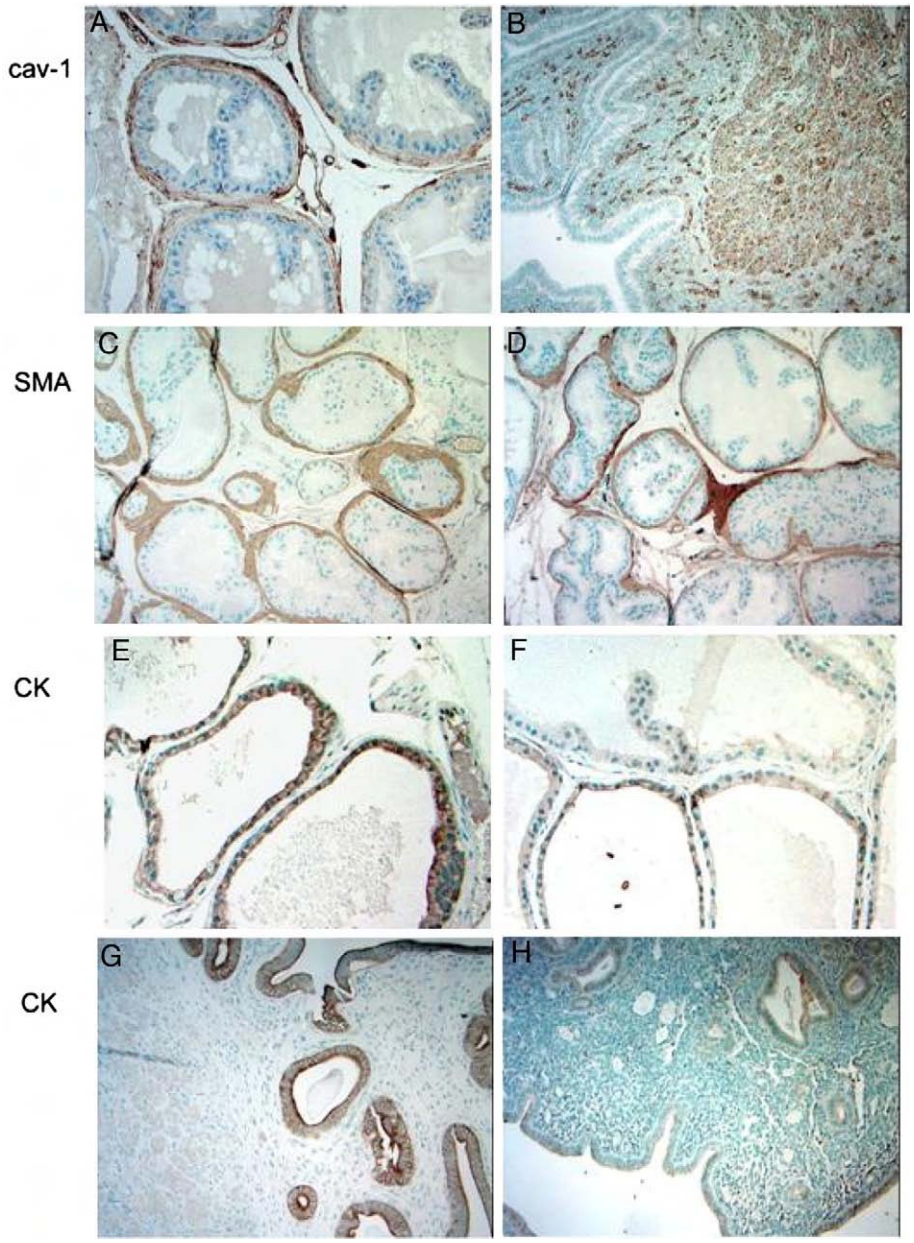

Fig. 6. Prostate and uterus tissues from *cav-1*$^{+/+}$ (A, B, C, E and G) and *cav-1*$^{-/-}$ (D, F and H) mice were stained for cav-1 (A and B), SMA (C and D) or cytokeratin (E–H). Cav-1 was present mainly in smooth muscles and vascular endothelia of the prostate (A) and uterus (B). In the prostates, no differences were evident in the fibromuscular layer surrounding the glandular epithelium between the *cav-1*$^{+/+}$ and *cav-1*$^{-/-}$ mice (C and D, respectively), whereas cytokeratin staining in the glandular epithelium was reduced in *cav-1*$^{-/-}$ (F) as compared with *cav-1*$^{+/+}$ mice (E). In female mice, the uterine epithelia of *cav-1*$^{-/-}$ mice (H) had reduced staining with cytokeratin compared to uterine sections from *cav-1*$^{+/+}$ mice (G). Original magnifications: B: 100×, others: 200×.

number of ovarian cysts observed in *cav-1*$^{-/-}$ mice but this did not achieve statistical significance ($P=0.1297$, χ^2 test, Table 2).

At necropsy, the seminal vesicles from *cav-1*$^{-/-}$ mice appeared to be swollen and enlarged in 67% of animals aged over 18 months ($P=0.0182$, χ^2 test, Table 2). Histological evaluation revealed a marked increase in seminal fluid with epithelial disorientation and a loss of the epithelial chords that normally protrude into the lumen in *cav-1*$^{-/-}$ mice (Figs. 7A and B). SMA staining delineated a thinner seminal vesicle smooth muscle layer in the *cav-1*$^{-/-}$ mice (Figs. 7E and F).

Breast tissues were harvested from *cav-1*$^{+/+}$ and *cav-1*$^{-/-}$ mice at ages ranging from 5 to 21 months. Cav-1 was mainly present in adipocytes, and myoepithelial cells surrounding the glandular epithelia (Fig 8A) in normal *cav-1*$^{+/+}$ breast. Benign epithelial hyperplastic lesions were apparent in H&E-stained sections from 46% of the *cav-1*$^{-/-}$ mice and only 6% of the *cav-1*$^{+/+}$ mice ($P=0.0072$, χ^2 test, Table 2). Features of *cav-1*$^{-/-}$ epithelial hyperplasia included increased numbers of ductal branches and mammary acini, as well as intraductal epithelial cells (Fig. 8). The myoepithelial cell layer that normally surrounds the mammary lining epithelial cells was obscured due to the tangled orientation of the intraductal cells. These morphological hyperplastic changes were also documented through IHC analysis. SMA-positive myoepithelial cells that

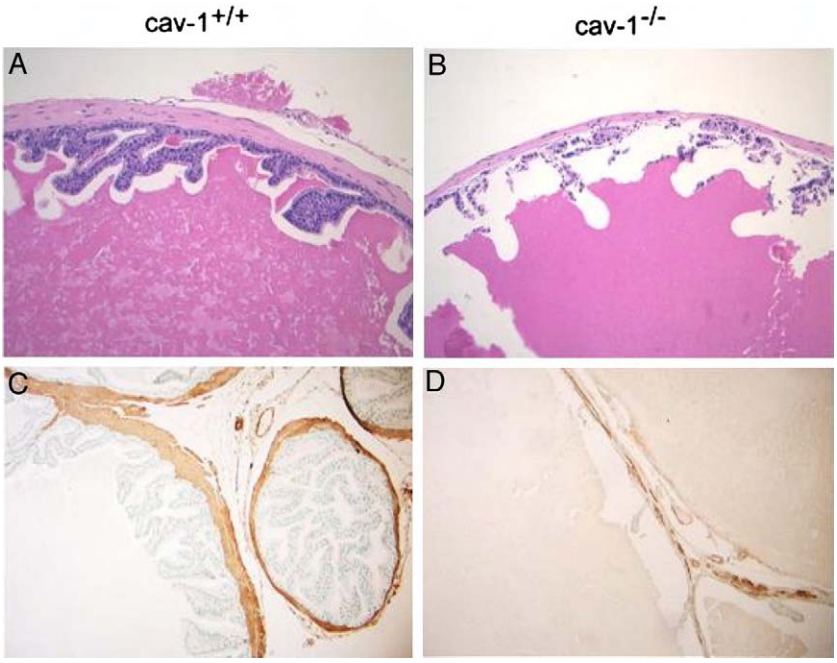

Fig. 7. Sections of seminal vesicle were stained with H&E (A and B) and SMA (C and D). Disorientation of the epithelial layer with a loss of protruding epithelial chords and epithelial detritus was evident in 10 month-old *cav-1*$^{-/-}$ mice (B). SMA staining appeared thinner in *cav-1*$^{-/-}$ mice (D). Original magnifications: 100×.

are normally orientated adjacent to mammary lining cells were admixed with epithelial cells in the *cav-1*$^{-/-}$ breast tissues (Figs. 8C and 8D). Interestingly, in 30% of the hyperplastic *cav-1*$^{-/-}$ breast specimens, SMA antibody strongly labeled intraductal cells (Fig. 8D). However, desmin antibody did not label the hyperplastic cells (data not shown). Vimentin-positive fibroblasts were not observed in the hyperplastic areas but were confined to connective tissue surrounding the hyperplastic epithelia (Fig. 8B). The hyperplastic epithelia in *cav-1*$^{-/-}$ breast sections exhibited attenuated cytokeratin expression compared to the *cav-1*$^{+/+}$ breast epithelia (Figs. 8E and F). Although the mammary hyperplasia-associated morphological and IHC changes were documented, mammary tumors were not observed in any *cav-1*$^{-/-}$ mice.

Discussion

The biological functions of cav-1 in cancer are complex and somewhat controversial (Massimino et al., 2002; Razani et al., 2001b; Thompson et al., 1999, 2001). Cav-1 is involved in multiple pathways that could influence cancer progression such as potocytosis, transcytosis, molecular transport and signal transduction in a cell and context-dependent fashion (Parton, 1996; Shaul and Anderson, 1998). The participation of cav-1 in these critical pathways involves interactions with a relatively large number of molecules in either a scaffolding binding-dependent or -independent manner (Carver and Schnitzer, 2003). The wide spectrum of molecular interactions involving cav-1 is consistent with important, context-dependent roles for cav-1 in signal transduction, molecular transport and other cellular regulatory events.

An association of reduced cav-1 expression in tyrosine kinase oncogene transformed NIH-3T3 cells (Koleske et al., 1995) led to the notion that cav-1 could function as a tumor suppressor gene (Galbiati et al., 1998; Razani et al., 2001b). Subsequent studies clearly demonstrated that overexpression of cav-1 in cells that constitutively express cav-1 (fibroblasts and selected breast cancer cell lines) can suppress growth in vitro (Engelman et al., 1997; Galbiati et al., 2001; Lee et al., 1998). The analysis of clinical specimens has yielded conflicting evidence for the concept of cav-1 as a tumor suppressor. There are several reports that cav-1 expression is down-regulated in cancer including specific types of lung cancer (Kato et al., 2004; Racine et al., 1999; Sunaga et al., 2004; Wikman et al., 2004), colon cancer (Bender et al., 2000), ovarian cancer (Bagnoli et al., 2000; Davidson et al., 2001; Wiechen et al., 2001), breast cancer (Sagara et al., 2004), follicular carcinoma of the thyroid (Aldred et al., 2003) and several types of sarcoma (Wiechen et al., 2001).

Conversely, cav-1 is up-regulated in many human malignancies and is associated with an unfavorable clinical prognosis (reviewed in Mouraviev et al., 2002). In prostate cancer, cav-1 was found to be over-expressed in human metastatic prostate cancer (Yang et al., 1998). Subsequently, positive correlations between cav-1 overexpression and clinical/pathological markers of cancer progression were reported for human prostate cancers (Satoh et al., 2003; Yang et al., 2000, 1999) as well as for other malignancies including metastatic colon cancer (Bender et al., 2000; Patlolla et al., 2004), renal cancer (Campbell et al., 2003; Carrion et al., 2003; Horiguchi et al., 2004; Joo et al., 2004), bladder cancer (Rajjayabun et al., 2001; Sanchez-Carbayo et al., 2002), urothelial carcinoma (Fong et al., 2003), oral squamous cancer (Hung et al., 2003), esophageal

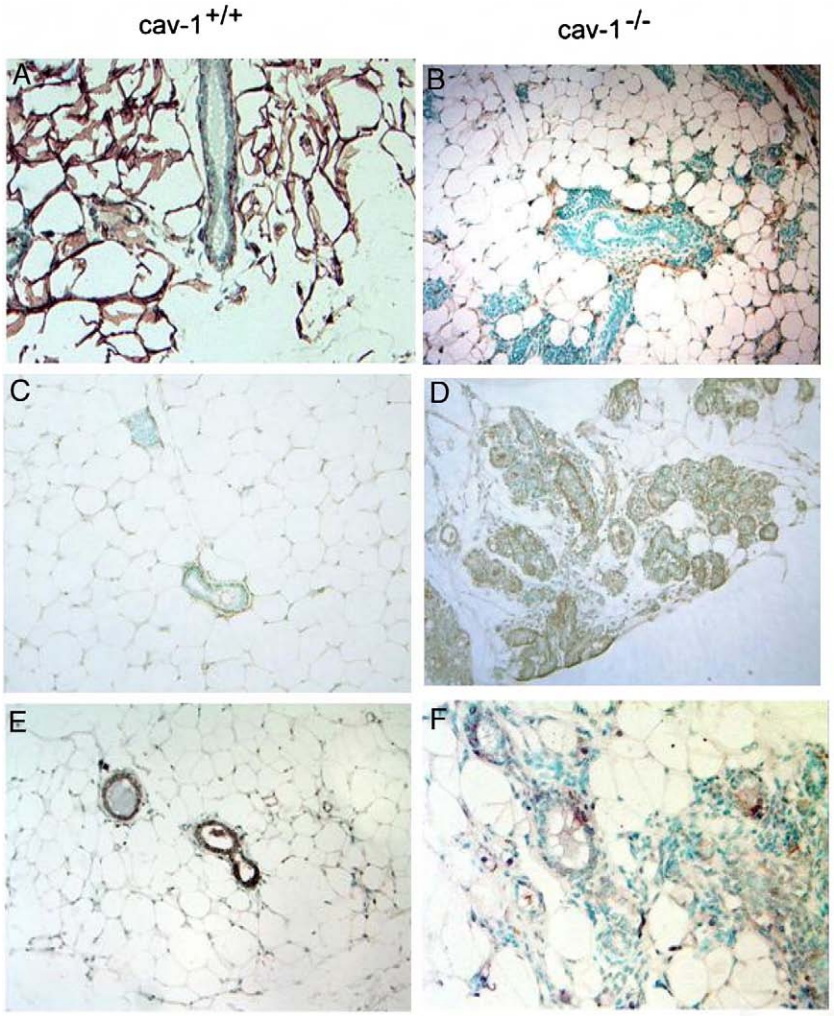

Fig. 8. Immunohistochemistry of mammary glands from 9- to 10-month-old virgin *cav-1*$^{+/+}$ (A, C and E) and *cav-1*$^{-/-}$ (B, D and F) mice as demonstrated by (A) cav-1, (C and D) SMA, (B) vimentin and (E and F) cytokeratin staining. Normal lobular development was apparent in *cav-1*$^{+/+}$ mice (A, C and E) whereas in *cav-1*$^{-/-}$ mammary glands there was pronounced epithelial hyperplasia (B, D and F). Original magnifications: 200×.

squamous cancer (Hu et al., 2001; Kato et al., 2002), papillary carcinoma of the thyroid (Ito et al., 2002), lung cancer (Ho et al., 2002; Sunaga et al., 2004; Yoo et al., 2003), pancreatic cancer (Suzuoki et al., 2002; Terris et al., 2002) and ovarian cancer (Davidson et al., 2002).

In this analysis of *cav-1*$^{-/-}$ and control *cav-1*$^{+/+}$ mice, we observed significantly increased wet weights of specific organs in 10-month-old mice, including kidney, spleen, liver and lung (see Table 1). This result prompted us to further investigate these differences using morphological and IHC analysis. Our studies revealed multiple abnormalities in specific cell types that were directly or indirectly related to growth control. In the lungs of *cav-1*$^{-/-}$ mice, we identified increased numbers of endothelial cells in regions of thickened alveolar septa. Since cav-1 plays an important role in endothelial cell growth, differentiation and maturation (Carver and Schnitzer, 2003) (Smart et al., 1999) this pathology may represent a failure of endothelial cells to properly differentiate, a condition that may contribute to the observed lung pathologies in these mice (Cao et al., 2003; Drab et al., 2001; Razani et al., 2001a; Zhao et al., 2002). In addition, the definitive identification of increased macrophages in these tissues further adds to the etiology of this cav-1-related disorder.

A novel observation of our study is significantly increased spleen size in *cav-1*$^{-/-}$ mice compared to *cav-1*$^{+/+}$ mice (see Table 1). We demonstrated increased splenocyte turnover (see Fig. 4) and suggest that failure of *cav-1*$^{-/-}$ splenocytes to differentiate contribute to the spleen enlargement. In the exocrine pancreas we observed increased numbers of pyramidal epithelial cells of smaller size that demonstrated fewer features of differentiated secretory epithelium in *cav-1*$^{-/-}$ mice. This phenomenon also appeared to be consistent with a failure to differentiate.

Our observations regarding bladder tissue of *cav-1*$^{-/-}$ mice support our previous observations of increased numbers of urinary calculi compared to *cav-1*$^{+/+}$ mice; however, the frequency of frank stone formation was significantly less than we previously observed (Cao et al., 2003). We attribute this to the difference in the age of the mice evaluated in this study (10 months to 1.5 years) compared to those previously evaluated

(3 to 5 months). In the present study, we also observed disorientation of the smooth muscle cell layer in the bladder of *cav-1*$^{-/-}$ mice (see Fig. 6). The intensity of actin staining in these cells was weaker in these cells suggesting that proper differentiation/organization was not achieved. Thickening of the smooth muscle layer in the bladder of *cav-1*$^{-/-}$ mice has been previously reported but the cellular disorganization we observed was not previously described (Woodman et al., 2004). Consistent with this previous study, we also observed a marked increase in the amount of fluid in the seminal vesicles of *cav-1*$^{-/-}$ mice compared to *cav-1*$^{+/+}$ mice with a thinner smooth muscle cell layer and epithelial disorientation accompanying this increased fluid retention.

In contrast with a previous report (Woodman et al., 2004), we did not observe a higher incidence of prostate growth abnormalities in *cav-1*$^{-/-}$ mice. This may be a reflection of differences in strain background.

It is important to note that our studies clarify the growth abnormalities associated with *cav-1*$^{-/-}$ breast that were reported previously (Williams et al., 2003). As in the previous report, we did document complex hyperplasia-related phenomena that involved increased numbers of ductal branches and increased numbers of acini per terminal ductal lobular unit. However, we showed that, at least in some animals, this hyperplastic condition involved myoepithelial cells as confirmed by positive SMA labeling. Since both the epithelial cells and myoepithelial cells may originate from a common progenitor stem cell (Bocker et al., 2002; Boecker and Buerger, 2003), our data suggest that the *cav-1* gene status may affect this differentiation pathway.

Finally, we show that there is markedly reduced cytokeratin expression in glandular epithelia of breast, prostate and uterus in *cav-1*$^{-/-}$ mice compared to *cav-1*$^{+/+}$ mice. It is conceivable that these abnormalities are related to inappropriate stromal differentiation and dysfunctional stromal–epithelial interactions.

The growth abnormalities that we document in this study could be interpreted as conditions that could evolve into a premalignant phenotype or possibly could render the affected cells susceptible to transformation under specific conditions. Indeed a recent study documents increased skin malignancies in *cav-1*$^{-/-}$ mice compared to *cav-1*$^{+/+}$ mice following topical application of a carcinogen (Capozza et al., 2003). However, most of the cell types observed to exhibit hyperplasia in *cav-1*$^{-/-}$ mice were smooth muscle cells that do not commonly undergo spontaneous malignant transformation in either rodents or humans. Furthermore, the hyperplastic pathologies apparent in *cav-1*$^{-/-}$ mice can be interpreted to result from incomplete differentiation that in some cases appeared to resolve to some extent in later years of life rather than progress to malignancy (see Table 2). Notably, we did not observe any increase in malignancies in *cav-1*$^{-/-}$ mice compared to *cav-1*$^{+/+}$ mice in our study. Additional studies will be required to determine the role of cav-1 in the development and progression of malignancy. This study demonstrates that loss of cav-1 function leads to abnormal growth and differentiation of specific cell types including stromal cells. We suggest that in some cases, loss of cav-1 function in stromal cells can lead to disruption of normal stromal–epithelial interactions and dysfunctional organ systems.

Acknowledgments

This work was supported by NIH grants U01-CA84295, P50-CA58204, RO1- CA68814 and a Department of Defence grant W81WH-06-1-116. A portion of these studies were conducted in facilities provided by the Michael E DeBakey VA Medical Center.

References

Aldred, M.A., et al., 2003. Caveolin-1 and caveolin-2, together with three bone morphogenetic protein-related genes, may encode novel tumor suppressors down-regulated in sporadic follicular thyroid carcinogenesis. Cancer Res. 63, 2864–2871.

Bagnoli, M., et al., 2000. Downmodulation of caveolin-1 expression in human ovarian carcinoma is directly related to alpha-folate receptor overexpression. Oncogene 19, 4754–4763.

Bender, F.C., et al., 2000. Caveolin-1 levels are down-regulated in human colon tumors, and ectopic expression of caveolin-1 in colon carcinoma cell lines reduces cell tumorigenicity. Cancer Res. 60, 5870–5878.

Bocker, W., et al., 2002. Common adult stem cells in the human breast give rise to glandular and myoepithelial cell lineages: a new cell biological concept. Lab. Invest. 82, 737–746.

Boecker, W., Buerger, H., 2003. Evidence of progenitor cells of glandular and myoepithelial cell lineages in the human adult female breast epithelium: a new progenitor (adult stem) cell concept. Cell Prolif. 36 (Suppl 1), 73–84.

Campbell, L., et al., 2003. Caveolin-1 overexpression predicts poor disease-free survival of patients with clinically confined renal cell carcinoma. Br. J. Cancer 89, 1909–1913.

Cao, G., et al., 2003. Disruption of the caveolin-1 gene impairs renal calcium reabsorption and leads to hypercalciuria and urolithiasis. Am. J. Pathol. 162, 1241–1248.

Capozza, F., et al., 2003. Absence of caveolin-1 sensitizes mouse skin to carcinogen-induced epidermal hyperplasia and tumor formation. Am. J. Pathol. 162, 2029–2039.

Carrion, R., et al., 2003. Caveolin expression in adult renal tumors. Urol. Oncol. 21, 191–196.

Carver, L.A., Schnitzer, J.E., 2003. Caveolae: mining little caves for new cancer targets. Nat. Rev., Cancer 3, 571–581.

Davidson, B., et al., 2001. Caveolin-1 expression in advanced-stage ovarian carcinoma—a clinicopathologic study. Gynecol. Oncol. 81, 166–171.

Davidson, B., et al., 2002. Caveolin-1 expression in ovarian carcinoma is MDR1 independent. Am. J. Clin. Pathol. 117, 225–234.

Drab, M., et al., 2001. Loss of caveolae, vascular dysfunction, and pulmonary defects in caveolin-1 gene-disrupted mice. Science 293, 2449–2452.

Engelman, J.A., et al., 1997. Recombinant expression of caveolin-1 in oncogenically transformed cells abrogates anchorage-independent growth. J. Biol. Chem. 272, 16374–16381.

Fielding, C.J., Fielding, P.E., 2001. Caveolae and intracellular trafficking of cholesterol. Adv. Drug Deliv. Rev. 49, 251–264.

Fong, A., et al., 2003. Expression of caveolin-1 and caveolin-2 in urothelial carcinoma of the urinary bladder correlates with tumor grade and squamous differentiation. Am. J. Clin. Pathol. 120, 93–100.

Galbiati, F., et al., 1998. Targeted downregulation of caveolin-1 is sufficient to drive cell transformation and hyperactivate the p42/44 MAP kinase cascade. EMBO J. 17, 6633–6648.

Galbiati, F., et al., 2001. Caveolin-1 expression negatively regulates cell cycle progression by inducing G(0)/G(1) arrest via a p53/p21(WAF1/Cip1)-dependent mechanism. Mol. Biol. Cell 12, 2229–2244.

Gavrieli, Y., et al., 1992. Identification of programmed cell death in situ via specific labeling of nuclear DNA fragmentation. J. Cell Biol. 119, 493–4501.

Hakem, R., Mak, T.W., 2001. Animal models of tumor-suppressor genes. Annu. Rev. Genet. 35, 209–241.

Ho, C.C., et al., 2002. Up-regulated caveolin-1 accentuates the metastasis capability of lung adenocarcinoma by inducing filopodia formation. Am. J. Pathol. 161, 1647–1656.

Horiguchi, A., et al., 2004. Impact of caveolin-1 expression on clinicopathological parameters in renal cell carcinoma. J. Urol. 172, 718–722.

Hu, Y.C., et al., 2001. Profiling of differentially expressed cancer-related genes in esophageal squamous cell carcinoma (ESCC) using human cancer cDNA arrays: overexpression of oncogene MET correlates with tumor differentiation in ESCC. Clin. Cancer Res. 7, 3519–3525.

Hung, K.F., et al., 2003. The biphasic differential expression of the cellular membrane protein, caveolin-1, in oral carcinogenesis. J. Oral Pathol. Med. 32, 461–467.

Ito, Y., et al., 2002. Caveolin-1 overexpression is an early event in the progression of papillary carcinoma of the thyroid. Br. J. Cancer 86, 912–916.

Joo, H.J., et al., 2004. Increased expression of caveolin-1 and microvessel density correlates with metastasis and poor prognosis in clear cell renal cell carcinoma. BJU Int. 93, 291–296.

Kato, K., et al., 2002. Overexpression of caveolin-1 in esophageal squamous cell carcinoma correlates with lymph node metastasis and pathologic stage. Cancer 94, 929–933.

Kato, T., et al., 2004. Difference of caveolin-1 expression pattern in human lung neoplastic tissue. Atypical adenomatous hyperplasia, adenocarcinoma and squamous cell carcinoma. Cancer Lett. 214, 121–128.

Koleske, A.J., et al., 1995. Reduction of caveolin and caveolae in oncogenically transformed cells. Proc. Natl. Acad. Sci. U. S. A. 92, 1381–1385.

Kurzchalia, T.V., et al., 1992. VIP21, a 21-kD membrane protein is an integral component of trans-Golgi-network-derived transport vesicles. J. Cell Biol. 118, 1003–1014.

Lee, S.W., et al., 1998. Tumor cell growth inhibition by caveolin re-expression in human breast cancer cells. Oncogene 16, 1391–1397.

Lee, H., et al., 2002. Caveolin-1 mutations (P132L and null) and the pathogenesis of breast cancer: caveolin-1 (P132L) behaves in a dominant-negative manner and caveolin-1 (−/−) null mice show mammary epithelial cell hyperplasia. Am. J. Pathol. 161, 1357–1369.

Massimino, M.L., et al., 2002. Involvement of caveolae and caveolae-like domains in signalling, cell survival and angiogenesis. Cell. Signal. 14, 93–98.

Mouraviev, V., et al., 2002. The role of caveolin-1 in androgen insensitive prostate cancer. J. Urol. 168, 1589–1596.

Park, D.S., et al., 2003. Caveolin-1 null (−/−) mice show dramatic reductions in life span. Biochemistry 42, 15124–15131.

Parton, R.G., 1996. Caveolae and caveolins. Curr. Opin. Cell Biol. 8, 542–548.

Parton, R.G., 2001. Cell biology. Life without caveolae. Science 293, 2404–2405.

Parton, R.G., 2003. Caveolae—from ultrastructure to molecular mechanisms. Nat. Rev., Mol. Cell Biol. 4, 162–167.

Patlolla, J.M., et al., 2004. Overexpression of caveolin-1 in experimental colon adenocarcinomas and human colon cancer cell lines. Oncol. Rep. 11, 957–963.

Racine, C., et al., 1999. Reduction of caveolin 1 gene expression in lung carcinoma cell lines. Biochem. Biophys. Res. Commun. 255, 580–586.

Rajjayabun, P.H., et al., 2001. Caveolin-1 expression is associated with high-grade bladder cancer. Urology 58, 811–814.

Razani, B., et al., 2001a. Caveolin-1 null mice are viable but show evidence of hyperproliferative and vascular abnormalities. J. Biol. Chem. 276, 38121–38138.

Razani, B., et al., 2001b. Caveolin-1, a putative tumour suppressor gene. Biochem. Soc. Trans. 29, 494–499.

Razani, B., et al., 2002. Caveolin-2-deficient mice show evidence of severe pulmonary dysfunction without disruption of caveolae. Mol. Cell Biol. 22, 2329–2344.

Rothberg, K.G., et al., 1992. Caveolin, a protein component of caveolae membrane coats. Cell 68, 673–682.

Sagara, Y., et al., 2004. Clinical significance of caveolin-1, caveolin-2 and HER2/neu mRNA expression in human breast cancer. Br. J. Cancer 91, 959–965.

Sanchez-Carbayo, M., et al., 2002. Molecular profiling of bladder cancer using cDNA microarrays: defining histogenesis and biological phenotypes. Cancer Res. 62, 6973–6980.

Satoh, T., et al., 2003. Caveolin-1 expression is a predictor of recurrence-free survival in pT2N0 prostate carcinoma diagnosed in Japanese patients. Cancer 97, 1225–1233.

Shaul, P.W., Anderson, R.G., 1998. Role of plasmalemmal caveolae in signal transduction. Am. J. Physiol. 275, L843–L851.

Smart, E.J., et al., 1999. Caveolins, liquid-ordered domains, and signal transduction. Mol. Cell Biol. 19, 7289–7304.

Sunaga, N., et al., 2004. Different roles for caveolin-1 in the development of non-small cell lung cancer versus small cell lung cancer. Cancer Res. 64, 4277–4285.

Suzuoki, M., et al., 2002. Impact of caveolin-1 expression on prognosis of pancreatic ductal adenocarcinoma. Br. J. Cancer 87, 1140–1144.

Terris, B., et al., 2002. Characterization of gene expression profiles in intraductal papillary—mucinous tumors of the pancreas. Am. J. Pathol. 160, 1745–1754.

Thompson, T., et al., 1999. Caveolin-1: a complex and provocative therapeutic target in prostate cancer and potentially other malignancies. Emerg. Ther. Targets 3, 337–346.

Thompson, T.C., et al., 2001. Molecular pathways that underlie prostate cancer progression: the role of caveolin-1. In: Chung, L. (Ed.), Prostate Cancer in the 21st Century. Humana Press.

Wiechen, K., et al., 2001. Down-regulation of caveolin-1, a candidate tumor suppressor gene, in sarcomas. Am. J. Pathol. 158, 833–839.

Wikman, H., et al., 2004. Caveolins as tumour markers in lung cancer detected by combined use of cDNA and tissue microarrays. J. Pathol. 203, 584–593.

Williams, T.M., et al., 2003. Loss of caveolin-1 gene expression accelerates the development of dysplastic mammary lesions in tumor-prone transgenic mice. Mol. Biol. Cell 14, 1027–1042.

Williams, T.M., et al., 2004. Caveolin-1 gene disruption promotes mammary tumorigenesis and dramatically enhances lung metastasis in vivo. Role of Cav-1 in cell invasiveness and matrix metalloproteinase (MMP-2/9) secretion. J. Biol. Chem. 279, 51630–51646.

Williams, T.M., et al., 2005. Caveolin-1 promotes tumor progression in an autochthonous mouse model of prostate cancer: genetic ablation of Cav-1 delays advanced prostate tumor development in TRAMP mice. J. Biol. Chem. 10, 1074.

Woodman, S.E., et al., 2004. Urogenital alterations in aged male caveolin-1 knockout mice. J. Urol. 171, 950–957.

Yang, G., et al., 1996. Perineural invasion of prostate carcinoma cells is associated with reduced apoptotic index. Cancer 78, 1267–1271.

Yang, G., et al., 1998. Elevated expression of caveolin is associated with prostate and breast cancer. Clin. Cancer Res. 4, 1873–1880.

Yang, G., et al., 1999. Caveolin-1 expression in clinically confined human prostate cancer: a novel prognostic marker. Cancer Res. 59, 5719–5723.

Yang, G., et al., 2000. Elevated caveolin-1 levels in African-American versus White-American prostate cancer. Clin. Cancer Res. 6, 3430–3433.

Yoo, S.H., et al., 2003. Expression of caveolin-1 is associated with poor prognosis of patients with squamous cell carcinoma of the lung. Lung Cancer 42, 195–202.

Zhao, Y.Y., et al., 2002. Defects in caveolin-1 cause dilated cardiomyopathy and pulmonary hypertension in knockout mice. Proc. Natl. Acad. Sci. U. S. A. 99, 11375–11380.